SURFACE MODIFIED VASCULAR TISSUE FOR TARGETED DELIVERY

by

Timothy Edward Deglau

B.S., Carnegie Mellon University, 1995

M.S.E., University of Pennsylvania, 1996

Submitted to the Graduate Faculty of

the School of Engineering in partial fulfillment

of the requirements for the degree of

Doctor of Philosophy

University of Pittsburgh

2005

UNIVERSITY OF PITTSBURGH

SCHOOL OF ENGINEERING

This dissertation was presented

by

Timothy Edward Deglau

It was defended on

July 5, 2005

and approved by

Eric J. Beckman, Ph.D.
Bayer Professor, Department of Chemical & Petroleum Engineering; Co-Director, Mascaro Sustainability Initiative

Harvey S. Borovetz, Ph.D.
Professor & Chair, Department of Bioengineering; Robert L. Hardesty Professor, Department of Surgery; Professor, Department of Chemical & Petroleum Engineering

Alan J. Russell, Ph.D.
Director, McGowan Institute for Regenerative Medicine; Professor, Department of Surgery; Executive Director, Pittsburgh Tissue Engineering Initiative, Inc.

Flordeliza S. Villanueva, M.D.
Associate Professor, Department of Medicine; UPMC Cardiovascular Institute

William R. Wagner, Ph.D.
Dissertation Director
Associate Professor, Departments of Bioengineering, Chemical & Petroleum Engineering, & Surgery

SURFACE MODIFIED VASCULAR TISSUE FOR TARGETED DELIVERY

Timothy Edward Deglau, Ph.D.

University of Pittsburgh, 2005

Thrombosis and restenosis are common problems associated with intravascular procedures such as anastomoses, balloon angioplasty, and carotid endarterectomies. Application of a molecular barrier at the site of injury to inhibit platelet deposition would be advantageous. Additional therapeutic benefit could be achieved if the modified surface provided a target for delivery of pharmaceuticals, vectors, or cells. This dissertation focuses on the development of an intravascular modification and targeted delivery system that possesses numerous potential applications in the treatment of vascular injury.

Polyethylene glycol is commonly used for modification of molecules and surfaces to increase biocompatibility, reduce immunogenicity, and provide stealth characteristics. Protein-reactive polyethylene glycol could be used to modify vascular surfaces forming a molecular barrier. In addition, the polymer could be used as a target for site-specific delivery of agents by applying a recognizable tag to the terminus of the polymer. For instance, agents could be targeted to modified vascular tissue via the biotin/avidin recognition system.

The ability to modify vascular surfaces with protein-reactive polyethylene glycols was confirmed using quantitative flow cytometry. Furthermore, *in vitro* perfusion studies with cultured human endothelial cells and scrape-damaged bovine carotid arteries demonstrated

preferential delivery of microspheres and cells to polyethylene glycol-biotin modified vascular surfaces.

An *in vivo* rabbit model provided a more rigorous assessment of the polymer modification and targeted delivery system. Polymer modification of balloon injured rabbit femoral arteries persisted for a minimum of 72 hours. Targeted microspheres preferentially adhered to uninjured and balloon injured arteries modified with the reactive polymer as opposed to untreated controls. Furthermore, the ability to target microspheres to the modified vascular surfaces persisted for a minimum of 72 hours.

In conclusion, it was shown that it is possible to modify vascular tissue with a protein-reactive polyethylene glycol and that applying a signaling molecule to the terminus can also provide a target for the site-specific delivery of vascular-infused agents. An intravascular targeted delivery system such as this might find numerous applications in the treatment of intravascular injury that is associated with anastomoses, angioplasty, and endarterectomy procedures.

TABLE OF CONTENTS

LIST OF TABLES

LIST OF FIGURES

PREFACE

I would like to start by thanking my advisor, Dr. William R. Wagner, for all of his assistance and guidance in my research efforts at the University of Pittsburgh. He has helped me with designing experimental studies, analyzing data, composing manuscripts, and presenting research at conferences. His guidance has provided me with all of the essential tools that I will need to survive and prosper in an academic research environment.

Along with my advisor, I would like to thank my committee members for all of their assistance with my project. Dr. Beckman, Dr. Borovetz, Dr. Russell, and Dr. Villanueva all took an active role in guiding me in my academic career, development of my dissertation, and completion of my doctorate. Their suggestions and guidance were imperative in designing my experimental studies and completing my dissertation.

Funding for this research was provided by the National Institutes of Health (grant # HL58617) and The National Tissue Engineering Center (log # 02059001). In addition, the staff and facilities at the McGowan Institute for Regenerative Medicine (MIRM) and Center for Biologic Imaging (CBI) at the University of Pittsburgh provided help and resources to enable completion of this dissertation. Specifically, I would like to recognize those that assisted in the animal studies, including Aaron Dean, Lisa Gordon, Dave Fischer, Dr. Kenneth Litwak, Dr. Elizabeth Tyler-Kabara, Dr. Yu Liu, Dr. Yiqun Ling, and Mary Watach. They devoted a great deal of time and effort in assisting me with completing the *in vivo* studies for this project.

Also, I would like to acknowledge my fellow lab members, Kenneth Gage, Jianjun Guan, Alexa Polk, Priya Ramaswami, Trevor Snyder, John Stankus, Eric Tom, and Greg Weller, who

provided support and assistance during the experimental work for this project. Furthermore, there were a number of undergraduate students that participated in my research over the summer or during academic semesters. They include the following: Rachelle Abati, Kim Albrecht, Katrina Dobbs, Jermaine Johnson, Carl Johnson Jr., Tamika Perry, Adam Pfeiffer, and Diana Yoon.

I would like to extend a special thank you to my aunts, uncles, cousins, in-laws, and friends for all of their support and encouragement over the years. My grandparents have always been the backbone of our family teaching the importance of hard work and perseverance. I would also like to acknowledge my sister for her thoughtfulness and friendship. All of their love and support have been instrumental in my growth as an individual.

I am indebted to my mother for her faith and encouragement, which provided me with the strength and conviction to follow my heart and achieve all of my goals. Her strong will and determination in the face of adversity provided me with the resolve to confront all of life's challenges along the way. Her belief in me provided me with the confidence to pursue my dreams and made me the person I am today. I am certain that I could not have completed this dissertation without her love, support, and guidance.

Furthermore, I owe a special thank you and debt of gratitude to my wife, Stephanie. She provided a great deal of moral support and motivation that assisted in completion of the necessary experiments and writing the dissertation. She was always there to lift my spirits and encourage me during the long hours and sleepless nights in completing this doctorate. In addition, she helped me with the arduous chores of editing and rewriting the dissertation. Without her love, support, and encouragement, I know that I would not have been able to achieve this milestone in my life.

Finally, I would like to honor and thank my father and grandfather who are no longer with me here, but have always been a guiding light in my life. They are deeply missed, but their memory and legacy lives on as an example of the kind of person I hope to emulate. In closing, I am forever grateful for the countless people that have touched my life and supported me throughout the years.

1.0 INTRODUCTION

1.1 ATHEROSCLEROSIS

Atherosclerosis is a complex, progressive disease affecting intermediate and large-sized arteries [1, 2]. Lipid accumulation in the arterial wall begins early in childhood, which can progress into formation of atheromatous plaques [1-3]. Atheroslcerotic plaques protrude into the lumen of the vessel and are subject to tears and fissures due to the shear forces of the surrounding blood flow [1, 2]. The surface of the plaque itself or the underlying lesion exposed by the tears and fissures leads to thrombus or embolus formation and occlusion of the artery at the site of the plaque or downstream in the case of embolization [1, 2]. Occlusion of arteries leads to development of serious life-threatening conditions.

A blockage in the coronary arteries can lead to heart muscle ischemia and myocardial infarction [1, 2]. Similarly, occlusion of a carotid or cerebral artery may result in cerebral ischemia or infarctions [1, 2]. Finally, obstructions can also form in arteries that supply blood to vital organs, such as the kidneys, liver, and intestine or even threaten body limbs [1, 2]. Atherosclerosis results from a myriad of factors such as endothelial dysfunction or injury, inflammation, matrix alterations, and vascular smooth muscle proliferation [4, 5]. Each of these processes and their effects on the development and growth of atherosclerotic plaques will be addressed in detail in the following sections.

1.1.1 Endothelial Dysfunction or Injury

The endothelial cells (ECs) lining all blood vessels are the primary regulators of vascular tone and homeostasis [6, 7]. A healthy endothelium exerts a number of protective effects upon the blood vessel to maintain homeostasis [6, 7]. In the normal state, the endothelium promotes vasodilation, suppresses smooth muscle cell migration and proliferation, controls inflammation, and inhibits platelet and leukocyte adhesion [6, 7]. In addition, endothelial cells support antioxidant, anticoagulant, and profibrinolytic effects [7].

Atherosclerotic plaques show a propensity to develop in areas of fluctuating hemodynamic shear stresses commonly where arteries branch or bifurcate [1]. At these sites, mechanical stresses along with other physical and chemical factors lead to endothelial injury and dysfunction and increased permeability [1, 4, 7]. Increased permeability of the endothelium permits infiltration of leukocytes, lipids, and free oxygen radicals into the vessel wall [4]. Free oxygen radicals obliterate the protective effects of nitric oxide (NO) such as vasodilation, inhibition of platelet adherence and aggregation, prevention of leukocyte adherence and infiltration, and reduction of smooth muscle cell proliferation and migration [4, 6]. Endothelial injury also leads to an upregulation endothelial-derived adhesion molecules leading to attachment of monocytes, macrophages, and platelets [4, 8]. Furthermore, endothelial dysfunction triggers a phenotypic change for the endothelial cells into a proinflammatory, procoagulant, and promitotic state that further enhances the progression of atherosclerosis [7].

1.1.2 Inflammation

Inflammation is another key contributor to atherosclerotic plaque formation. Adhesion molecules expressed on dysfunctional or injured endothelial cells encourage adhesion of

circulating monocytes and extravasation into underlying tissue [1, 4, 9]. The monocytes transform into macrophages and phagocytize oxidized low-density lipoprotein-cholesterol (LDL-C) resulting in the formation of foam cells in the early stages of atherosclerosis [4, 9]. This creates a positive feedback loop whereby buildup of low-density lipoprotein (LDL) in the macrophages further activates the cells leading to recruitment of additional monocytes, macrophages, T lymphocytes, and mast cells [1, 8].

Accumulation of the immune cells within the vessel wall increases inflammation at the site, which can result in activation of the classical and alternative complement pathways and release of cytokines and chemokines [8]. Progression of the inflammatory state leads to further endothelial dysfunction, which stimulates vascular smooth muscle cell (VSMC) migration and proliferation [8]. Current research suggests that both local and systemic inflammation play a crucial role in the progression of atherosclerosis [8].

1.1.3 Matrix Alterations

The extracellular matrix (ECM) of atherosclerotic plaques is altered as compared to the ECM of normal arteries [10]. Matrix composition and structure regulates the behavior of cells in the vessel wall and can influence their ability to migrate, proliferate, and even their resilience to withstand trauma [10]. As mentioned earlier, endothelial injury and dysfunction results in an increased permeability of the endothelium permitting an influx of proteins and cells into the vessel wall [4]. Free radicals oxidize native LDLs resulting in activation of monocytes and macrophages, build-up of intracellular free oxygen radicals, increased expression of adhesion molecules, and cytokine and chemokine release [4, 9].

In addition, there is significant evidence of matrix degradation by matrix metalloproteinases (MMPs) and cathespins within atherosclerotic plaques [10]. Increased MMP expression and activation is associated with all of the major factors contributing to atherosclerosis [11]. Structural changes and remodeling are required for plaque development as evidenced by an accumulation of cells, matrix, and lipids within the intimal layer of the vessel wall [11]. Recruitment and extravasation of inflammatory cells through the endothelial layer into the underlying matrix also contribute to disease progression [11]. There is evidence suggesting that MMPs play a significant role in both of these processes [11].

Other matrix proteins are more commonly found in atherosclerotic lesions than in healthy vasculature. Matrix-associated glycoproteins such as osteopontin, thrombospondin, and tenascin are found in atherosclerotic plaques, which possess properties that assist in cell migration and proliferation [10]. Osteopontin and vitronectin, found in atherosclerotic lesions, encourage smooth muscle cell (SMC) proliferation and migration [10]. Alterations in ECM composition and structure can influence the responses of vascular cells and result in further development of atherosclerotic plaques [10].

1.1.4 Vascular Smooth Muscle Cell Proliferation and Migration

Another contributing factor to the pathobiology of atherosclerosis is VSMC proliferation and migration [1, 5]. VSMCs are primarily responsible for management of blood vessel tone, blood pressure, and flow distribution [12]. Normally, SMCs within adult blood vessels proliferate at an exceptionally slow pace, possess little synthetic activity, and express a specific collection of contractile proteins, ion channels, and signaling pathways necessary to support the contractile function of the cell [12]. However, as atherosclerosis progresses, the phenotype of VSMCs

converts from a contractile to a synthetic state [12]. In the synthetic phenotype, smooth muscle cells become activated and begin to migrate and proliferate [12]. The change in phenotype of the VSMCs is likely a direct result of the other factors discussed previously such as endothelial dysfunction, inflammation, and matrix alterations [5].

Growth factors, cytokines, inflammatory mediators, lipid deposits, free radicals, and MMPs, are all postulated to have a role in the migration and proliferation of VSMCs [12]. Initially, it was assumed that all of the smooth muscle cells that participate in migration and proliferation in the atherosclerotic plaque arise from preexisting medial SMCs within the vessel wall [5, 12]. Nevertheless, new evidence suggests that a portion of the SMCs that contribute to neointima formation may evolve from subpopulations of bone marrow cells in the circulating blood or perhaps develop from ECs and adventitial fibroblasts in the vessel [5, 12]. Vascular smooth muscle cells migrate into the intima and proliferate resulting in increased production of pro-inflammatory factors [5].

Furthermore, the smooth muscle cells accumulating in the neointima secrete disproportionate amounts of collagen and other connective tissue leading to formation of a fibrous cap [1]. Underneath the plaque surface, the inflammatory environment along with VSMC migration and proliferation results in the production of increasing amounts of collagenases and MMPs along with a reduction in proteolytic inhibitors [1, 5]. All of these factors contribute to deterioration and rupture of the atherosclerotic plaque [5]. Fissures and tears in the lesion result in subsequent thrombus and embolus formation, which may occlude the artery and produce an ischemic event [1, 2, 5].

1.2 ISCHEMIC HEART DISEASE

With an average of 698,000 deaths per year from the years 2000 to 2003, diseases of the heart remains the leading killer in the United States of America accounting for 29% of the total mortality [13-16]. The most common form of heart disease, also known as ischemic heart disease, is attributed to inadequate coronary blood flow to the heart muscle often caused by atherosclerosis [2]. As mentioned previously, atherosclerosis is a chronic, progressive disease that ultimately results in the formation of plaques or lesions in the arterial wall [4]. Over time, the fatty lesions continue to grow and change into fibrous, calcified plaques that cause a narrowing and hardening of the arteries that can ultimately occlude blood flow to the heart muscle [17].

Additionally, thrombosis at the site of the atherosclerotic lesion, as a result of erosion or rupture of the plaque, is a another key contributor leading to unstable angina and acute myocardial infarction [18, 19]. Ruptures and erosion of the atherosclerotic plaques elicit procoagulant and prothrombotic events such as activation of the coagulation cascade, platelet aggregation, fibrin deposition, and entrapment of red blood cells generating a thrombus or embolus that can obstruct or diminish coronary blood flow [18]. The primary treatment modalities for ischemic heart disease are pharmacological (including anti-platelet) therapy, coronary artery bypass grafting, and percutaneous coronary interventions (PCIs) with the primary goal of restoring blood flow as rapidly as possible through the atherosclerotic vessel to prevent additional ischemic events in the cardiac muscle [20, 21].

1.2.1 Pharmacological Therapy

Aggressive pharmacological therapy is usually the first treatment option employed in the management of acute coronary syndromes (ACS) to try and stabilize the plaque and minimize further ischemic events [1]. The standard pharmacological therapy in treating acute coronary syndromes is low-dose aspirin to suppress platelet activation and aggregation and inhibit thrombosis [1, 20-22]. Alternative pharmacological strategies involving the use of anticoagulant and antithrombin agents, vasodilators, Beta (β)– blockers, and statins are also employed [23].

Aspirin is one of many anti-platelet agents designed to inhibit platelet activation, aggregation, and release of platelet agonists [22]. However, there are significant limitations such as resistance, allergic reactions, peptic ulceration, and intracranial hemorrhage associated with aspirin [18]. Due to the noted limitations with administration of aspirin, more effective anti-platelet therapies are continually under development. Agonists for the platelet receptor GP IIb-IIIa are the most promising at inhibiting arterial thrombosis because this integrin is involved in both adhesion and aggregation of platelets [1, 20-24]. Abciximab (ReoPro), eptifibatide (Integrilin), and tirofiban (Aggrasat) are three GP IIb-IIIa agonists currently being evaluated [22, 25].

The most commonly used anticoagulant and antithrombin is unfractionated heparin [1, 20, 21, 24]. However, variations in its anticoagulant effect, failure to inhibit thrombin in a clot, risk of thrombocytopenia, and requirement for diligent monitoring have led to development of low molecular weight heparins and direct antithrombins, such as hirudin, as alternatives [18]. Hirudin binds to both the active catalytic site and substrate recognition site of thrombin [18]. Low-molecular-weight heparins are produced through enzymatic or chemical fractionation of heparin molecules [18, 24]. Less nonspecific binding to plasma proteins, a greater inhibitory

effect on Factor Xa, and a more predictable anticoagulatory effect are some of the benefits associated with low-molecular-weight heparin [18, 24].

Nitrovasodilators act to increase NO levels leading to vasodilation and increased perfusion through collateral coronary arteries in an attempt to alleviate ischemia of the myocardium [1, 26]. β-blockers are administered to diminish myocardial contractility and reduce wall stress to enhance perfusion of the left ventricle thereby decreasing the oxygen requirements of the ischemic tissue [1, 27]. A number of adverse effects, such as fatigue, reduced left ventricular function, hypotension, and severe bradycardia, are associated with the use of β-blockers [1, 27].

Another class of pharmacologic agents utilized in the treatment of ischemic heart disease is the lipid-lowering statins [1, 28]. Statins represent a class of drugs that inhibit hydroxymethylglutarylcoenzyme A (HMG-CoA) reductase thereby decreasing cholesterol synthesis in the liver [28]. As the intracellular cholesterol levels drop, LDL receptor expression on the cell surface of hepatocytes is upregulated capturing LDL-C from the bloodstream, which may lead to shrinkage of the lipid core in atherosclerotic plaques [28].

Aggressive pharmacological therapies are usually the first treatment modality utilized in management of ischemic heart disease. A number of therapeutic strategies, including anti-platelets, anticoagulants, antithrombins, vasodilators, and lipid-lowering agents, are exploited to try and minimize ischemic events. Unfortunately, there are a number of adverse side effects associated with pharmacological therapies. More aggressive surgical or catheter-based procedures, such as coronary artery bypass grafting and percutaneous coronary interventions, are often mandated in higher risk patients due to the chronic, progressive nature of atherosclerosis [1]. Pharmacological therapy is frequently used in conjunction with these procedures as well as

providing therapy for atherosclerotic lesions in other locations that have not resulted in obvious ischemic symptoms [1].

1.2.2 Coronary Artery Bypass Grafting (CABG)

The first CABG surgical procedures were completed over forty years ago [1]. Coronary artery bypass grafting (CABG) is usually indicated if other less invasive therapies, such as drug therapy or balloon angioplasty, are unable to control angina pain [1, 29]. CABG is also indicated in cases of multiple-vessel (≥3) disease, or where severe left ventricular dysfunction occurs [1, 29]. CABG restores blood flow to the ischemic myocardium by connecting unessential vessels harvested from other locations in the body between the aorta and coronary arteries distal to any blockages [1].

Originally, the long superficial saphenous vein was used as the vessel conduit in CABG procedures; but problems developed that brought into question the long-term patency of the graft [1]. More commonly, the left internal mammary artery (LIMA) is now used to provide an alternate, unobstructed route for blood flow past the stenosis [1, 2, 30]. The LIMA is not detached from the subclavian artery as was the case with the saphenous vein, but the LIMA is severed distally and anastomosed to the coronary artery beyond any occlusions [1, 2, 30]. Mammary artery bypass grafts demonstrate improved long-term results as compared to saphenous vein grafts [1]. Additionally, the right internal mammary, radial, and gastroepiploic arteries all can be utilized in bypass procedures [1]. The anastomosed vessel bypasses the constriction in the coronary artery restoring adequate blood flow to the ischemic heart muscle thus leading to its name, coronary-aortic or coronary artery bypass grafting. During the surgery

one to five grafts are commonly used to supply the peripheral coronary arteries with adequate blood flow to provide the necessary nutrients and oxygen to the heart [2].

One major drawback to the coronary-aortic bypass surgery is the initial expense. Over 553,000 CABG procedures were performed in 1998 with average costs ranging between $41,500 and $45,000 per procedure for a total of more than $24 billion annually [29, 31-33]. Another disadvantage of CABG is that it is an invasive surgical procedure. New key-hole procedures are being tested to minimize the severity of the surgery and reduce the recovery time. However, the majority of the coronary-aortic bypass surgeries performed today still involve large incisions in the chest and sometimes the leg, fracturing the sternum to expose the heart, and the patient being placed on a heart-lung bypass machine while the graft is inserted. Thus, CABG results in significant discomfort to the patient, extended hospital stays, and prolonged recovery times. Consequently, percutaneous transluminal coronary angioplasty (PTCA), which is minimally invasive and more cost-effective, has surpassed CABG as the most commonly employed treatment modality for coronary atherosclerosis to restore blood flow [29, 34].

1.2.3 Percutaneous Coronary Interventions (PCIs)

Since its inception in the late 1970s, percutaneous coronary interventions (PCIs) have increasingly been used as an alternative to coronary-aortic bypass surgery [35]. PCIs have become the leading treatment option for those afflicted with coronary heart disease in the United States with an estimated 686,000 procedures completed in 1997 [31, 35]. In addition, PCIs can be completed at a reduced cost as compared to CABG. PCIs average between $12,500 and $17,000 per procedure depending upon whether or not stents were deployed, which is one-third of the cost of CABG procedures [29, 31-33].

1.2.3.1 Percutaneous Transluminal Coronary Angioplasty (PTCA)

Percutaneous transluminal coronary angioplasty (PTCA) is achieved by guiding a balloon angioplasty catheter over a wire to the site of the lesion using radiography and inflating the balloon [35]. Inflation of the balloon catheter results in compression and radial displacement of the plaque [35]. PCIs can enhance coronary perfusion by several methods including: compression, fissure, or stretching of the plaque; stretching the vessel wall; and medial dissection [36]. Despite the rudimentary mechanism of arterial expansion employed by the balloon catheter, it enjoys an initial success rate of >90% [36]. However, there are some complications associated with PCIs such as vasospasm, acute thrombus formation, dissection of the vessel, and restenosis [37].

Even with an initial success rate in excess of 90% for balloon angioplasty alone, 30-60% of the patients require repeated revascularization therapy due to restenosis in the treated vessels within six months of having the PCI completed [38-42]. PTCA causes extensive arterial injury destroying the endothelial layer, subendothelial matrix, medial, and adventitia components [38, 39]. The damaged vascular surface exposed following angioplasty is exceedingly thrombogenic, which leads to deposition of circulating platelets and leukocytes [38, 39]. Countless chemotactic and mitogenic factors are contained inside the developing thrombus that ultimately lead to migration and proliferation of the vascular smooth muscle cells within the intima [38, 39].

1.2.3.2 Bare Metal Stents

In order to try and reduce restenosis and abrupt vessel closure, the deployment of metal, expandable stents is now common practice in the field of PCIs [35]. Metallic stents are frequently deployed during balloon angioplasty procedures to provide mechanical support to the vessel wall in the hopes of preserving lumen increases during expansion and inhibiting vessel

recoil and remodeling [41, 43]. Coronary stent implantation during PCIs results in a significant reduction of restenosis in the treated vessels from 30-60% [39-42] with angioplasty alone to only 20-30% [40, 41] when combined with stenting. However, restenosis still remains a considerable concern even with the advent of stents [40, 41].

Stent implantation elicits a number of physiologic responses from the injured vascular tissue resulting that leads to restenosis in a number of patients. The stents are usually metallic and represent a foreign body that initiates a robust inflammatory response [44]. In addition, stent deployment can increase and prolong the insult to the vascular wall leading to localized thrombus formation [43]. Furthermore, stent implantation is also associated with greater neointimal growth than with angioplasty alone [40, 41, 43, 44]. The benefit from stenting during PCIs is attributed to their superior initial gain in lumen diameter and impediment to vessel wall recoil and remodeling [41]. Further advancements attempted to use radiation, laser, and atherectomy to try and improve outcomes following PCIs; however, none of these techniques have proven to be more effective than stenting alone [35, 37].

1.2.3.3 Drug-Eluting Stents (DESs)

Bare metal stents improved the effectiveness of angioplasty procedures, but failed to eliminate all instances of restenosis in the treated vessels. As a result, stents with drug-eluting coatings have been developed try improve long-term patency of the stents by further inhibit in-stent restenosis [45-49]. Many of the pharmacological therapeutics loaded into the DES coating were previously mentioned in the pharmacological therapies section. Ineffectiveness of systemic administration of pharmacological therapies can be attributed, in large part, to inadequate local concentrations at the treatment site as well as systemic toxicity associated with higher doses [49]. Drug-eluting coatings have been constructed with anti-thrombotic (heparin and hirudin), anti-

inflammatory (dexamethasone and sirolimus), and anti-proliferative (paclitaxel and ABT-578) pharmaceutics [48-50]. Pharmaceutics can be chemically attached to the metal stent; however, entrapment of the therapeutics in a polymer matrix coated onto the stent is more common [50].

To date, the sirolimus (Cypher, Cordis J&J) and paclitaxel (Taxus, Boston-Scientific) drug eluting stents have undergone the most testing and have even received market approval from the U.S. Food and Drug Administration (FDA). Clinical studies and post-approval use of the Cypher and Taxus DESs have demonstrated considerable success in preventing neointima formation [46-51]. Sirolimus is a powerful immune modulator that inhibits proliferation of lymphocytes and vascular smooth muscle cells mediated by cytokines and growth factors [45, 46, 49]. Paclitaxel, a microtubule stabilizing compound that prevents transition into the M phase of the cell cycle, is a potent anti-proliferative agent that has been used in treating malignant neoplasms [45, 46]. In randomized-controlled trials, the use of drug-eluting stents resulted in reduced neointima formation and a decline in repeat revascularization procedures as compared to bare metal stents [46-52].

Some of the initial studies with drug-eluting stents suggested restenosis rates as low as 0% [53, 54]. However, the exclusion criteria for the studies was restrictive limiting the use of DESs to relatively simple lesions in noncomplex patients [46, 55, 56]. As drug-eluting stents are applied to increasingly complicated lesions and more challenging patient populations, the restenosis rates increased. Depending upon the study, restenosis rates of 0-9% for the Taxus [54] and 0-12% for the Cypher [57, 58] drug-eluting stents have been documented. The possibility exists for these rates to continue to increase as DES implantation is on the rise since their FDA approval. The documented reduction restenosis rates from 20-30% [40, 41] when deploying bare

metal stents to 0-12% when utilizing DESs [54, 57, 58] demonstrates a significant improvement in PCIs for the treatment of ischemic heart disease that should be noted.

Even with the substantial benefits observed with drug-eluting stent implantation, there are a number of concerns and complications that still must be addressed. A number of experts are urging caution with the application of DESs in more complex lesions where they have not been tested and evaluated [59]. Long-term efficacy in the prevention of restenosis and associated toxicity with the eluted therapeutic remain unknown [59, 60]. A number of possible complications associated with the use of DESs have surfaced, including failure of complete vessel healing, lack of re-endothelialization, delayed in-stent thrombosis, weakening of the vessel wall, persistent fibrin deposition, intimal hemorrhage, and inflammation [45, 46, 50, 55, 56, 58, 59].

The polymer substrate for delivery of the drug has also come under scrutiny. There are numerous reports suggesting a possible hypersensitivity reaction to the polymer coating on the stents resulting in extensive inflammation of the vessel wall [56, 58, 59]. Evidence of delayed thrombosis, re-endothelialization, inflammation, and vessel wall weakening complications exposes the possibility that drug-eluting stents simply delay, but do not abolish restenosis following intravascular procedures [46, 58].

1.3 CEREBROVASCULAR DISEASE

Cerebrovascular disease is currently the third leading killer in the United States with an average of 163,000 deaths per year from the years 2000 to 2003 accounting for 7% of the total mortality each year [13-16]. Almost all elderly patients have some degree of blockage in the arteries

supplying blood to the brain and up to 10% of these might be severe enough to result in a loss of function, otherwise known as a stroke [2]. The majority of cerebral ischemic events (cerebral infarctions) can be attributed to the development of atherosclerotic plaques in one or more of the feeder arteries to the brain [2, 61].

Carotid artery stenosis is a result of atherosclerotic plaque development just as was described with coronary artery stenosis in ischemic heart disease [61]. Lesions that occlude greater than 60-70% of the carotid diameter pose a significant risk of stroke and must be treated surgically [61]. The two principal treatment modalities for cerebral ischemia are carotid endarterectomies and carotid angioplasty and stenting [61-64]. Carotid procedures such as these endeavor to minimize the risk of stroke and death if completed before an ischemic event or reduce the possibility or subsequent infarctions leading to further neurological impairment [63].

1.3.1 Carotid Endarterectomies

Carotid endarterectomy (CEA) remains the most successful treatment and current standard of care for management of carotid artery stenosis [62, 64]. This procedure was developed more than half a century ago, in 1954, and continues as the principal surgical solution in the treatment of carotid arterial occlusive disease [64, 65]. CEAs involve the following: isolation and dissection of the carotid artery, incision along the length of the plaque in the carotid, separation of the lesion from the arterial wall, closure of the artery and initial incision [62].

A number of complications are associated with CEAs, including myocardial infarctions (MIs), transient ischemic attacks (TIAs), neurovascular injury, plaque rupture, and vessel thrombosis [62, 64] Extreme caution must be exercised in all phases of the endarterectomy so as not to rupture the plaque leading to embolization [62]. Even in the absence of procedural

difficulties during the surgery, post-operative thrombosis of the vessel lumen can occur and result in ischemic complications [62]. Consequently, treatments that alleviate or minimize thrombus formation in the vessel lumen after the vascular procedure should improve the effectiveness of the treatment. CEAs have even proven superior to pharmacological management of carotid artery stenosis in a number of studies especially in more advanced disease states [64].

1.3.2 Carotid Angioplasty and Stenting

Percutaneous transluminal angioplasty and stenting have proven effective in alleviating ischemia in coronary and peripheral artery diseases [61]. As a result, carotid angioplasty and stenting have been suggested as a potential lower risk and less invasive alternative to CEAs [61, 64]. In recent years, carotid angioplasty and stenting has gained popularity as a viable substitute to carotid endarterectomy procedures for treatment of cerebral ischemia and could replace endarterectomies altogether within the next ten years [63]. Carotid angioplasty can be performed at a reduced cost, with a shorter hospital stay, fewer surgical complications, and increased comfort for the patients when compared to carotid endarterectomies [63].

Complications are possible with carotid angioplasty and stenting similar to those associated with endarterectomies [64]. In addition, the long-term results of carotid angioplasty and stenting are limited by restenosis as documented in coronary, renal, and peripheral interventions [61]. Thus far, carotid angioplasty and stenting have failed to match the positive early outcomes and some studies even suggest higher rates of complications than those witnessed following CEAs [64]. In the future, carotid angioplasty and stenting may prove to be a less invasive, cost-

effective remedy to alleviate carotid stenosis provided techniques or therapies are developed to reduce or minimize restenosis following the procedure.

1.4 RESTENOSIS

Coronary and carotid interventions aim to restore adequate blood flow to ischemic tissues. Unfortunately, procedures such as PCIs, CEAs, carotid angioplasty and stenting, and anastomoses during CABG used to alleviate ischemia are considerably hindered by restenosis [40]. Restenosis rates for the aforementioned revascularization procedures vary depending upon the particular treatment. However restenosis remains a significant limitation associated with all intravascular procedures. Patients that experience considerable restenosis usually suffer from ischemic events, such as angina, and require additional revascularization procedures (PCIs, CABG, or CEAs) [42].

1.4.1 Etiology

Restenosis is the subsequent re-narrowing of vessels due to neointima formation after intravascular procedures such as balloon angioplasty, stenting, and endarterectomies [41, 66]. A healthy, uninjured rabbit femoral artery (Figure 1-1, A) shows the normal arterial structure with the endothelium, media, and adventitia. Contrastingly, a rabbit femoral artery (Figure 1-1, B) harvested 5 weeks following balloon injury shows significant intimal hyperplasia and reduction in the vessel lumen. The neointima formation (Figure 1-1, B) results in a marked decrease in lumen area available for blood flow and demonstrates the deleterious effects of restenosis following intravascular injury.

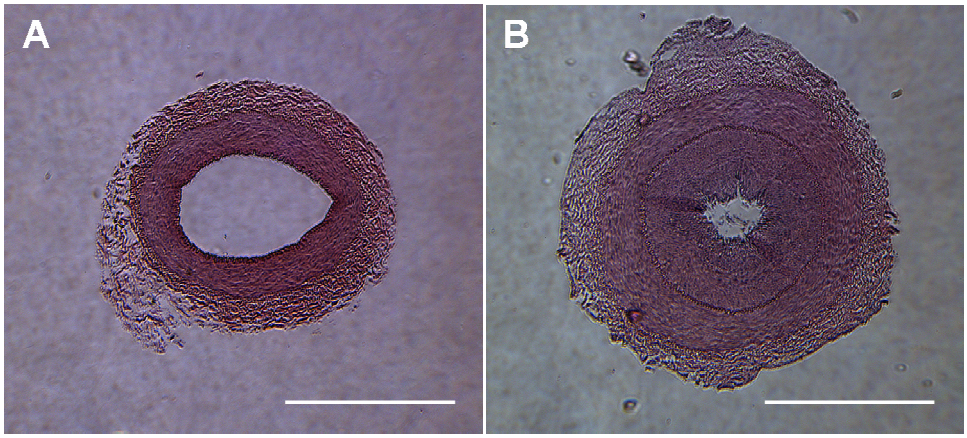

Figure 1–1 Micrographs of (A) un-manipulated and (B) balloon injured rabbit femoral arteries harvested after 5 weeks, paraffin embedded, stained with hematoxylin and eosin, and observed on a light microscope. The scale bar is 1 mm.

Substantial research efforts have attempted to elucidate the underlying mechanisms following intravascular injury that ultimately lead to restenosis [39, 40, 42, 66]. Restenosis is a complex process initiated by tears, fractures, and dissection of the arterial plaque and wall following intravascular procedures [66]. Many of the same factors that lead to development of atherosclerosis are also involved with restenosis; however, the exact mechanisms and response to injury differ [41]. Lipids, calcification, and fibrosis characterize atherosclerotic plaques, whereas neointima formation with cells and matrix epitomize restenosis [41]. The major factors thought to play a role in the development of restenosis are de-endothelialization and endothelial injury, platelet deposition, inflammation, smooth muscle cell migration and proliferation, and vessel wall remodeling [39-42, 44, 66].

1.4.1.1 De-Endothelialization and Endothelial Injury

An intact, healthy endothelium provides continuous vasodilation, inhibition of thrombus formation, and prevention of platelet and leukocyte adhesion as part of its protective effects on vascular homeostasis [44]. However, all of these protective effects are lost following

intravascular procedures such as angioplasty, stenting, and endarterectomies providing the first trigger for initiation of restenosis [44]. PCIs cause extensive de-endothelialization and injury that can persist for months following the revascularization procedure [42, 44].

Loss and injury of the endothelium seriously diminishes its anti-thrombotic effect with a reduction in NO, prostacyclin, and tissue plasminogen activator production [41]. In addition, the endothelial denudation, retraction of remaining cells, and loose intracellular connections leads to an increased permeability of factors and cells as well as exposure of underlying matrix [44]. The exposed underlying matrix induces platelet adhesion and activation [41]. Furthermore, the increased permeability and exposed matrix induces monocyte and leukocyte adhesion and infiltration into the vascular wall inducing an inflammatory response [40]. Endothelial cells also modulate growth, differentiation, and migration of smooth muscle cells, but this control over proliferation and migration is lost after injury or denudation [44]. Re-endothelialization of the injured surface can take a month or longer depending upon the severity of injury and this closely correlates with the extent of neointimal thickening observed [42, 44].

1.4.1.2 Platelet Deposition

The underlying lipid and collagen matrix, exposed following intravascular injury, presents an extremely thrombogenic surface with many adhesive ligands [39, 66, 67]. Platelet deposition occurs immediately following vascular injury as the exposed adhesive ligands interact with receptors found on circulating platelets [66, 67]. Platelets continue to adhere, activate, and aggregate on the injured vascular surface initiating thrombus formation with the release of numerous procoagulant factors [41, 66]. Thrombotic deposition continues for several hours following intravascular injury [66].

Platelet activation and degranulation releases copious amounts of growth factors and chemo-attractants, which contribute to smooth muscle cell migration and proliferation in the neointima [39, 41]. Factor release and surface receptor expression from activated platelets also contribute to adhesion of leukocytes and inflammation at the site of injury [67]. Approximately 24 hours after the intervention, passivation of the injured arterial surface occurs resulting in a less thrombogenic state [39, 66].

1.4.1.3 Inflammation

Inflammation is now thought to play a vital role in restenosis following intra-arterial procedures like angioplasty, stenting, and endarterectomy [39, 40]. P-selectin from the alpha (α)-granules of activated platelets is expressed on the cell surface, which can lead to rolling of leukocytes over the platelet-covered surface [40, 67]. The ligand on leukocytes that interacts with P-selectin is P-selectin glycoprotein ligand (PSGL)-1 [67]. Interactions between P-selectin and PSGL-1 initiate the inflammatory response triggering the release of inflammatory mediators, such as cytokines, chemokines, and reactive superoxide anions [67].

After rolling over the activated platelets, the neutrophils begin to firmly adhere to platelet receptors expressed on their surface [40, 67]. Arrest of leukocytes on the platelet surface can occur either by formation of fibrinogen bridges between MAC-1 integrins of neutrophils with GP IIb/IIIa platelet receptors or interactions between MAC-1 and GP Ib-IX-V platelet receptors [40, 67]. This process further enhances the inflammatory response as platelet and leukocyte interactions lead to activation, upregulation of cell adhesion molecules, integrin activation, chemokine production, and recruitment of leukocytes [40]. Upon firm adhesion to the injured vascular surface, leukocytes extravasate through the adhered platelet layer into the vessel wall

coordinating an inflammatory and healing process, which further contributes to the pathology of restenosis [67].

1.4.1.4 Smooth Muscle Cell Migration and Proliferation

In addition to endothelial denudation and injury, angioplasty, stenting, and endarterectomy produce deep tears and fissures of the media and direct injury to smooth muscle cells [41]. The extensive injury to smooth muscle cells results in substantial apoptosis of the cells with as many as 70% of the medial cells displaying apoptotic characteristics following intravascular injury [39]. In addition, the remaining smooth muscle cells become activated and undergo a change in phenotype from a contractile to a synthetic state [39, 42].

Platelet deposition and cell lysis leads to proliferation of smooth muscle cells in the media [39]. Chemo-attractants released from platelets and leukocytes also promote migration of smooth muscle cells into the neointima where these cells begin to proliferate [39, 42]. However, not all of the smooth muscle cells migrating into the neointima originate in the media layer of the vessel [68, 69]. There is increasing evidence that smooth muscle-like cells derived from circulating bone marrow cells are recruited to sites of vascular injury and participate in the healing process [68, 69]. Smooth muscle cells in the neointima generate substantial quantities of new extracellular matrix through production of hyaluron and chondroitin sulfate [39]. Migration and proliferation of smooth muscle cells in the neointima begins within a few days of intravascular injury and persists for 1 to 4 months depending upon the extent of injury and the individual [39]. Neointima formation stabilizes sometime during this period and then usually begins to regress to some degree as the vessel wall is remodeled through the removal of extracellular matrix [39].

1.4.1.5 Vessel Wall Remodeling

Vessel wall remodeling is a new area of focus into the mechanisms behind restenosis. A number of recent studies are focusing on identifying the role vessel wall remodeling plays in restenosis and how this response differs from smooth muscle cell migration and proliferation. However, in many respects the vessel wall remodeling seems to be related to the smooth muscle response to injury. Smooth muscle cells in the neointima proliferate and synthesize additional extracellular matrix contributing to intimal thickening [39].

However, at some point, the smooth muscle cells produce matrix metalloproteinases (MMPs) and begin to remodel the neointima through removal of matrix [39]. The balance between matrix synthesis and removal and cell death and proliferation at the site of vascular injury all contribute to the thickness and remaining lumen for blood flow of the vessel [70]. In addition, the importance of vascular remodeling should not only be considered in the neointima, but applies to the media and adventitia as well [70, 71]. Inward remodeling of all the layers within the vessel wall is considered a crucial factor in restenosis and it cannot be solely attributable to intimal hyperplasia [70, 71].

1.4.2 Treatments

Restenosis remains a significant limitation with intravascular procedures such as angioplasty, stenting, anastomoses, and endarterectomy as noted previously. The incidence and rate of restenosis is accelerated in PCIs as opposed to more invasive surgical procedures such as CABG and CEA [42, 67]. However, the use of angioplasty and stenting shows no evidence of decline and is, in fact, on the rise due to a number of factors, including its less invasive nature, reduced cost, shorter hospitalization requirement, and reduced patient discomfort [29, 31-34]. Patients

that experience considerable restenosis must endure additional revascularization procedures [42]. As a result, supplementary therapies that further reduce or prevent restenosis are vital to ensure the success and effectiveness of intravascular procedures in the future. A number of areas are under investigation to inhibit restenosis, including pharmacological therapy, gene therapy, molecular barriers, and re-endothelialization [41].

1.4.2.1 Pharmacological Therapy

A number of pharmacological strategies have been employed to try and inhibit and prevent restenosis following intravascular injury. One such tactic was systemic administration of pharmacological agents to inhibit restenosis. In order to increase the therapeutic benefit and reduce systemic toxicity, local deliveries of pharmacological therapies have also been attempted. Site-specific delivery of agents can be accomplished by targeting drugs or carriers to markers present at the site of vascular injury. One other option for locally delivering agents to sites of vascular injury is through the utilization of specialized delivery techniques such as drug delivery catheters.

Initially, systemic administration of pharmacological therapies was first attempted to try and prevent restenosis following intravascular procedures. Many of the pharmacological agents used to treat atherosclerosis have also been employed in the prevention of restenosis. The therapies have focused on agents to inhibit platelet deposition, prevent vessel wall recoil and remodeling, or reduce inflammation and cell proliferation [41].

A number of anti-platelet agents such as aspirin, thienopyridines, and GP IIb/IIIa agonists have been used to prevent platelet, adhesion, activation, and aggregation at the site of vascular injury [41, 67, 72, 73]. Another approach attempts to deliver anticoagulants in order to inhibit thrombus formation on the damaged vascular surface. Pharmacological agents such as heparin,

low molecular weight heparin (LMWH), coumadin, hirudin, urokinase, and thrombomodulin have all been utilized to inhibit thrombus formation in an attempt to curb restenosis [41, 72-74]. Other therapeutics target vascular recoil and remodeling or cell proliferation [41]. Angiotensin-converting enzyme (ACE) inhibitors, Ca-channel agonists, NO, and serotonin receptor agonists aim at reducing vessel wall recoil and reducing vasoconstriction following an intravascular procedure [41, 73]. Trapidil, angiopeptin, colchicines, and statins have all demonstrated anti-proliferative effects on smooth muscle cells that aim to curb intimal hyperplasia [41, 73]. One final approach targets inflammation and its role in restenosis by delivering immunosuppressants and anti-inflammatory pharmaceutics [41]. Corticosteroids, tranilast, and growth factor inhibitors produce immunosuppressive effects curbing the release of pro-inflammatory factors in an attempt to limit their role in restenosis [41].

Systemic delivery of pharmacological agents has demonstrated limited success in the prevention of restenosis following intravascular procedures thus far [41, 73]. In addition, there are a number of serious complications and systemic toxicity associated with administration of such agents [72]. One other issue with systemic delivery is that the concentration of the compounds found at the site of vascular injury is, often times, lower than what is required to elicit a therapeutic effect [72]. Consequently, a shift from systemic to local delivery of therapeutics should maximize the effectiveness of the agents at the site of injury and minimize adverse systemic effects [72].

Local delivery of therapeutics can be achieved by targeting the therapeutic molecules themselves or using targeted carriers for site-specific delivery to injured vascular segments. One such technique combines heparin or low molecular weight heparin (LMWH) with antibodies to cross-linked heparin to direct the compounds to sites of arterial injury in an attempt to reduce

neointima formation [75]. Another scheme targets microspheres or particle carriers through the use of antibodies against exposed ligands in the extracellular matrix or cell surfaces at injured vascular sites [76-80].

Hyaluron microspheres conjugated to antibodies against E- and P-selectin preferentially adhered to inflammatory vascular sites and successfully delivered plasmid DNA [81]. Antibodies against E- and P-selectin, ICAM-1, and VCAM-1 demonstrated the ability to target biodegradable particles to inflamed endothelium [78]. Similarly, liposomes conjugated to antibodies for type I and III collagen or fibronectin selectively adhere to de-endothelialized vascular segments [79, 80]. Furthermore, it is possible to target drug carrying liposomes using a model ligand, such as arginine-glycine-aspartic acid (RGD), to the GP IIb/IIIa integrin found on activated platelets [76, 77]. As mentioned previously, platelet deposition and activation occurs immediately following vascular injury [66, 67]. Consequently, platelets deposited on the injured vascular surface could be used as a target for the site-specific delivery of therapeutics or carriers to platelet markers [76, 77].

However, there are some limitations with the local delivery of therapeutics and carriers investigated thus far. The ability to specifically deliver agents to injured vascular segments depends upon the expression and availability of specific surface markers and their persistence on the surface. Several of the therapies target molecules up-regulated in certain disease states, but most are still commonly found at various levels in healthy vasculature. In addition, the injured vascular surface is constantly fluctuating, which can limit the time where targeted therapies can be administered.

Another method to locally administer treatments following intravascular procedures employs the use of specialized catheters. There are four basic types of balloon catheters that are used for

localized delivery of therapeutics: passive diffusion, active or pressure driven devices, and mechanically assisted technologies [82-86]. Passive diffusion is accomplished using double, coiled-helical multichamber, channeled, and coated balloon catheters [82-88] These systems utilize a secondary balloon for angioplasty and rely on passive diffusion of infused therapeutics to locally inhibit restenosis [82-88]. Active or pressure driven catheters employ micro- and macroporous, multiple, and infusion sleeve balloon designs to increase penetration of the pharmaceutics into the vessel wall using high pressures [82-88]. The final method of localized catheter delivery uses iontophoresis, electric charge, or microneedles to facilitate infiltration of the pharmacological agents into the vessel wall [82-92]. Specialized drug delivery balloon catheters have been used to deliver such therapeutics as urokinase [93, 94], dexamethasone [95], heparin or LMWH [96-103], enoxaparin [104], and caspase inhibitors [105] following PCIs in the hopes of inhibiting or preventing restenosis.

The localized treatment of intravascular injury possesses several advantages over systemic delivery of pharmaceutics including the ability to deliver locally higher concentrations, maximize delivery of expensive or difficult to synthesize agents, and decreased systemic toxicity [89, 91, 92]. However, local administration of pharmaceutics has encountered its own set of complications leading to limited efficacy in the prevention of restenosis [89, 91, 92]. For instance, passive diffusion does not result in significant penetration of agents into deeper layers of the vessel wall [89]. In addition, passive diffusion often requires extended incubation periods to allow adequate delivery to the vessel surface or into the wall itself since many coronary procedures are often restricted to less than 1 min [89]. Localized delivery with specialized balloon catheters can also be limited by more extensive arterial injury that often occurs with pressure driven devices [88]. Finally, using specialized catheters for local administration of

therapies only affords one opportunity to treat the vascular segment, which may require multiple treatments or even continuous administration to elicit a beneficial effect.

1.4.2.2 Gene Therapy

Gene therapy is also under investigation as an adjunct therapy following intravascular procedures due to inadequate results following systemic and targeted pharmacological therapies in the treatment of restenosis [106]. A number of potential genetic targets exist for modulation to inhibit restenosis, including thrombosis, platelet deposition, vessel wall remodeling; but most of the attention has been directed at controlling cell proliferation and migration [107]. Viral envelopes, plasmid DNA, polymer complexes, and liposomes are all possible vectors for transfer of genes to the vasculature [107, 108].

Viral vectors are the most efficient vehicle for delivering new genetic material into transfected cells, but possess limitations which hinder their usefulness [108]. Retroviruses stably integrate the new genetic material into the host genome, but they can only infect proliferating cells and insertion of the new DNA can lead to mutagenesis [107, 108]. Adenoviruses are able to infect replicating and non-replicating cells with a higher efficiency of gene transfer than the other vectors; however, its success is limited by transient expression of the encoded protein and induction of inflammatory and immune responses [107, 108]. Liposome, polymer and plasmid complexes do not elicit the inflammatory or immune responses found with viral vectors, but suffer from low transfection rates and degradation of the transfer gene in endosomes [107, 108]. Gene therapy vectors can be delivered to vascular segments using targeted complexes and with specialized delivery catheters as described in Subsection 1.4.2.1 [107].

Targets of gene therapy for the prevention of restenosis following intravascular procedures include cell cycle regulators, apoptotic or cytotoxic products, signaling pathways, transcription

factors, cytokines, and growth factors [106]. Vectors encoding cytotoxic products like herpes virus thymidine kinase and cytosine deaminase result in significant cell mortality to the transfected and neighboring cells with a subsequent reduction in neointimal hyperplasia [106, 107]. Gene transfer of a cyclin-dependent kinase inhibitor p21, c-myc, c-myb, or a mutated retinoblastoma protein leads to arrest of cell division and reduction of restenosis [106-110]. Introduction of an inducible nitric oxide synthase gene at the site of vascular injury should lead to inhibition of platelet and leukocyte adhesion, reduction in smooth muscle cell migration and proliferation, and increased survival and proliferation of endothelial cells [106, 111-115]. A number of animal studies have demonstrated a reduction in neointima formation following gene transfer of an inducible nitric oxide synthase [106, 111-115]. Gene transfer of vascular endothelial growth factor (VEGF) has also demonstrated some success at inhibiting restenosis by promoting re-endothelialization on the denuded vessel wall reducing thrombus formation and curbing neointimal hyperplasia [106, 108, 116-118].

Gene transfer is an emerging therapy for the prevention of restenosis following intravascular procedures [119]. Some animal studies using gene therapy have shown promise in reducing restenosis following percutaneous arterial interventions, but difficulties remain with this technique [107, 119, 120]. Delivery of the therapeutic genes is often inefficient resulting in poor expression of the encoded molecule [119, 120]. Transfection of the target cells usually requires extended incubation periods of 30 min or more, which is impractical in time-sensitive coronary procedures [121, 122]. In addition, viral vectors tend to elicit inflammatory and immune reactions, which can limit expression and injure or kill the transfected cells [107, 120]. Another setback encountered with gene therapy strategies is evidence of gene transfer in peripheral

organs even after local administration of the vectors, which could produce systemic toxicity [119].

1.4.2.3 Molecular Barriers

Formation of a molecular barrier following intra-arterial procedures to inhibit platelet deposition is another approach designed to inhibit restenosis at the site of vascular injury. Coatings have been constructed on injured vascular surfaces to create a physical barrier to inhibit platelet deposition. In addition to coatings, synthesis of hydrogel matrices on the injured vascular surface has been utilized as a barrier to platelet deposition and for the elution of therapeutics.

One example of molecular barrier formation at the site of vascular injury involves creation of nanocoatings to inhibit platelet deposition [123]. Nanocoatings of hyaluron and chitosan were formed by alternating deposition of the polyelectrolyte layers [123]. Unfortunately, establishment of an effective barrier via deposition of the hyaluron and chitosan nanocoatings involves multiple administrations of each individual polyelectrolyte [123]. The requirement of multiple administrations to develop the nanocoating increases the time necessary for successful treatment, which might be a limiting factor in its applicability to coronary procedures.

A surgical fibrin glue, Tisseel from Baxter, has also been evaluated on injured vascular surfaces [124]. The fibrin glue is composed of thrombin, factor XIII, fibrinogen, plasminogen, and plasmafibronectin [124]. When mixed together, the constituents rapidly react to form a coagulum [124]. However, in this case, the coagulum showed no barrier effects on preventing thrombus formation [124]. Instead, the fibrin glue was used as a matrix for the elution of pharmacological agents to assist in preventing restenosis [124]. Actually contributing to thrombus formation at the site of vascular injury might be counterproductive as platelet deposition on the injured vascular surface has been shown to contribute to the restenotic process

[39, 41, 66]. In addition, formation of the coagulum excluded some therapeutic agents and elution of the incorporated pharmaceutics occurred swiftly in under 4 hours [124].

Another tactic attempted to shield extracellular matrix (ECM) ligands with a polyethylene glycol-modified fibronectin [125]. Fibrillar collagens constitute a significant portion of the ECM exposed following intravascular injury [125]. Fibronectin interacts with fibrillar collagens and platelets, which might allow for targeting of the fibronectin modified with polyethylene glycol to sites of vascular injury [125]. Covalent modification of proteins and surfaces with polyethylene glycol blocks undesirable interactions, such as protein adsorption, immune responses, and cell adhesion [125]. The benefits and applications of polyethylene glycol modification are discussed in greater detail in Chapter 2. For this application, the polyethylene glycol-modified fibronectin molecules should amass on injured vascular surface forming a molecular barrier that should reduce platelet recognition and binding [125]. However, the establishment of an effective blockade to platelet deposition with the fibronectin modified with polyethylene glycol required extensive incubation periods of 30 min or more, which would be impractical in a number of intravascular procedures that are time-sensitive [125].

Photopolymerization of hydrogel barriers onto injured vascular surfaces have demonstrated an ability to inhibit platelet deposition as well as reduce neointima formation [126, 127]. The photopolymerized hydrogel creates a barrier on the injured vascular surface preventing blood form contacting the thrombogenic surface, which blocks platelet adhesion [126]. However, there are obstacles to successful formation of hydrogels on vascular surfaces during intravascular time-sensitive procedures. Hydrogel formation on vascular surfaces requires multiple steps, including adsorption of a photoinitiator on the injured vessel surface, flushing of excess initiator, and then subsequent administration of the hydrogel precursors [126, 127]. Additionally, adequate external

or internal illumination is required for proper photopolymerization of the hydrogel precursors into a stable gel [126, 127]. Internal illumination requires specialized illuminators and procedures while external illumination would prove difficult in minimally-invasive procedures. In addition to their barrier effect, photopolymerized hydrogels have also been developed to release therapeutics, such as NO or benzyl indazole derivatives (YC-1), to further reduce platelet deposition and inhibit smooth muscle cell proliferation at injured intravascular sites [128, 129].

1.4.2.4 Re-Endothelialization

A healthy, intact endothelium provides continuous vasodilation, inhibition of thrombus formation, prevention of platelet and leukocyte adhesion, and regulation of smooth muscle cell growth and migration as a portion of its protective effects on vascular homeostasis [44]. The protective effects endothelial cells exert in order to maintain vascular homeostasis are lost upon endothelial injury and denudation following intravascular procedures, such as balloon angioplasty, stenting, and endarterectomy [44, 130]. Consequently, strategies to assist in re-endothelialization of the denuded vessel wall have received a great deal of attention in the hopes of restoring the beneficial effects of an intact endothelium and prevent restenosis [130]. Several techniques have been attempted to assist with expedited re-endothelialization following intravascular injury, including endothelial seeding of the injured vessel wall, promoting endogenous endothelial recruitment and recovery, and application of perivascular endothelial cells engrafted in matrices [130].

One approach to re-endothelialization of the mechanically injured vessel wall focuses on seeding previously harvested ECs on the injured vascular surface using specialized catheters [130]. A number of studies have attempted to delivery harvested cells with specialized catheters back to injured arterial segments following percutaneous interventions [131-134]. The seeded

endothelial cells accelerated re-endothelialization on the denuded vessel wall resulted in decreased platelet deposition [133, 134]. This approach was further confirmed as seeding of endothelial cells on vascular surfaces injured during endarterectomy procedures demonstrated a significant reduction in neointimal hyperplasia [135, 136]. The inhibitory effects of endothelial cells on thrombus formation and neointimal hyperplasia could further be enhanced through the use of genetically modified cells for continuous release of anticoagulants like tissue-type plasminogen activator and hirudin [137].

However, there are a number of limitations with the applicability of endothelial delivery to injured surfaces. Transport of endothelial cells to the injured vascular surface is difficult requiring development of specialized catheters [130]. In addition, adequate endothelial cell attachment and retention requires considerable incubation periods of anywhere from 20-45 min, which would be unsuitable for time-sensitive coronary interventions [131-134, 138]. Another difficulty encountered with cell seeding techniques is inefficient circumferential coverage due to gravity-dependent settling [138]. Inefficient coverage could be diminished using endothelial cells containing paramagnetic particles and magnets, but this still required extended incubation periods and rotation of the subject [138]. The ability to harvest adequate quantities of endothelial cells is also a concern. This dilemma could be alleviated by noting the ability of bone marrow-derived peripheral blood mononuclear cells to transdifferentiate into cells with endothelial characteristics [139-141]. Delivery of peripheral blood derived monocytes accelerated re-endothelialization after balloon injury and reduced neointima formation [139-141]. Unfortunately, this did not solve the problem of the lengthy incubation periods for cell attachment [139-141]. Furthermore, although endothelial seeding of the injured surface reduced platelet deposition, it did not always translate into an inhibition of intimal hyperplasia [130].

Re-endothelialization of the denuded surface could also be enhanced by encouraging endogenous endothelial recruitment and recovery [130]. Systemic administration of endothelial growth factors, including VEGF, basic fibroblast growth factor (bFGF), and estrogen hastens re-endothelialization after vascular injury [130]. However, there are a number of deleterious side effects associated with systemic delivery so local delivery of such factors is more applicable [130]. Evidence suggests a population of bone marrow-derived stem and progenitor cells, known as endothelial progenitor cells (EPCs), that participate in repair and regeneration of injured vessels [142-145]. Mobilization of endothelial progenitor cells can be aided with administration of estradiol or granulocyte-macrophage colony-stimulating factor (GM-CSF) [142, 143]. In animal studies, recruitment of endothelial progenitor cells resulted in accelerated re-endothelialization, reduced monocyte infiltration, and decreased neointima formation [142-145]. However, these results have not been confirmed in human clinical trials and more information about the precise precursor population, how to home them to regions of injury, and their differentiation and function at the site of injury is essential [146].

Perivascular transplantation of matrix engrafted endothelial cells represents another strategy to restore the beneficial effects of endothelium to injured vessels even though it does not restore the endothelial layer intraluminally [147-150]. A suspension of endothelial cells injected into the perivascular space around injured vessels undergo apoptosis or migrate to other locations [130]. Implants of biopolymeric matrices seeded with endothelial cells in the perivascular space at sites of vascular injury reduced neointimal hyperplasia [147-150]. Reduction of neointima formation must be attributed to biochemical effects provided by the endothelial cells in the matrix to regulate smooth muscle cell migration and proliferation since they could not participate in re-endothelialization inside the lumen [147-150]. However, these results were only demonstrated in

animal studies and application of a matrix seeded with endothelial cells would prove difficult in minimally-invasive procedures.

1.4.3 Clinical Significance

Diseases of the heart and cerebrovascular diseases represent two of the top three causes of mortality in the United States accounting for 36% of all fatalities [13-16]. Both ischemic heart disease and cerebral ischemia can be attributed to the development of atherosclerosis in blood vessels that nourish the heart and brain, respectively [2, 61]. Interventions to alleviate ischemic events include vascular procedures such as bypass grafting, angioplasty, stenting, and endarterectomy. However, the ultimate success of these therapeutic strategies are plagued by occurrences of restenosis in the treated vessels [40]. Often times, restenosis results in a substantial reduction in the lumen of the treated vessel leading to recurring ischemia necessitating additional revascularization therapies [42].

Pharmacologic, genetic, barrier, stent, and re-endothelialization strategies are all under investigation as potential therapies to alleviate restenosis [41]. Results of the various techniques are mixed. Many strategies have demonstrated beneficial effects in a variety of animal models, but frequently suffer from poor clinical outcomes. Consequently, there still exists a considerable need for the development of innovative strategies as stand alone or adjuncts to current therapies in the prevention of restenosis.

This dissertation attempts to address this dilemma. A novel intravascular modification and targeted delivery system is investigated. A protein-reactive polyethylene glycol is used to modify vascular surfaces. The addition of biotin to the terminus of the covalently linked polyethylene glycol provides a target for the site-specific delivery of agents using the biotin and

avidin chemistry. This should provide an opportunity for the targeted delivery of pharmaceutics, vectors, or cells to injured vascular sites following procedures such as angioplasty and endarterectomy.

2.0 INTRAVASCULAR MODIFICATION AND TARGETED DELIVERY SYSTEM

2.1 POLYETHYELENE GLYCOL (PEG)

2.1.1 Properties

The effects of polyethylene glycol (PEG) modification of molecules and surfaces is increasingly exploited for countless pharmacologic and biomedical applications [151]. Effects of PEG modification are likely due to its distinctive chemical and physical properties [152, 153]. Polyethylene glycol is a neutral charged, crystalline, thermoplastic polyether that exhibits a high degree of solubility in water and organic solvents [152, 153]. The basic chemical structure of PEG is H-(O-CH_2-CH_2)OH [152]. PEGs exceptional solubility in aqueous environments can be attributed to its superior structural fit with water [152, 153]. Water, in its liquid state, maintains a highly structured tetrahedral lattice shaped by hydrogen bonds linking individual molecules [152, 153]. It is postulated that the PEG chain structure essentially fits into the tetrahedral lattice of water with hydrogen bonding occurring between the water molecules and ether oxygens in PEG, which results in minimal disturbance of water structure [152, 153].

Additionally, it has been demonstrated that water molecules associate with individual ethylene glycol subunits forming a hydration shell and resultant large excluded volume associated with the PEG molecule [152, 153]. The linear, uncharged PEG molecule, without inclusion of large side groups, allows for substantial chain flexibility and rapid motion [152,

153]. High solubility , neutral charge, large excluded volume, chain flexibility, and rapid motion are all characteristics of polyethylene glycols that contribute to its beneficial effects when modifying molecules and surfaces [152, 153].

2.1.2 PEGylation Chemistry

In order for PEG to exert its unique properties, a linkage must exist between the polymer and another molecule or surface. For surface modification, this can be accomplished using a variety of techniques, including bulk modification, physical adsorption, covalent grafting, and graft copolymerization [152]. However, the only effective method to modify molecules of interest with PEG is through covalent attachment [152]. A discussion of these techniques will demonstrate how to impart the unique properties of PEG onto molecules or surfaces of interest.

Bulk modification of surfaces is usually accomplished through block copolymerization or crosslinking of PEG networks to form modified surfaces [152]. This technique involves formation of a sizable layer of polymer network, which is not applicable to creation of thin polymer layers on biomedical devices, liposomes, or cells. Another method involves physical adsorption of the PEG chains onto pre-existing surfaces [152]. Physical adsorption is usually achieved through the utilization of amphiphilic copolymers of PEG with hydrophobic segments that will associate with hydrophobic surfaces common with many commonly used medical materials [152]. However, no covalent bonds are established so the association may be interrupted and the beneficial effects of PEG modification lost. Covalent grafting of PEG onto surfaces results in a stable, durable linkage that also applies to modification of target molecules [152]. Graft copolymerization starts with covalent attachment of polymer chains onto the surface, but uses initiators to incorporate additional chain growth and branching of the original

engrafted polymers [152]. This type of process would likely be unsuitable for biologic compounds, liposomes, or cell surfaces because of denaturation or toxicity associated with the initiators.

Covalent modification of molecules and surfaces with PEG provides the most effective method of forming a stable, durable linkage [152]. In addition, this is the method of choice for most application involving PEG modification. This process for covalently attaching PEG onto molecules or surfaces is termed PEGylation [151, 152]. Polyethylene glycol chains are terminated with hydroxyl groups in its basic form [151]. As a result, PEG must be activated by incorporation of a reactive group at one or both ends to enable covalent modification of another molecule [151]. Selection of the specific reactive group is based upon the available functional groups for modification of the molecule of interest [151]. Proteins and peptides are of particular interest for PEG modification in pharmacological and biomedical applications. In this case, lysine, cysteine, histidine, arginine, aspartic acid, glutamic acid, serine, threonine, tyrosine, N-terminal amine, and C-terminal carboxyl represent active residues that can participate in formation of covalent bonds [151]. Covalent linkage of reactive PEGs with proteins will depend upon the number of available active sites and the nature of the bond formed. Precise selection of the reactive PEG for specific proteins or peptides permits significant control in the placement and magnitude of PEG attachment [151].

2.1.3 Applications

As noted previously, the high degree of solubility, neutral charge, large excluded volume, chain flexibility, and rapid motion associated with PEG makes it an ideal candidate for modification of molecules and surfaces to modulate their properties [152, 153]. The unique chemical and

physical properties of PEG camouflage and exhibit repulsive effects on molecules and surfaces [152]. PEG interfaces with water display extremely low free energies, which decreases the driving force for adsorption of molecules, like proteins [152]. Steric hindrance or stabilization from the PEG chain on a molecule or surface also leads to repulsion because the encroaching object compresses the excluded volume allowing fewer possible conformations of the polymer, decreasing entropy and repelling the other entity [152]. Another mechanism that PEG attachment facilitates in decreasing interactions between molecules or surfaces involves the chain motion [152]. The increased chain mobility and hydration due to PEG modification prevents stagnation decreasing the time the two molecules or surfaces are in contact thus reducing the chances for interaction [152].

PEG modification of surfaces have demonstrated decreased protein adsorption and inhibition of cell adhesion [154-156]. Proteins and peptides modification with PEG reduces toxicity, immune responses, and rapid clearance [157, 158]. In addition, PEG attachment to proteins and peptides can result in improved pharmacokinetics [157]. The unique physical and chemical properties of polyethylene glycol lend itself to modification of proteins and peptides, biomaterials, cells, and tissues to modulate responses.

2.1.3.1 Protein and Peptide Modification

Proteins and peptides are commonly linked with PEG to reduce adverse events, such as toxicity, immunogenicity, antigenicity, proteolysis, kidney filtration, and liver clearance [157, 158]. In addition, PEGylation of proteins and peptides can produce a number of beneficial effects, including increased solubility, stability, pharmacokinetics, bioactivity, and residence times [157, 158]. PEG modification of pharmaceutical agents, cytokines, and antibodies or antibody

fragments have all demonstrated increase therapeutic benefit and blood circulation times as well as reduced toxicity and immunogenicity [159-161].

The PEGylated drugs pegadamase and pegaspargase have already been approved for clinical use by the FDA [161]. Pegadamase replaces an adenosine deaminase (ADA) deficiency associated with severe combined immunodeficiency disease (SCID) [161]. Covalent attachment of PEG to ADA boosts the circulating half-life from only a few minutes to 24 hrs [161]. Therapeutic enhancement of pegaspargase occurs through a different mechanism. Asparaginase is one of the primary factors administered for leukemia treatments [161]. In this instance, PEG modification reduces the incidence of hypersensitivity reactions and the formation of neutralizing antibodies to asparaginase [161]. Circulation half-life of pegadamase increased 18-fold as compared to the un-modified agent [161]. Reduction of immune reactions and augmented circulation times leads to superior therapeutic effects with fewer doses.

PEGylation of cytokines can also lead to improved therapies in the treatment of various cancers and chronic diseases [160]. This is accomplished by modifying cytokines with PEGs of molecular weight (MW) $\geq$ 30,000 [158]. Attachment of large PEG chains results in an increase in the molecular size of the combined agent above the pore size of the kidney glomerular membrane preventing its removal [158]. In addition, polyethylene glycol modification of recombinant proteins reduces its immunogenicity and decreases production of neutralizing antibodies [160]. PEG modification of interferon-alpha (IFNα) markedly increased circulation times with less frequent injections in the treatment of chronic hepatitis B and C virus infections and cancer [160]. PEGylation of granulocyte colony-stimulating factor (G-CSF) increases the quantity of neutrophilic granulocytes in an attempt to alleviate the neutrophilia resulting from chemotherapy [160]. Covalent modification of cytokine inhibitors with PEG would enhance

their ability to regulate adverse immune responses associated with conditions such as toxic shock, arthritis, asthma, and Crohn's disease [160].

Antibody-based therapies are increasing for the treatment of cancer and chronic conditions [159]. However, immunogenicity, degradation, and reduced longevity have limited antibody-based remedies [159]. PEGylation of antibodies and antibody fragments has been utilized to prevent removal in the kidneys, inhibit proteolysis, and reduce antigenicity [159]. Site-specific PEG modification techniques of antibody-based therapies are typically required to prevent interference with the antigen binding domains and effector functions [159]. Random PEG modification of antibodies frequently results in a marked reduction of antigen binding ability and an inability to interact with their target cells [159]. Antibodies modified with PEG have demonstrated increased longevity and enhanced tumor targeting [159]. Furthermore, PEGylated antibody fragment therapies for rheumatoid arthritis, Crohn's disease, and coronary restenosis are under investigation.

2.1.3.2 Biomaterial Surface Modification

Surface modifying with PEG can increase the biocompatibility of biologic or synthetic materials by decreasing protein and cell adsorption when exposed to blood [156, 162]. Previously, our lab demonstrated a significant reduction in platelet deposition following PEG modification of fibrinogen and collagen adsorbed microconduits and pre-clotted Dacron fabric [162-164]. These results suggest that protein-reactive PEGs are able to conceal adhesive ligands and agonists present on thrombogenic surfaces thereby reducing platelet deposition [162-164]. PEG modification on biomaterial surfaces contacting blood would be useful in cardiovascular applications where thrombosis can lead to device failure [162-164].

This effect could be further augmented by incorporation of sulfonate groups on the free terminus of the polyethylene glycol molecules [156]. Surfaces grafted with PEG containing the negatively charged sulfonate groups resulted in superior thrombus resistance as compare to PEG alone [156]. Negatively charged surfaces tend to exhibit anti-thrombotic characteristics; consequently, the combination of sulfonate groups on PEG should enhance its blood biocompatibility [156].

The concept of PEG surface modification enhance biocompatibility can be extended to include liposomes, microspheres, and viral vectors [165-167]. PEGylation of galactosylated liposomes diminished removal of the particles by the liver without impeding their targeting capabilities [167]. Similarly, surface modification of poly(lactic –co-glycolic acid) microspheres with PEG demonstrated a substantial reduction of adsorbed proteins, which may abrogate removal of microspheres by phagocytic cells [167]. One final example of PEG modification as a mechanism to alter surface properties involves adenoviral vectors [166]. Adenoviral vectors are extremely effective in delivering genetic constructs, but possess a tendency for robust immune responses ultimately leading to failure of the treatment [166]. PEGylation of adenoviral vectors reduced innate immune responses and vector uptake by macrophages without a decline in transduction efficiency [166]. Modulation of surface properties with PEG modification of liposomes, microspheres, and viral vectors diminishes immune responses and prolongs their duration in the circulation to maximize therapeutic benefit.

2.1.3.3 Cell and Tissue Modification

Polyethylene glycol modification of cells and tissues is also possible. Cell membranes contain a large number transmembrane (or integral membrane) and peripheral membrane proteins [168]. These proteins can be covalently linked to PEG in the same manner as a protein in solution.

PEG modification of cell and tissue surfaces can have a myriad of effects on the modified surfaces. Immunogenicity of transplanted cells and tissues could be abrogated by attachment of PEGs [169]. Another potential benefit of PEG modification on cells and tissues is a reduction in protein and cell adhesion to the modified surfaces that may inhibit restenosis following intravascular procedures.

Modification of transplanted cells and tissues could be valuable in a number of clinical circumstances, including blood transfusions, acute organ rejection, and diabetes. Patients with rare blood types or those that require repeated transfusions may suffer from immune rejection of the donor blood [170-172]. PEG modification of donor erythrocytes can create stealth-like properties by mitigating immune responses, prevention of monocyte phagocytosis, and promote tolerance [169-174].

In the case of acute organ rejection, the endothelium of the transplanted organ undergoes immediate attack by the host immune system [175]. Antibodies bind to the foreign endothelial cells leading to complement activation and rejection of the transplanted organ [175]. Rejection of the donor organ is prevented by systemic administration of immunosuppressive agents like cyclosporine [169]. However, lifelong immunosuppression leads to compromised immune function predisposing the individual to infection and certain forms of cancer [169]. PEG modification of endothelium of the transplanted organ might be able to mask the antigenic determinants and prevent organ rejection [175].

Insulin-dependent diabetes mellitus is caused by an autoimmune response that destroys the beta cells in the pancreas [176]. A possible treatment to alleviate this condition involves transplantation of islet cells back into diabetic patients [176]. However, the success of the therapy is dependent upon the ability to protect the transplanted cells from the host's immune

system [176]. A number of studies have demonstrated a protective effect of PEG modification of pancreatic islet capsules against immune rejection without any deleterious effects on the islets biochemical activity [169, 176-180].

As noted previously, restenosis represents a significant problem to the success of revascularization strategies such as balloon angioplasty, stenting, and endarterectomies [41, 66]. Upon endothelial denudation, the underlying lipid and collagen matrix is exposed presenting an extremely thrombogenic surface with many adhesive ligands [39, 66, 67]. Platelets deposition occurs immediately following vascular injury activating the cells and initiating thrombus formation with the release of numerous procoagulant factors [41, 66].

Prior studies in our lab demonstrated and ability to significantly reduce platelet deposition following PEG modification of protein adsorbed biomaterials [162-164]. Thus, the concept of PEGylation to prevent adverse cell and protein interactions was expanded to injured arteries. PEG modification of scrape-damaged human placental arteries resulted in decreased platelet deposition when perfused with blood [163, 181]. These results were validated in an animal model where balloon injured vessels were treated with a reactive PEG. [182]. A reduction in platelet deposition onto balloon injured arteries modified with PEG was observed following restoration of blood flow [182].

2.2 BIOTIN AND AVIDIN

2.2.1 Biotin

Biotin is a naturally occurring vitamin found in all cells [183]. Some other commonly used names for biotin are vitamin H or Bw and coenzyme R. The liver, kidney, and pancreas contain the largest quantities of biotin [183]. Biotin serves as a carbon dioxide (CO_2) carrier utilized in fat synthesis, amino acid metabolism, and glycogen formation [3, 17, 184]. The molecular formula of biotin is $C_{10}H_{16}N_2O_3S$ and its structure contains an imidazoline ring fused to a tetrahydrothiophene ring with a valerate side chain [3, 17, 183].

Biotin deficiency is rare due to the fact it synthesized by intestinal bacteria and contained in many foods such as legumes, vegetables, and meats [17, 184]. Symptoms of inadequate levels of biotin include fatigue, depression, dermatitis, nausea, and muscle pains [3, 184]. Biotin insufficiency in humans is primarily due to the consumption of large quantities of raw eggs, which contain the protein avidin [17].

2.2.2 Avidin

Avidin is a glycoprotein commonly found in egg whites as well as the tissues of birds, amphibians, and reptiles [183, 185, 186]. Its exact biological function is still uncertain, but it may serve as an antibiotic [185]. Avidin is a tetrameric protein composed of four identical subunits consisting of 128 amino acids [183, 186]. In addition, approximately 10% of the structure of avidin is composed of carbohydrates [186]. Heterogeneous oligosaccharide units are attached at identical locations on each subunit of the avidin protein [183].

Other variations of avidin exist possessing altered structures or formulations with similar functionality. Certain strains of Streptomyces were shown to possess avidin-like activity [185]. The isolated protein, with avidin-like properties, was also a tetrameric protein consisting of four identical subunits of 159 amino acids and was named streptavidin [183, 186]. 33% of the amino acid structure is conserved when comparing avidin and streptavidin [183]. The other commonly used form of avidin involves deglycosylation of native avidin [183, 186]. NeutrAvidin (Pierce Biotechnology, Inc., Rockford, IL) biotin-binding protein represents a customized avidin derivative where attached carbohydrates moieties have been eliminated and modification of surface charges result in a more neutral isoelectric point [186].

2.2.3 Interaction

The interaction between biotin and avidin forms an exceptionally robust noncovalent linkage between protein and ligand that resembles antigen and antibody binding [183, 185]. Bond formation between biotin and avidin transpires quickly [183]. Additionally, the biotin-avidin complex and bond is extremely stable, resisting harsh organic solvents and denaturing agents, withstanding extremes of both temperature and pH, and enzymatic proteolysis [183, 186]. The strength of the biotin-avidin interactions is further demonstrated by noting the exceptionally high binding constant, K_a, of 10^{15} M^{-1} [183, 186].

Each subunit of the avidin protein is capable of binding one molecule of biotin [183]. This tetravalent nature of avidin enables the binding of up to four molecules of biotin per avidin [183]. The amino acids tryptophan and lysine in the biotin binding site of avidin mediate bond formation [183]. Considerable hydrogen bonding, van der Waals interactions, and conformational changes facilitate the strong interaction between biotin and avidin making their

association virtually irreversible [186]. There are minor differences in MW, isoelectric points, binding constants, and nonspecific binding associated with various avidin derivatives as noted in Table 2-1.

Table 2–1 Properties of Different Avidin Derivatives [183, 186]

	Avidin	Streptavidin	NeutrAvidin
MW	67,000	53,000-60,000	60,000
Biotin-Binding Sites	4	4	4
Isoelectric Point	10-10.5	5-7.5	6.3
Binding Constant (K_a) for Biotin (M^{-1})	10^{15}	10^{13}-10^{15}	10^{15}
Nonspecific Binding	High	Low	Lowest

Neither streptavidin nor NeutrAvidin contain carbohydrate residues leading to their reduced MW as compared to avidin. The binding constants for avidin, streptavidin, and NeutrAvidin for biotin are nearly identical with some variation observed with streptavidin [186]. The isoelectric points vary greatly between the various avidin derivatives. Streptavidin and NeutrAvidin have lower isoelectric points, which can reduce non-specific interactions with other molecules [186]. The lack of carbohydrates and reduced isoelectric points make streptavidin and NeutrAvidin superior to avidin for many biotin binding applications. Of the three avidin derivatives, NeutrAvidin demonstrates the lowest nonspecific binding [186].

2.2.4 Applications

Biotin and avidin interactions have been employed in a wide variety of biochemical and targeting applications. The ability to bind four biotin molecules at the same time and the high affinity of the biotin-avidin interaction make it an ideal system for assays [186]. Avidin's tetravalent nature

enables it to amplify signals and permits cross-linking of different biotin-containing molecules [187]. Biotin and avidin binding resembles the strong interactions usually only found with antibody and antigen interactions [185].

A number of detection, purification, diagnostic, and targeted delivery systems employ biotin and avidin interactions [183, 187]. Some of the detection systems that utilize biotin and avidin are immunoassays, histochemistry, and blotting technologies [183, 187]. Biotin and avidin binding permits purification of proteins and cells using affinity chromatography and column separations [183, 187]. Diagnostic procedures, such as bioaffinity sensors, gene probes, cytological probes, and flow cytometry, regularly exploit the favorable binding characteristics of biotin and avidin [187] Numerous detection and targeted delivery systems, especially in the treatment of malignant neoplasms, are constructed based on biotin and avidin chemistry [188-200]. Biotin and avidin systems enjoy numerous advantages over other binding strategies [187]. A few of these distinctive features are their high affinity, retention of activity after linking to other molecules, tetravalent interaction, adaptability, and vast numbers of reagents containing biotin or avidin [187].

2.3 INTRAVASCULAR POLYETHYLENE GLYCOL (PEG) MODIFICATION

Intrvascular surfaces are usually lined with a confluent layer of endothelial cells that regulate vasomotor responses and vascular homeostasis [44]. However, after damaging vascular procedures, such as angioplasty, stenting, and endarterectomy, a thrombogenic, protein-rich matrix surface is uncovered with many adhesive ligands [39, 66, 67]. An effective intravascular modification technique necessitates applicability to both situations. Abundant quantities of

proteins are found on cell membrane and matrix surfaces [168]. The presence of proteins on cell membranes and in matrix permit covalent modification with reactive PEGs as discussed in Subsection 2.1.3.

PEG conjugation to proteins is frequently accomplished by activation with functional groups that react with primary amines [151]. Primary amines are present on the amino acid lysine or N-terminus of protein molecules [151]. The lysine content of many proteins can be in excess of 10% since it is one of the most prevalent amino acids comprising proteins [151]. Acylating PEGs, typically N-hydroxysuccinimidyl esters of carboxylated PEGs, normally react with several amines in a single protein molecule [151, 201]. The reactivity of PEG is easily controlled by the spacing distance between the active ester and the PEG units to influence aminolysis and hydrolysis rates [201].

Protein-reactive PEGs are available with a N-hydroxysuccinimide (NHS) ester that covalently links with accessible amine groups in proteins. This dissertation concentrates on covalently modifying vascular surfaces with N-hydroxysuccinimide-polyethylene glycol-biotin (NHS-PEG-biotin). The NHS active ester reacts with primary amines, the most prevalent being the epsilon amine of lysine [183]. NHS reactivity should permit modification of proteins found on cell membranes and in the extracellular matrix with PEG-biotin. NHS-PEG-biotin, in solution, approaches primary amines on cell membranes or exposed matrix (Figure 2-1, A) resulting in a nucleophilic attack and formation of a stable amide bond (Figure 2-1, B) [151, 202]. The protein-reactive PEG used for modification of vascular surfaces rapidly links with amine groups in under a minute requiring only a single application.

As mentioned previously, modification of biomaterial surfaces with a protein-reactive PEG has been shown to reduce thrombosis and platelet deposition [162-164]. Additionally, reactive

PEG modification of injured vascular surfaces has demonstrated an ability to inhibit thrombosis and platelet deposition on theses surfaces [163, 181, 182]. Protein-reactive PEG solutions can easily be administered to vascular tissue with specialized delivery catheters during or immediately following intravascular procedures for rapid modification of the surfaces.

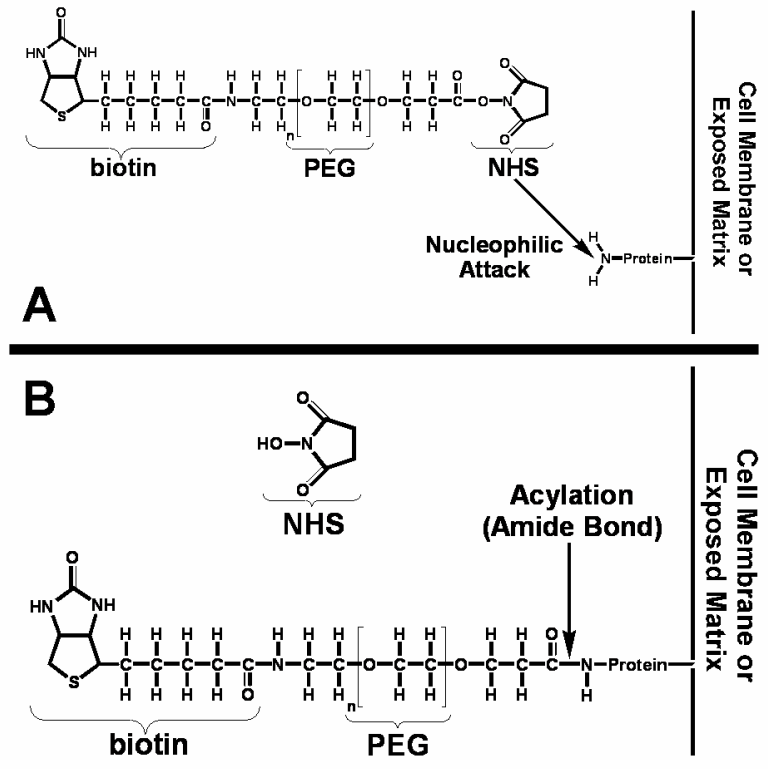

Figure 2–1 Covalent modification of cell membrane or matrix surfaces utilizing a protein-reactive polymer. (A) Chemical structure of protein-reactive polymer and surface amine. (B) Formation of covalent bond between the polymer and the vascular surface.

2.4 AVIDIN-BIOTIN TARGETED DELIVERY SYSTEM

Reactive polyethylene glycols can be used to covalently modify proteins on cell membranes and in the exposed extracellular matrix of denuded vascular tissue. Modification of the vascular

surfaces with the protein-reactive PEG should provide a molecular barrier to prevent platelet deposition following intravascular injury (Figure 2-2) as demonstrated previously [162-164, 181, 182]. Furthermore, a number of bi-functional PEGs have been synthesized with a reactive group on one terminus and a target molecule on the other that could enable site-specific delivery of pharmaceutics, carriers, vectors, and cells to the modified vascular segments.

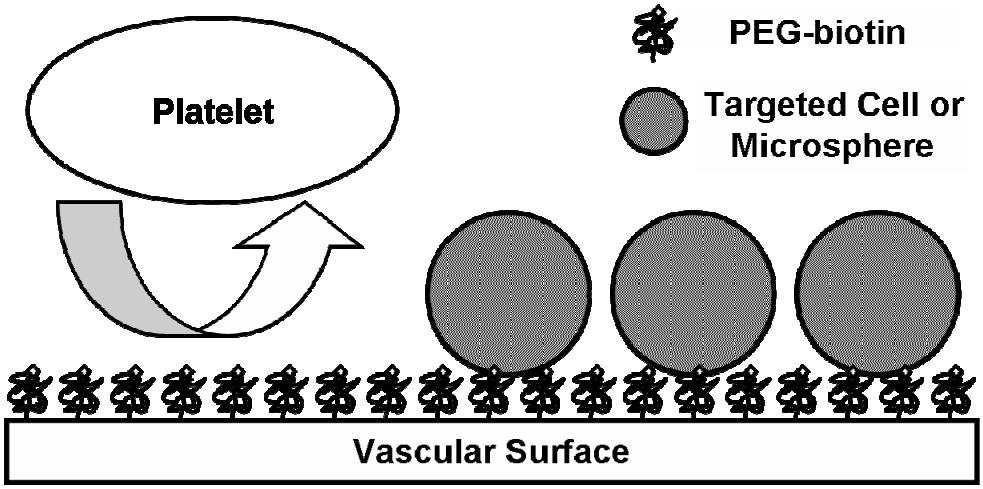

Figure 2–2 Schematic of the proposed targeted delivery system. The reactive polymer is covalently attached to the vascular surface forming a molecular barrier. Microspheres or cells are targeted to the modified surface.

Specifically, in the system under investigation in this dissertation, we chose biotin as the tag molecule on the reactive PEG. The addition of biotin to the terminus of the reactive PEG should provide a site for the targeted delivery of agents based on the high affinity between biotin and avidin interactions. In order to reduce the problem of non-specific binding, often associated with the use of avidin in biological applications, two common derivatives of avidin (NeutrAvidin and streptavidin) were investigated for this application. This dissertation focuses on the development of a technique to modify vascular tissue with a reactive N-hydroxysuccinimide polyethylene

glycol-biotin [NHS-PEG-biotin] molecule to allow for targeting of microspheres and cells to the labeled vascular tissue (Figure 2-2).

Microspheres serve as a model for evaluating the ability to target particulate drugs, liposomes, vesicles, or vectors. NeutrAvidin and streptavidin-coated microsphere should directly interact with PEG-biotin modified surfaces. In addition, the system ought to allow for targeting of biotin-coated microspheres to PEG-biotin modified vascular tissue using NeutrAvidin as a bridge. Similarly, the site-specific delivery of cells would occur via a two-step process. First, both the cells and the vascular surface are modified with NHS-PEG-biotin. NeutrAvidin should allow for linkage of the two PEG-biotin modified surfaces based on its tetravalent nature.

2.5 SPECIFIC AIMS

The purpose of this dissertation is to investigate the hypothesis that a protein-reactive polymer can be utilized as a target for the site-specific delivery of microspheres and cells. NHS-PEG-biotin covalently modifies proteins on cell and matrix surfaces. Biotin provides the target for delivery of agents because of its strong affinity for avidin and its derivatives. Neutravidin-coated microspheres should specifically adhere to PEG-biotin modified vascular surfaces. In addition, it should be possible to target PEG-biotin modified cells to vascualr surfaces labeled with PEG-biotin using NeutrAvidin as a bridge. Such a technique might ultimately be utilized for cell therapy, drug delivery, or gene therapy to specific vascular regions following catheter-based or surgical procedure.

2.5.1 PEG Modification of Cell Surfaces

As discussed earlier, polyethylene glycol modification has been applied for a vast number of applications. The first goal of this project is to confirm that protein-reactive NHS-PEG-biotin is capable of modifying cultured human coronary artery endothelial cell surfaces (HCAEC), a model vascular surface. In addition, quantitative flow cytometry will be employed to try and determine the actual number of PEG covalently linked to the endothelial cell surfaces. Modification of cell surfaces with varying solution concentrations and incubation periods for the reactive PEG will be quantified. Additionally, two other common agents to modify proteins with biotin, termed biotinylation, will be evaluated and compared to PEG-biotin modification. The persistence of the covalently bound PEG molecules on the cell membranes will also be explored. Chapter 3 tackles the question of the feasibility, extent, and persistence of PEG modification on endothelial cell surfaces.

2.5.2 Targeted Delivery to PEG-Modified Cell Surfaces

Chapter 4 takes a first look at the feasibility of the targeting system. Once the modification of endothelial cells is confirmed, the ability of the modification to direct the site-specific delivery of microspheres and cells to treated vascular surfaces will be explored. Cultured HCAECs are grown on coverslips for use in a parallel plate chamber. Fluid dynamic relations allow for calculation of the shear rates based upon the volumetric flow rate of the perfused fluid. The cells on the coverslip will be treated with a reactive polymer solution or a control solution consisting of the vehicle alone using defined incubation periods that are relevant to clinical applications. After modification, microspheres and cells will be perfused over the surface and epi-fluorescence microscopy will confirm adherence. NeutrAvidin-coated microspheres should bind to PEG-

biotin modified cell surfaces in a one step process. PEG-biotin modified cells in suspension ought to bind to PEG-biotin modified cell surfaces using NeutrAvidin as a bridge in a two step process.

2.5.3 Targeted Delivery to PEG-Modified Vascular Surfaces

Cultured cells are unable to reproduce the complex multilayer structure of actual blood vessels. In addition, it is difficult to reproduce the endothelial denudation and injury and exposed extracellular matrix in a simple endothelial cell culture. Injured blood vessels test the ability of the proposed modification and targeting system following intravascular procedures such as angioplasty, anastomoses, and endarterectomy. The endothelium of bovine carotid arteries could be denuded by scraping the lumen with a weighing spatula to mimic the damage evident after intravascular procedures. Vascular segments can then be loaded into a tubular perfusion chamber and treated with the reactive PEG solution or the vehicle for predetermined incubation periods that are appropriate for clinical applications. After modification, microspheres and cells will be perfused over the surface and epi-fluorescence microscopy will confirm attachment. NeutrAvidin-coated microspheres should adhere to PEG-biotin modified cell surfaces in a one step process. A two step process ought to permit the site-specific delivery of PEG-biotin modified cells in suspension to PEG-biotin modified injured vessels using NeutrAvidin as a bridge. Chapter 5 aims at investigation the feasibility of modifying injured vascular surfaces for the targeted delivery of microspheres and cells.

2.5.4 *In Vivo* Modification of Blood Vessels with PEG

In vitro studies provide initial insight in evaluation of the intravascular modification and targeting system. However, a more vigorous *in vivo* animal model is required to determine if the system is applicable as a treatment modality following procedures such as balloon angioplasty and endarterectomy. A rabbit femoral artery balloon injury model should provide a suitable trial to determine the feasibility of modifying injured vascular tissue in a more clinically relevant setting. Rabbit femoral arteries can be isolated and balloon injured with an embolectomy catheter. Following injury, a drug delivery catheter or small diameter tube will allow injection of a reactive PEG solution to modify the injured surface forming a molecular barrier. The duration of the PEG modification will be evaluated to determine the window for blocking undesirable adhesion and delivering targeted microspheres. Additionally, a five week study will assess the effectiveness of the PEG molecular barrier in preventing restenosis following balloon injury. Chapter 6 examines the ability to modify balloon injured vascular surfaces, different delivery techniques, the persistence of the PEG, and its ability to inhibit restenosis in a rabbit femoral artery balloon injury model.

2.5.5 *In Vivo* Targeting to PEG-Modified Vessels

Chapter 7 concentrates on verifying the ability of the targeted delivery system under investigation to deliver microspheres and cells to modified healthy and injured vascular tissue. PEG modification of healthy or balloon injured rabbit femoral arteries should be possible utilizing specialized delivery catheters or a small diameter tube. After modification of the vascular tissue, targeted microspheres or cells can be administered intravenously to the animal. It is postulated that the targeted microspheres and cells will specifically bind to the modified

vascular segments. NeutrAvidin-coated microspheres should adhere to PEG-biotin modified healthy and balloon injured vascular tissue in a one step process. However, the delivery of PEG-biotin modified rabbit endothelial progenitor cells will require a second incubation of the PEG-biotin treated vascular segments with NeutrAvidin, which will link the two biotinylated surfaces.

3.0 PEG MODIFICATION OF CELL SURFACES

3.1 INTRODUCTION

Previous work completed in our lab demonstrated that modification of injured vascular surfaces with a protein-reactive PEG inhibited platelet deposition [163, 181, 182]. This dissertation employs a similar protein-reactive PEG for the modification of vascular surfaces. Cultured human coronary artery endothelial cells in tissue culture well plates will be utilized as the model vascular surface. NHS-PEG-biotin is the protein-reactive polymer under investigation. The HCAECs will be incubated with various concentrations of NHS-PEG-biotin in solution and incubation periods to establish if the polymer is capable of covalently modifying endothelial cell surfaces. Modification of the cells will be confirmed using a fluorescein conjugated NeutrAvidin and analyzing the cell samples on a flow cytometry. Furthermore, reference fluorescence standards will enable computation of the number of PEG-biotin molecules linked to the cell surface using quantitative flow cytometry. Covalent modification of the HCAECs will be charted for different NHS-PEG-biotin concentrations and incubation times and compared.

PEG-biotin modification of HCAECs will also be compared to sulfo-NHS-biotin and sulfo-NHS-LC-LC-biotin, two other common biotinylation reagents. The sulfo-NHS-biotin molecule has no spacer between the reactive group and biotin. In contrast, the sulfo-NHS-LC-LC-biotin has two PEG monomers between the reactive ester and biotin. Sulfo-NHS-LC-LC-biotin

represents an extremely short PEG chain spacer. Comparing the three biotinylation reagents should provide some insight into the effect of MW on the modification of vascular surfaces. In addition, the time interval that the covalently linked PEG-biotin molecules remain on the cell surface will be established. Over time, it is believed that natural cellular process should degrade the polymer resulting in its elimination from the cell membrane.

3.2 METHODS

3.2.1 Cell Culture

Frozen ampules of human coronary artery endothelial cells (HCAECs) (Cambrex, Walkersville, MD) were thawed and placed into BD Falcon 75 cm^2 tissue culture flasks (Fisher Scientific, Pittsburgh, PA). Endothelial cells were grown in EGM-2 BulletKit media composed of EBM-2 basal medium and SingleQuots with 5% FBS (Cambrex, Walkersville, MD). Cell cultures were grown in a Thermo Forma (Thermo Electron Corporation, Waltham, MA) water jacketed CO_2 incubator maintained at 37°C with 5% CO_2 in a humidified environment. Standard aseptic cell culture techniques were utilized [203]. Upon reaching 70-90% confluence, the HCAECs were subcultured into 12 well tissue culture plates (Fisher Scientific, Pittsburgh, PA) using ReagentPack containing Hank's Balanced Salt Solution (HBSS), trypsin/EDTA (T/E), and trypsin neutralizing solution (TNS) (Cambrex, Walkersville, MD). The EC subculture procedure was completed as instructed in Clonetics Endothelial Cell Systems – Instructions for Use (Cambrex, Walkersville, MD). HCAECs in the 12 well plates were grown until confluence and then used in the PEG modification experiments.

3.2.2 PEG Surface Modification of Endothelial Cells

A pre-weighed sample of NHS-PEG-biotin (Nektar Therapeutics, San Carlos, CA) was removed from storage in the -80ºC freezer and warmed to room temperature. Previous studies completed in the lab used higher concentrations of the reactive polymer to modify surfaces [162-164, 181, 182, 203], but this was not applicable to modification of the endothelial cell surfaces employed here (APPENDIX B). Phosphate buffered saline (PBS) (Cambrex, Walkersville, MD) was added to the sample of NHS-PEG-biotin to yield a 10 mM stock solution. Aliquots of the stock solution were diluted with PBS to make 5, 2.5, 1.25, and 0.625 mM solutions of the reactive polymer. Media on the endothelial cells in 6 wells of a 12 well plate were removed and replaced with 0.5 mL of a 0, 0.625, 1.25, 2.5, 5, or 10 mM solution of the NHS-PEG-biotin. The reactive polymer was then allowed to incubate on the cell surface for 1 or 5 min. After the desired incubation time, the solution was removed and the cells were washed three times with Dulbecco's Modified Eagle's Medium (DMEM) (Cambrex, Walkersville, MD). This procedure was repeated for the other biotinylation reagents, Sulfo-NHS-biotin (Pierce Biotechnology, Inc., Rockford, IL) and Sulfo-NHS-LC-LC-biotin (Pierce Biotechnology, Inc., Rockford, IL).

3.2.3 Persistence of PEG Modification on Endothelial Cells

Similarly, a sample of NHS-PEG-biotin was removed from the -80ºC freezer and allowed to warm to room temperature. Once thawed, PBS was added to the sample to make a 10 mM stock solution. Media on endothelial cells in 11 of 12 wells of a 12 well plate were removed and replaced with 0.5 mL of the 10 mM NHS-PEG-biotin solution. The reactive polymer was allowed to incubate on the cells for 1 min. After the 1 min incubation time, the solution was removed and the cells washed three times with DMEM. Samples were collected at time points

of 0.5, 2, 4, 6, 9, 12, 24, 48, 72, 96, and 120 hrs with a control for comparison to background. Additionally, a separate 12 well plate was treated with PBS alone to provide control samples for all of the extended time points.

3.2.4 Flow Cytometry Analysis of PEG Surface Modification

Modified cells were removed from the plate with ReagentPack as described in Subsection 3.2.1 and individual samples collected in correspondingly labeled 16 x 75 mm round bottom polystyrene tubes (Fisher Scientific, Pittsburgh, PA). The tubes were then centrifuged at 220g for 5 min in a Sorvall Legend RT (Kendro, Asheville, NC) centrifuge and the supernatants removed. A 15 µL aliquot of a 5 mg/mL solution of fluorescein conjugated NeutrAvidin (Pierce Biotechnology, Inc., Rockford, IL) was removed form the -20ºC freezer and allowed to thaw. Once thawed, the fluorescein conjugated NeutrAvidin solution was diluted 1:40 with PBS and 100 µL of the diluted solution added to each tube. Cell pellets were then resuspended in the tube by vortexing and allowed to incubate for 30 min at 4ºC in the dark. After 30 min, the tubes were centrifuged at 220g for 5 min once again and the supernatants removed. Cell pellets were then fixed and resuspended with 500 µL of a 1% paraformaldehyde solution (Sigma, St. Louis, MO). Cells samples were analyzed on a BD FACScan (San Jose, CA) flow cytometer and the fluorescence intensity data collected.

3.2.5 Standardization of Fluorescence Intensity

Quantum Fluorescein Isothiocyanate (FITC) MESF High Level standard beads (Bangs Laboratories, Inc., Fishers, IN) were added to 500 µL of a 1% paraformaldehyde solution in another 16 x 75 mm round bottom polystyrene tube. Analysis of the standard beads on a BD

FACScan enabled standardization of the values for the molecules of equivalent soluble fluorophore (MESF) unit to known quantities [204-208]. The MESF values obtained from the standard beads permitted construction of a standardized fluorescence calibration plot [205]. Using the calibration plot, the MESF values for the cell samples could be related to the known fluorescein quantities on the standard beads. Conjugation of molecules to fluorophores alters their fluorescence intensity. Thus, 0.5, 1, and 2 μM solutions of fluorescein and fluorescein conjugated to NeutrAvidin were prepared for analysis. The fluorescence intensity of the two compounds was quantified on a LS-50B Luminescence Photometer (PerkinElmer Optoelectronics, Fremont, CA). Both the fluorescein and the fluorescein conjugated NeutrAvidin were excited at 488 nm and the emission intensity collected at 530 nm, which correlates with the excitation and emission spectra of the FL 1 channel on the BD FACScan flow cytometer. Relating the two fluorescence intensities permitted calculation of the effective fluorophore to protein (F/P) ratio. Using the Effective F/P ratio, the fluorescence intensity of the cell samples from the flow cytometer could be correlated with an actual number of fluorescein conjugated NeutrAvidin molecules. The number of fluorescein conjugated NeutrAvidin molecules could be used to approximate the number of PEG-biotin molecules on the cell surface.

3.3 RESULTS

3.3.1 Construction of Standardized Fluorescence Calibration Plots

Fluorescein and fluorescein conjugated to NeutrAvidin solutions of 0.5, 1, and 2 μM were excited at 488 nm and the emission data gathered at 530 nm to duplicate the excitation and

emission spectra of the FL 1 channel on the BD FACScan flow cytometer. Identical excitation and emission parameters were used to permit direct comparison of the fluorescence intensities in solution to the MESF values from the flow cytometer. The fluorescence intensities of the various solution concentrations are shown in Table 3-1.

Table 3–1 Calculation of the Effective F/P Ratio for Fluorescein and Fluorescein Conjugated NeutrAvidin

	Fluorescence			
Solution Concentration (µM)	**Fluorescein**	**Fluorescein Conjugated NeutrAvidin**	**Effective F/P Ratio**	
0.5	148.77	29.92	0.20	
1.0	286.30	58.06	0.20	
2.0	540.44	100.59	0.19	
			0.20	**Average**

Conjugation of fluorescein to NeutrAvidin results in a substantial decrease in fluorescence intensity at identical concentrations. The Effective F/P ratio is calculated by dividing the fluorescence intensity of the fluorescein conjugated to NeutrAvidin by the fluorescein fluorophore itself, which is then used in the calculation of the number of PEG-biotin molecules. This procedure was repeated whenever a new lot of fluorescein conjugated NeutrAvidin was used in the protocol to ensure accuracy.

Quantum FITC MESF high level beads were analyzed on the BD FACScan flow cytometer using the same settings and at the same time as when the HCAECs were examined to permit direct comparison. Five distinct bead populations of differing fluorescence intensity were evident (Figure 3-1). Markers were placed around each of the five distinct bead populations and the median fluorescence intensity of each individual standard determined. A certificate of analysis accompanies every set of Quantum FITC MESF high level beads with the actual MESF

value for each bead. Table 3-2 illustrates the histogram channels and actual MESF values for each bead.

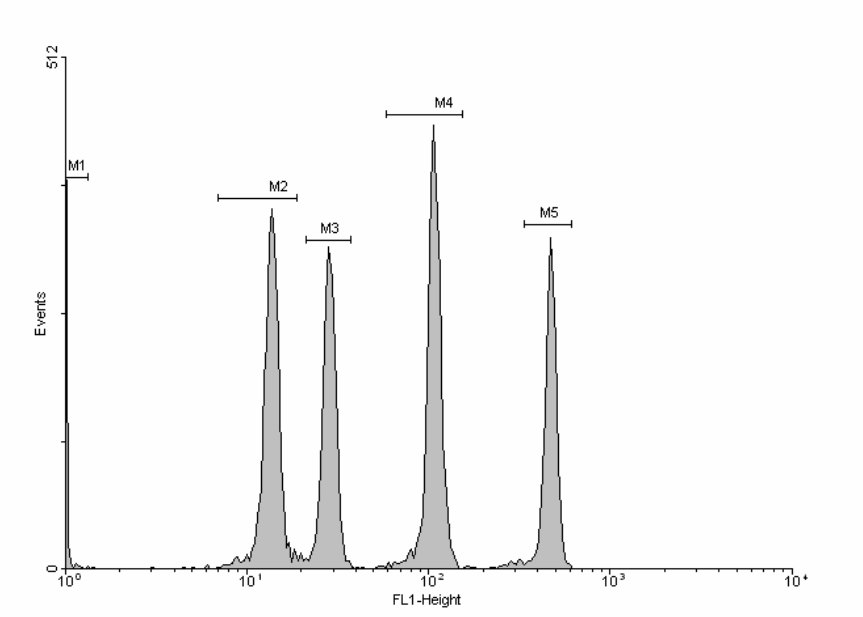

Figure 3–1 Fluorescence intensity histogram of Quantum FITC MESF high level standard beads.

Table 3–2 Histogram Channel and MESF Data for Quantum FITC MESF High Level Standard Beads

Standard Bead	Actual MESF	Histogram Channel
Blank	0	1
1	23,411	13.34
2	52,837	28.39
3	210,425	107.46
4	912,535	469.76

Using the median histogram channel information and the actual MESF values (Table 3-2); a calibration curve is generated using linear regression (Figure 3-2). Linear regression is a statistical analysis that utilizes the relationship between two variables to predict the value of one from the other [209-211]. In this case, the MESF values for the samples can be calculated from the histogram channel data obtained from the flow cytometer. The calibration curve is depicted

as a straight line (Figure 3-2) fitted to the data obtained from the flow cytometer and the actual MESF values of the Quantum FITC MESF High Level standard beads. In addition, the measured MESF values form the standard beads are displayed in Figure 3-2 as squares.

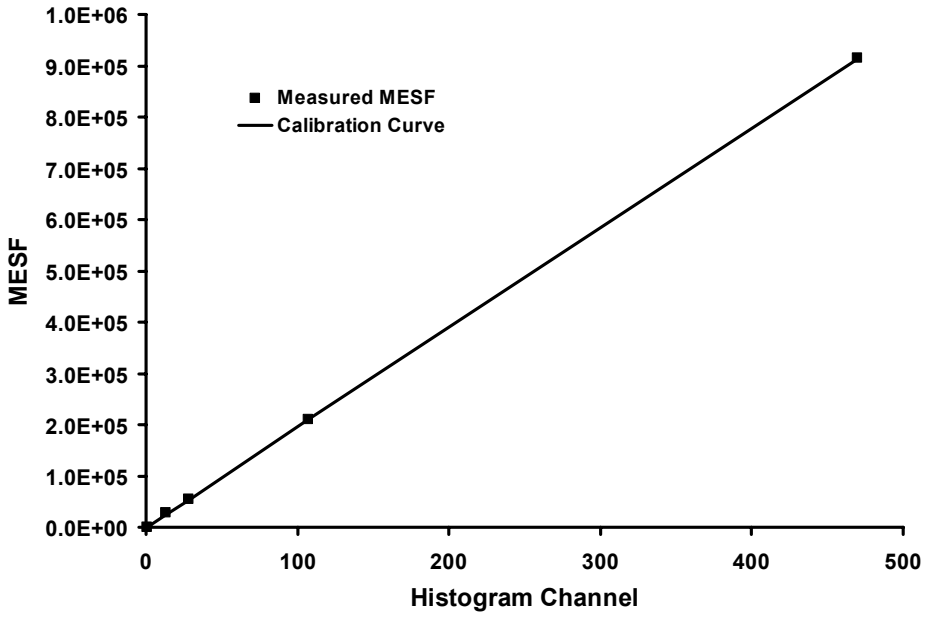

Figure 3–2 Plot of the calibration curve and measured MESF values.

By fitting a straight line to the data the Actual MESF can be calculated from the Histogram Channel as shown in Equation 3-1 with a coefficient of determination (R^2) of 1.00.

Equation 3-1 MESF Calculation

$$\text{Sample MESF} = (1947 \times \text{Histogram Channel}) - (1578)$$

There is excellent agreement between the actual and measured MESF values as demonstrated by the R^2 of 1.00 for the fitted linear regression and graphically in Figure 3-2.

HCAECs were analyzed on the BD FACScan in a similar manner as the standard beads. PEG-biotin modification was tracked using fluorescein conjugated NeutrAvidin. The histogram

channel information and the calibration curve enabled calculation of MESF values for the modified cells. All cells possess some level of auto-fluorescence [212]. Most cellular auto-fluorescence can be attributed to nicotinamide adenine dinucleotide (NADH), riboflavins, and flavin coenzymes [212]. To account for auto-fluorescence of the cells, the calculated MESF for control, un-modified ECs was subtracted from the values for ECs modified with NHS-PEG-biotin. Multiplying the calculated MESF value by the Effective F/P ratio converted the MESF value into the number of molecules of fluorescein conjugated NeutrAvidin. Equation 3-2 demonstrates how to calculate the number of PEG-biotin molecules per cell using the calculated sample MESF values generated from Equation 3-1 and the Effective F/P ratio.

Equation 3-2 PEG-biotin Quantification

$$\#\text{ of PEG - biotin Molecules/Cell} = \left(\frac{\text{Sample MESF - Control MESF}}{\text{Effective F/P Ratio}} \right)$$

This provided an estimate of the number of PEG-biotin molecules present on the cells surface. However, this may have resulted in underestimating the actual number of PEG-biotin molecules because NeutrAvidin is tetravalent for biotin. Consequently, one fluorescein conjugated NeutrAvidin molecule could potentially interact with more than one PEG-biotin molecule.

3.3.2 Determination of PEG Modification on Endothelial Cells

The number of PEG-biotin molecules per cell was calculated using Equations 3-1 and 3-2 as described in Subsection 3.3.1. These results are shown as a function of solution concentration and incubation time in Figure 3-3. Over 110 million molecules of PEG-biotin per cell were observed with a 10 mM solution and 5 min incubation time. Even at 1 min, it was possible to bind approximately 80 million molecules of PEG-biotin per cell. Furthermore, we demonstrated that if the N-hydroxysuccinimide reactive group is removed by hydrolysis, then no modification

of the endothelial cells was observed. This was verified by the two inactive NHS-PEG-biotin curves. In summary, it was shown that the number of PEG-biotin molecules covalently linked per cell increases with increasing solution concentration and increasing incubation time (Figure 3-3).

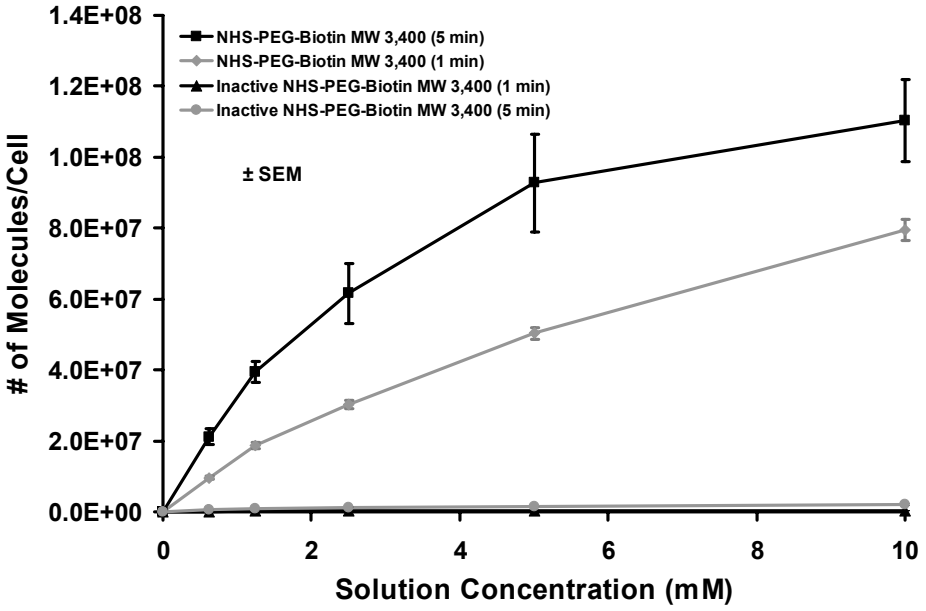

Figure 3–3 The number of molecules of PEG-biotin per EC as a function of solution concentration and incubation time. Data is shown ± SEM with a sample size (n) = 6-9 for all solution concentrations and times.

It is important to compare the modification of cell surfaces with other commonly employed biotinylation reagents. For most applications, shorter length biotinylation reagents are used for labeling of a surface or protein for subsequent detection with an avidin derivative. NHS-PEG-biotin has the added advantage of inhibiting platelet deposition on modified surfaces [162-164, 181, 182]. However, the kinetics and degree of PEG-biotin modification could be markedly different than those encountered with other biotinylation reagents, such as sulfo-NHS-biotin and sulfo-NHS-LC-LC-biotin. As mentioned previously, the sulfo-NHS-biotin and sulfo-NHS-LC-

LC-biotin are similar to NHS-PEG-biotin with either no PEG monomers or only two monomers, respectively. As a result, they should provide some insight into the role MW plays on modification of vascular surfaces. As before, quantitative flow cytometry enabled calculation of the number of biotin molecules per cell and the results are presented in Figure 3-4.

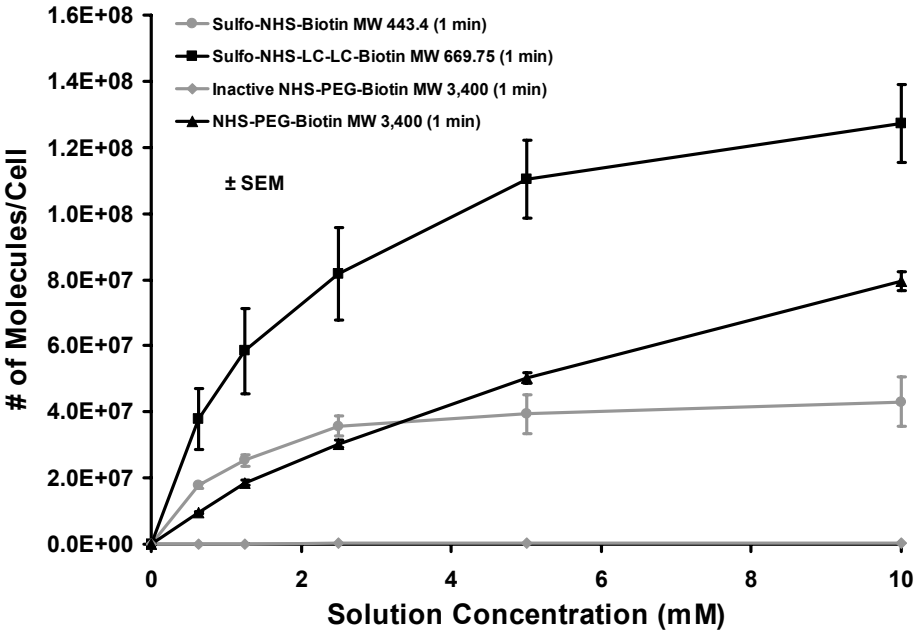

Figure 3–4 The number of molecules of NHS-X-biotin per EC as a function of solution concentration with a 1 min incubation. Data is shown ± SEM with n = 6-9 for all solution concentrations and treatments.

In this instance, only the 1 min incubation period was investigated. Trying to keep modification times as brief as possible, especially under 1 min, makes the process more applicable to time-sensitive intravascular procedures. After a 1 min incubation, sulfo-NHS-LC-LC-biotin showed significantly increased biotinylation (Figure 3-4) of the cell surfaces at all concentrations as compared to NHS-PEG-biotin with 160% more molecules per cell when using a 10 mM solution. Contrastingly, sulfo-NHS-biotin was initially more effective at biotinylating the cell surface than NHS-PEG-biotin, but trailed at higher reactive solution concentrations. At 10 mM, the number

of molecules per cell for sulfo-NHS-biotin was almost half that seen with NHS-PEG-biotin modification (Figure 3-4). Similarly to NHS-PEG-biotin, the modification of cell surfaces with the other biotinylation reagents increased with increasing solution concentrations (Figure 3-4). As the modifying solution concentrations approach 10 mM a plateau effect begins to appear, which may indicate a saturation of surface protein modification.

3.3.3 Persistence of PEG Modification on Endothelial Cells

The duration of the PEG-biotin modification on the cell surface was established by quantifying the number of PEG-biotin molecules at various time points post-modification. This was accomplished by comparing the fluorescence intensity of the cell samples to the standard beads, as described previously. The number of PEG-biotin molecules per cell for up to 120 hrs post-modification was charted in Figure 3-5.

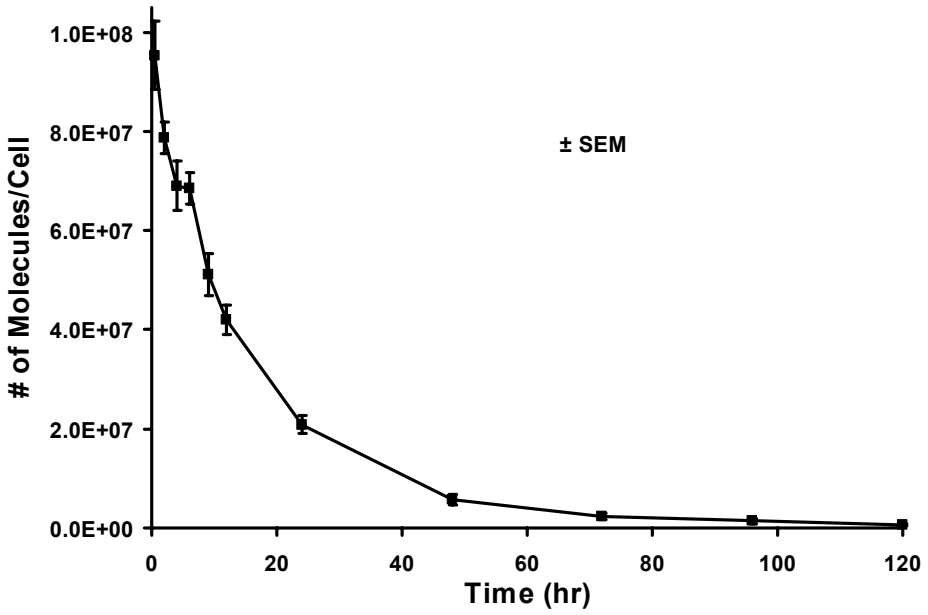

Figure 3–5 Persistence of PEG-biotin modification following a 1 min incubation with a 10 mM solution of the reactive PEG over a period of 120 hrs. Data is shown ± SEM with n = 6 for all times.

It was determined that the number of PEG-biotin molecules decreases sharply over the first 24 hrs post-modification followed by a gradual decrease in the number of remaining molecules for the duration of the 120 hrs (Figure 3-5). Over half the initial number of PEG-biotin molecules per cell was lost in the first 12 hrs following modification (Figure 3-5). Thus, the data illustrated a rapid decrease in the number of PEG-biotin molecules in the first 24 hrs followed by a gradual decrease out to 120 hrs. Less than 1% of the initial PEG-biotin modification remains on the cell surface at 120 hrs post-modification. Further analysis of the PEG-biotin modification data revealed that a transformation could be used to establish a relation between the number of PEG-biotin molecules per cell and the time post-modification [209, 211]. Transformation of the number of molecules per cell was accomplished by taking the natural logarithm (ln) of the values. A plot of the ln of the number of PEG-biotin molecules per cell versus time yielded a linear fit (Figure 3-6).

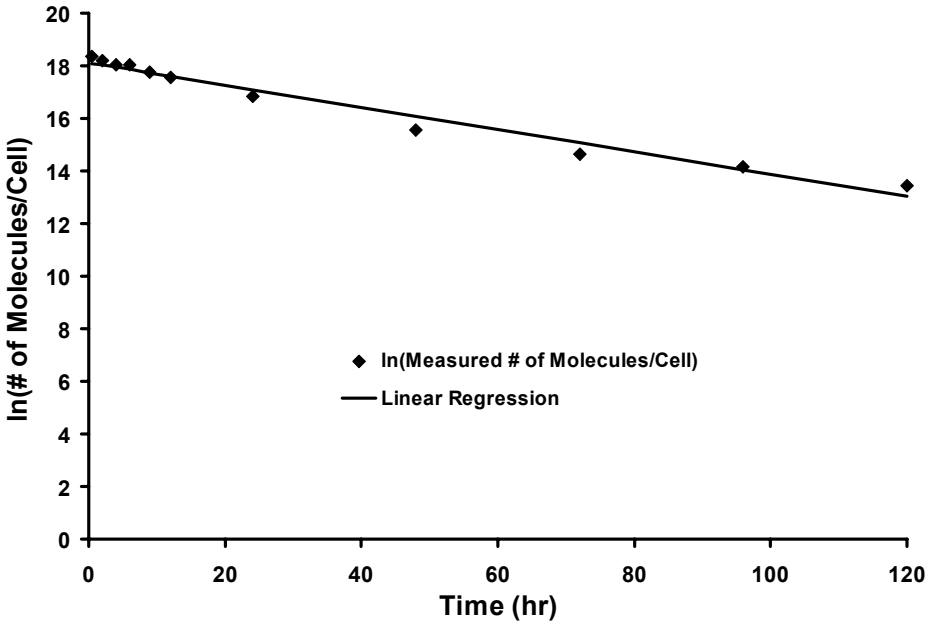

Figure 3–6 Persistence of PEG-biotin modification after a natural logarithmic transformation following a 1 min incubation with a 10 mM solution of the reactive PEG over a period of 120 hrs. Data is shown ± SEM with n = 6 for all times.

As a result, the number of PEG-biotin molecules as a function of time (t) can be approximated by an exponential function as shown in Equation 3-3.

Equation 3-3 PEG-biotin Persistence

$$\#\text{ of PEG - biotin Molecules/Cell} = (7.4\times10^{7})\times\left(e^{-0.04t}\right)$$

Using Equation 3-3, the exponential function can be plotted along with the actual values for the number of PEG-biotin molecules per cell as a function of time (Figure 3-7). The number of PEG-biotin molecules per cell exponentially decays over time (Equation 3-3 & Figure 3-7). Equation 3-3 provides an estimate of the PEG-biotin modification as a function of time, but there is some divergence of the calculated and actual number, especially at early time points post-modification (Figure 3-7).

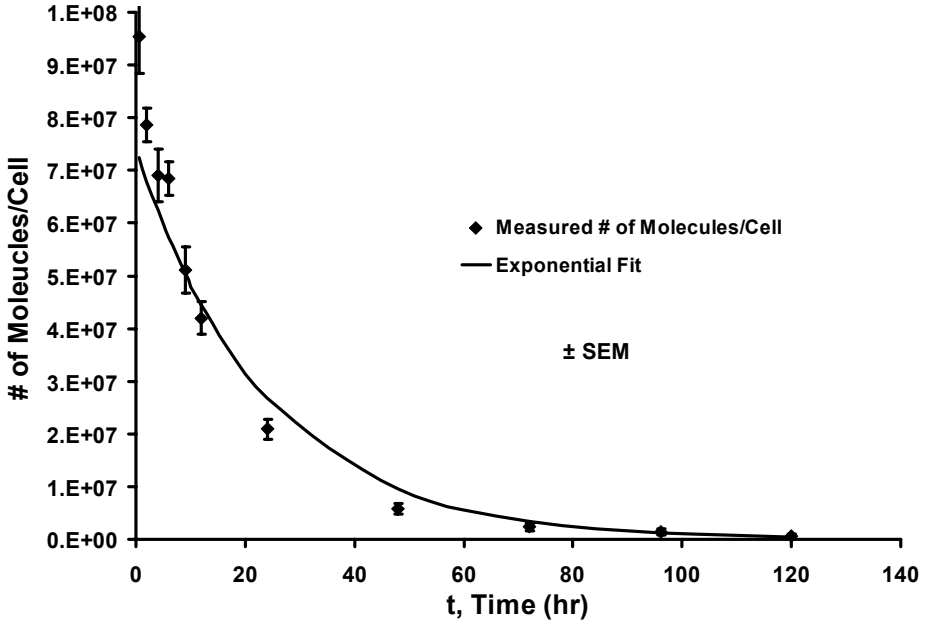

Figure 3–7 Exponential fit of the PEG-biotin modification along with the actual measured number of molecules per cell following a 1 min incubation with a 10 mM solution of the reactive PEG over a period of 120 hrs. Data is shown ± SEM with n = 6 for all times.

3.4 DISCUSSION

The results presented in this chapter confirm that a protein-reactive PEG is capable of modifying a model vascular surface, cultured endothelial cells. In addition, quantitative flow cytometry provided a means to evaluate the extent of modification on endothelial cell surfaces. As expected, modification with the reactive PEG-biotin increased with increasing solution concentrations of the reactive polymer and longer incubation periods. However, the modification occurs quickly and significant attachment is possible in less than 1 min. These results are paralleled for the sulfo-NHS-biotin and sulfo-NHS-LC-LC-biotin, but the overall modification varies depending upon the specific reagent used. Sulfo-NHS-LC-LC-biotin was the most effective biotinylation reagent at modifying the HCAECs. With solution concentrations of 2.5 mM or less sulfo-NHS-biotin was the second most effective biotinylation agent. Contrastingly, when the reactive solutions were at 5mM or greater, NHS-PEG-biotin was more effective than sulfo-NHS-biotin. Regardless, modification with sulfo-NHS-biotin and NHS-PEG-biotin trailed sulfo-NHS-LC-LC biotin at all solution concentrations.

These results are likely due to the different molecular sizes of the various biotinylation reagents and the properties of PEG itself. Based solely on the molecular size of the molecules the sulfo-NHS-biotin is smaller so more molecules should be able to attach to a surface of defined size. However, the results did not support this notion. One possible explanation for this relates to the large size of NeutrAvidin and the lack of a flexible spacer. In the case of sulfo-NHS-biotin, the biotin is covalently linked directly to the surface, which may result in steric hindrance preventing the larger NeutrAvidin molecule from interacting with the biotin. Additionally, as more and more biotins are attached to the surface they may obstruct neighboring biotins from interacting with the fluorescein conjugated NeutrAvidin molecules. The NHS-PEG-

biotin molecule provides a long spacer between the covalent linkage and the biotin; however, the large excluded volume, chain flexibility, and rapid motion of PEG [153, 213] may actually diminish NeutrAvidin attachment. A more rigorous evaluation of the probable PEG-biotin conformations covalently linked to the cell surfaces appears in APPENDIX C. Of the reagents evaluated, sulfo-NHS-LC-LC-biotin seems to provide an ideal overall size and spacer length to permit biotinylation and interaction with NeutrAvidin. Even though sulfo-NHS-LC-LC-biotin is more effective at biotinylating cell membranes than NHS-PEG-biotin, no studies have evaluated if it possesses the same ability to inhibit undesirable protein and cell adhesion on modified surfaces as has been demonstrated with MW 3,400 PEGs. Many experimental studies indicate that short PEG oligomers do not resist protein and cell adhesion as effectively as long chain PEGs [214]. As a result, NHS-PEG-biotin was employed as the intravascular modification agent in the targeted delivery system in the hopes of retaining the molecular barrier effect of the polymer layer.

The Quantum FITC MESF high level standard beads and calculation of the Effective F/P ratio for fluorescein conjugated to NeutrAvidin permitted estimation of the number of covalently linked molecules on endothelial cells. However, this provides a basis for quantifying the modification and the ability to compare different factors even though the absolute values are uncertain. One such factor is the tetravalent nature of NeutrAvidin. NeutrAvidin can bind up to four molecules of biotin simultaneously. Consequently, determining that one molecule of fluorescein conjugated NeutrAvidin is present does not exclude the possibility that it is interacting with 2 or more biotins. Computation of the number of PEG-biotin molecules per cell assumed only a single PEG-biotin interacted with one NeutrAvidin molecule, but this may not be

the case. Consequently, the results presented here may be an underestimation of the actual modification of the cell surfaces.

The standard beads themselves contribute to another possible problem. Quantum standard beads were designed for determination of the quantities of cell surface markers. Contrastingly, the modification process evaluated here has the potential of indiscriminately modifying every protein on the cell surface. Most of the MESF values for the modified cells rest outside of the region covered by the standards so the calibration curve had to be extrapolated to values greater than those found on any bead. This might not be a significant issue as the relation of MESF to histogram channel appeared to remain linear over the entire region. Even with these limitations, the calculation of the number of covalently attached molecules per cell provides an approximation of the extent of modification. Furthermore, it provides a basis to discern how alterations in MW, solution concentration, incubation time, and reactive group can influence the degree of modification.

Another possible error in the quantitative determination of the number of PEG-biotin molecules per cell stems from a propagation of error analysis. The computed number of PEG-biotin molecules per cell is calculated from measured quantities that have their own associated error. As a result, the error in the measured quantities carries over into the computed number of PEG-biotin molecules. Calculation of the propagation of error in computed quantities as a function of the error in the measured quantities is illustrated in APPENDIX D. In the case of calculating the number of PEG-biotin molecules per cell, the propagation of error analysis is presented in APPENDIX E. Based on the errors in the measured quantities, calculated MESF and Effective F/P ratio, the expected total error in the calculation of the number of PEG-biotin molecules per cell is 9%.

The data presented in this chapter also verified that the polymer modification persists for a period of days on the endothelial cell surface. PEG-biotin molecules were present on the cell surface out to 120 hrs following modification, but at that point, less than 1% of the initial number remained. Over 50% of the initial PEG-biotin attachment is lost within the first 12 hrs. This accelerated removal of PEG-biotin molecules from the surface continued for the first 24 hrs post-modification. After this point, the loss of PEG-biotin molecules form the surface occurred at a slower rate. An exponential function could be fitted to the data points to provide the number of PEG-biotin molecules per cell as a function of time post-modification.

Generally, PEG is considered a non-biodegradable polymer since the polymer chain resists most mechanisms of hydrolytic cleavage [158]. However, there is new evidence of alternative biological and chemical processes that can result in the breakdown of PEG chains [158]. Alternative factors, such as cytochrome P450 dependent enzymes, alcohol dehydrogenases, and aldehyde dehydrogenases, have been implicated in oxidation of PEG chains [158, 215]. The hydrolytic and enzymatic oxidation of PEG occurs at a low frequency [158], which does not explain the rapid loss of PEG modification from endothelial surfaces. Consequently, additional mechanisms must exist that are capable of rapidly degrading and removing PEG from cell membranes. Unfortunately, these supplementary processes for PEG processing, degradation, and removal from cell surfaces have not been identified to date. Additional research into the cellular pathways and molecules that are capable of degrading PEG is crucial to gain a better understanding of PEG modification of cell surfaces and its persistence over time.

We have demonstrated that it is possible to modify vascular cell surfaces with a protein-reactive NHS-PEG-biotin. Furthermore, the modification can be controlled by varying the solution concentration and the incubation time of the NHS-PEG-biotin. This is the first step in

evaluating the intravascular modification and targeted delivery system under investigation in this dissertation. Quantitative flow cytometry confirmed that NHS-PEG-biotin is capable of modifying endothelial vascular surfaces. In addition, modification of the cells occurs rapidly with reaction conditions that are within physiologic norms for temperature and pH. The extent of PEG-biotin modification can be controlled by using different solution concentrations and incubation times. In addition, varying the MW of the PEG chain could also have profound effects on the extent of modification as well as the properties of the surface and its interactions. Modification of cell membranes with PEG-biotin should provide a target for the site-specific delivery of targeted microspheres and cells, which will be addressed in the following chapter.

4.0 TARGETED DELIVERY TO PEG-MODIFIED CELL SURFACES

4.1 INTRODUCTION

Flow cytometry confirmed the ability to modify endothelial cells with a protein-reactive PEG. This PEG modified surface could serve as a target for the site-specific delivery of therapeutics if a target molecule could be incorporated at the free terminus of the polymer. Biotin was chosen as the target molecule because of its strong interaction with avidin [183, 186]. For the proposed targeting system, NeutrAvidin and streptavidin will be employed as opposed to avidin to reduce the problem of nonspecific binding, which would limit the ability to specifically target agents. A perfusion system utilizing a parallel plate will be employed to determine if targeted microspheres and cells will bind to PEG-biotin modified endothelial cell surfaces. Cultured HCAECs are grown on coverslips for use in the parallel plate chamber. Fluid dynamic relations allow for calculation of the shear rates based upon the volumetric flow rate in order to reproduce relevant physiologic conditions. The cells on the coverslip will be treated with NHS-PEG-biotin or PBS as a control for a 1 min incubation, which is relevant in clinical applications. After modification, NeutrAvidin-coated microspheres suspended in solution will be perfused over the cell surface to determine if they are targeted to PEG-biotin modified surfaces. NeutrAvidin-coated microspheres should bind to PEG-biotin modified cell surfaces in a one step process. Targeting of PEG-biotin modified cells will require a second incubation of the PEG-biotin modified

surface with NeutrAvidin first. PEG-biotin modified cells in suspension ought to bind to PEG-biotin modified cell surfaces using NeutrAvidin as a bridge in a two step process. This should validate the PEG- biotin modification and biotin/avidin targeted delivery system.

4.2 METHODS

4.2.1 Cell Culture

HCAECs were cultured with the same techniques as described in Subsection 3.2.1. However, for these experiments the cells were subcultured on 24 x 50 mm Gold Seal cover glasses in Fisherbrand 100 x 15 mm I-Plate compartmentalized petri dishes (Fisher Scientific, Pittsburgh, PA) and in BD Falcon 75 cm^2 tissue culture flasks.

4.2.2 Microsphere Targeting in a Parallel Plate Perfusion Chamber

The HCAECs cultured on 24 x 50 mm Gold Seal cover glasses in Fisherbrand 100 x 15 mm I-Plate compartmentalized petri dishes were labeled with a 5 μM CellTracker Orange CMTMR (Molecular Probes, Eugene, OR) solution in EGM-2 media for 45 min in the incubator. After the incubation, the CellTracker Orange CMTMR solution was replaced with fresh EGM-2 media. Bovine Serum Albumin (BSA) (Sigma, St. Louis, MO) at a concentration of 4.5 g/dL was added to DMEM and warmed to 37°C for the perfusion media. The coverslip was loaded into a rectangular, parallel plate perfusion chamber (Figure 4-1) to allow for targeting of microspheres under physiologic flow conditions [216-220]. A silicon gasket and vacuum system were

employed to secure the coverslip in the chamber creating an air-tight seal. The chamber dimensions are 2.95 cm long by 0.9 cm wide by 200 μm high [216-220].

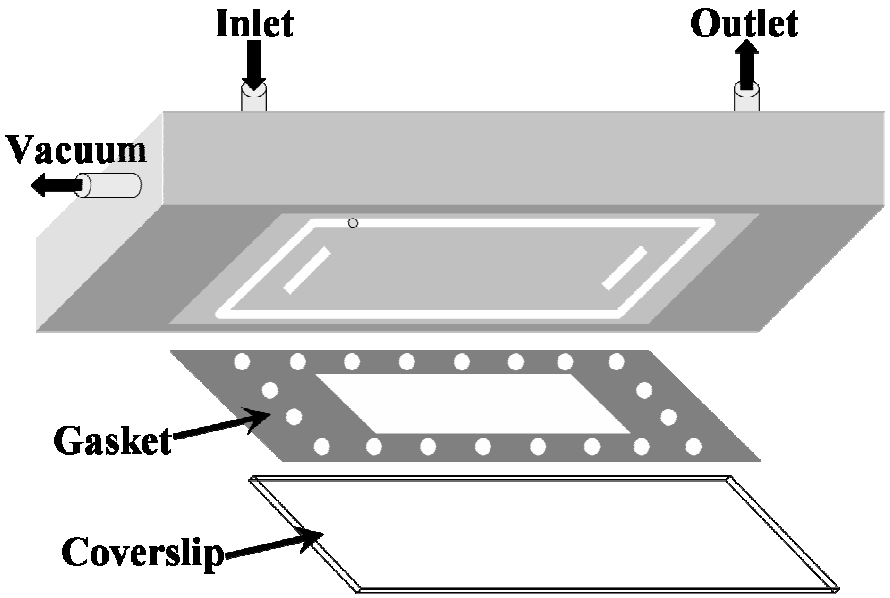

Figure 4–1 Schematic diagram of the parallel plate perfusion chamber.

Perfusion media could be drawn through the chamber at precisely controlled physiologic shear rates using a Harvard PHD 22/200 Infuse/Withdraw Syringe Pump (Harvard Apparatus, Holliston, MA). A detailed derivation of the velocity profile, shear rate, shear stress, volumetric flow rate, and Reynolds number equations for the parallel plate perfusion chamber appears in APPENDIX F. The shear rate, $\dot{\gamma}$, on the endothelial surface of the coverslip can be calculated from the volumetric flow rate, Q, chamber width, w, and chamber height, h, as shown in Equation 4-1.

Equation 4-1 Shear Rate for Parallel Plate Perfusion Chamber

$$\dot{\gamma} = \left(\frac{6Q}{wh^2} \right)$$

A shear rate of 100 or 1,000 s^{-1} was used for the microsphere targeting experiments.

Once the coverslip was loaded into the perfusion chamber, the system was primed with perfusion media using the syringe pump. Next, a 1.5 mL solution of 10 mM NHS-PEG-biotin or the vehicle (PBS) control was injected into the chamber through a stopcock and incubated for 1 min. After the incubation, the coverslip is perfused with perfusion media for 10 min. For the low shear rate experiments (100 s^{-1}), a 4 μL aliquot of Fluospheres NeutrAvidin labeled microspheres, yellow-green fluorescent (Molecular Probes, Eugene, OR) was mixed with 200 μL of BlockAid Blocking Solution (Molecular Probes, Eugene, OR) and sonicated for 5 min to reduce non-specific binding. Contrastingly, the high shear (1,000 s^{-1}) experiments did not require incubation of the NeutrAvidin labeled microspheres with BlockAid Blocking Solution. As in the previous case, a 4 μL aliquot of Fluospheres NeutrAvidin labeled microspheres (yellow-green fluorescent) was collected and diluted to 10 mL with perfusate media. A 7.28 x 10^6 part/mL suspension of microspheres is drawn through the chamber at the specified shear rate for 10 min followed immediately by another 10 min flush with the perfusion media alone. Finally, the number of bound microspheres is counted using epi-fluorescence microscopy.

4.2.3 Cell Targeting in a Parallel Plate Perfusion Chamber

The HCAECs cultured on 24 x 50 mm Gold Seal cover glasses in Fisherbrand 100 x 15 mm I-Plate compartmentalized petri dishes were labeled with a 50 μM CellTracker Blue CMAC (Molecular Probes, Eugene, OR) solution in EGM-2 media for 45 min in the incubator. HCAECs grown in a BD Falcon 75 cm^2 tissue culture flask were also labeled with a 5 μM CellTracker Orange CMTMR solution in EGM-2 media for 45 min in the incubator. After the incubation, the CellTracker Blue CMAC and CellTracker Orange CMTMR solutions were

replaced with fresh EGM-2 media. Cells grown in the BD Falcon 75 cm^2 flask were removed from the flask using ReagentPack with trypsin and collected in a BD Falcon BlueMax Jr. 15 mL Graduated tube (Fisher Scientific, Pittsburgh, PA). The tube was then centrifuged at 220g for 5 min in a Sorvall Legend RT and the supernatant removed. The cell pellet was dispersed and modified with 1 mL of a 10 mM NHS-PEG-biotin solution for 1 min. After modification, 9 mL of PBS was added to the cell suspension and the tube vortexed. Again, the cell suspension was centrifuged at 220g for 5 min and the supernatant removed. Next, the cells were resuspended in 10 mL of perfusate media and kept at 37°C in a Fisher Isotemp Economy water bath (Fisher Scientific, Pittsburgh, PA).

The same perfusate media and perfusion system (Figure 4-1) was employed for these experiments. A shear rate of 100 s^{-1} was used for the cell targeting experiments as calculated utilizing Equation 4-1. Once the coverslip was loaded into the perfusion chamber, the system was primed with media using the syringe pump. Next, a 1.5 mL solution of 10 mM NHS-PEG-biotin or the vehicle (PBS) control was injected into the chamber through a stopcock and incubated for 1 min. After the incubation, the coverslip is perfused with media for 10 min. Now, a 2 mg/mL solution of NeutrAvidin Biotin-Binding Protein (Pierce Biotechnology, Inc., Rockford, IL) or the vehicle (PBS) control was injected into the chamber through a stopcock for a 1 min incubation. After the incubation, the coverslip is perfused with media for 10 min. The PEG-biotin modified cell suspension is then drawn through the chamber at the specified shear rate for 10 min followed immediately by another 10 min wash with the media alone. This ensures that the cells in suspension adhere to the endothelial surface under shear and not from stagnation or settling resulting from a stoppage in flow. Finally, the number of adherent cells is counted using epi-fluorescence microscopy.

4.2.4 Epi-Fluorescence Microscopy of Samples

The number of adherent microspheres or cells was tracked using a Zeiss Axiovert 35 Epi-Fluorescence Microscope (Carl Zeiss, Inc., Thornwood, NY) with a MicroMAX 5 MHz CCD Camera (Princeton Instruments, Trenton, NJ), Mac G4 computer (Apple, Cupertino, CA), and IP Lab software (Scanalytics, Inc., Billerica, MA) for digital image processing. The yellow-green fluorescent Fluospheres NeutrAvidin labeled microspheres had excitation/emission spectra of 505 nm and 515 nm, respectively. CellTracker Orange CMTMR had maximum absorption at 541 nm and emission at 565 nm. CellTracker Blue CMAC had absorption/emission spectra of 353 nm and 466 nm, respectively. The IP Lab software was used to quantify the number of adherent microspheres or cells to PEG-biotin modified and control surfaces. A Stage Micrometer (Fisher Scientific, Pittsburgh, PA) was used to determine the width and height of the micrograph field. All measurements were made using a Zeiss LD Plan Neofluar 20x objective (Carl Zeiss, Inc., Thornwood, NY). The micrograph field measures 0.68 mm wide by 0.54 mm high for a total area of 0.36 mm^2. The number of adhered microspheres per mm^2 of vascular surface, #Micro/mm^2, can be computed by dividing the microsphere count from an individual micrograph, $Micro_{Count}$, by the micrograph area, $Area_{Field}$ as illustrated in Equation 4-2.

Equation 4-2 Microsphere Calculation

$$\#Micro/mm^2 = \left(\frac{Micro_{Count}}{Area_{Field}} \right)$$

Similarly, the number of attached cells per mm^2 of vascular surface, Cells/mm^2, can be computed by dividing the cell count from an individual micrograph, $Cell_{Count}$, by the micrograph area, $Area_{Field}$ as illustrated in Equation 4-3.

Equation 4-3 Cell Calculation

$$Cells / mm^2 = \left(\frac{Cell_{Count}}{Area_{Field}} \right)$$

4.2.5 Statistical Analysis

The Analysis Toolpak of Microsoft Excel and SPSS 12.0 were used for statistical analyses to look for differences in data points. The number of microspheres and cells binding to vascular surfaces per mm^2 was calculated as mean + standard error of the mean (SEM). The control and treated groups were compared using an unpaired, two-sample Student's *t*-test assuming unequal variances using the two-tailed distribution and the p values calculated to determine significant variations.

4.3 RESULTS

4.3.1 Targeted Delivery of Microspheres to Cultured Cells on Coverslips

Two-color epi-fluorescence microscopy was used to visualize the HCAECs on the coverslip and the adherent NeutrAvidin-coated microspheres. Representative micrographs of microspheres adhering to PEG-biotin modified and control treated coverslips are shown in Figure 4-2. The cells were labeled with CellTracker Orange CMTMR which appeared red (Figure 4-2). Microspheres were yellow-green fluorescent and looked green (Figure 4-2) on the epi-fluorescent microscope. The number of microspheres bound to control treated coverslips (Figure 4-2, A) was significantly less than the number bound to NHS-PEG-biotin treated coverslips (Figure 4-2, B). The total number of BlockAid treated NeutrAvidin-coated microspheres at 100

s^{-1} that adhered to NHS-PEG-biotin treated coverslips was 115 ± 9 per mm^2 as compared to only 10 ± 2 per mm^2 for control coverslips (Figure 4-3).

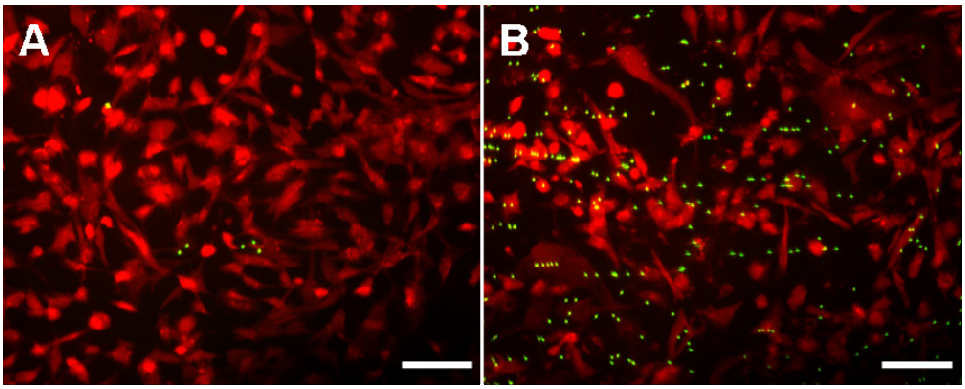

Figure 4–2 Targeted microspheres (green) adhering to control (A) and PEG-biotin modified (B) cultured cells (red) in a parallel plate chamber. The scale bar is 100 µm.

These results were found to be significant with $p < 0.0001$. The difference in binding to PEG-biotin modified cell surfaces was even more pronounced with NeutrAvidin-coated microspheres at 1,000 s^{-1} (Figure 4-4). BlockAid was not required for experiments at 1,000 s^{-1} as there was minimal non-specific binding. In this case, a total of 212 ± 32 per mm^2 adhered to PEG-biotin modified cell surfaces while only 8 ± 2 per mm^2 attached to control coverslips (Figure 4-4).

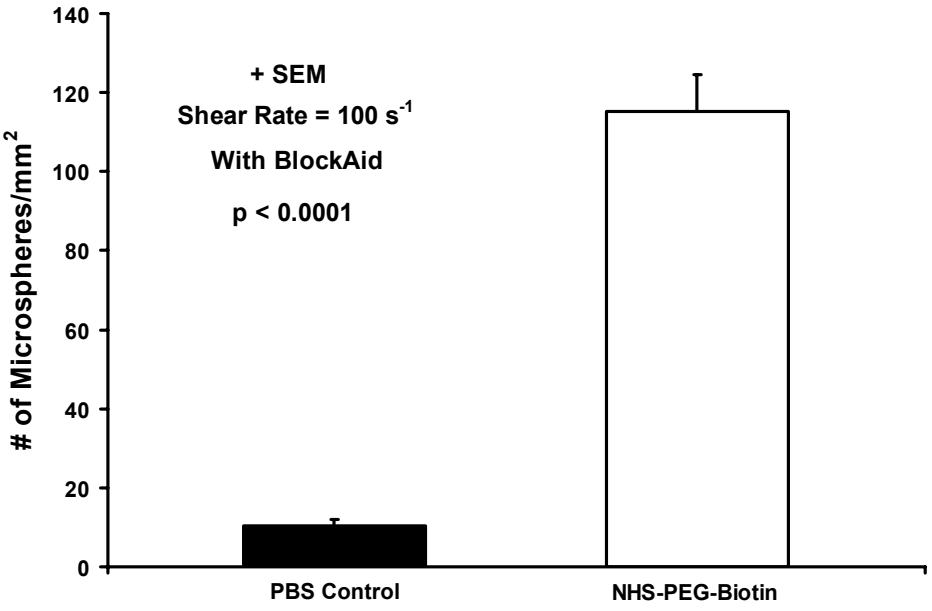

Figure 4–3 Number of adherent NeutrAvidin-coated microspheres treated with BlockAid solution on control and PEG-biotin treated coverslips at 100 s^{-1}. Data is shown +SEM with n = 6 and the results are significant with p < 0.0001.

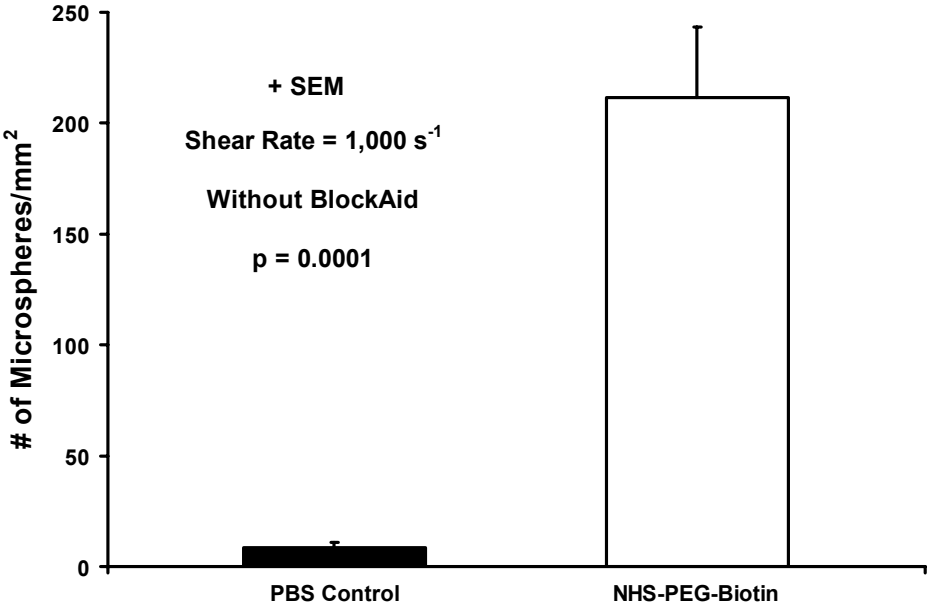

Figure 4–4 Number of adherent NeutrAvidin-coated microspheres on control and PEG-biotin treated coverslips at 1,000 s^{-1}. Data is shown +SEM with n = 9 and the results are significant with p = 0.0001.

4.3.2 Targeted Delivery of Perfused Cells to Cultured Cells on Coverslips

Again, two-color epi-fluorescence microscopy was used to visualize the HCAECs on the coverslip and the cells bound to the treated and control coverslips. The cultured cells on the coverslip were labeled with CellTracker Blue CMAC which appeared blue (Figure 4-5). Targeted cells that adhered to the coverslips from flow were labeled with CellTracker Orange CMTMR and appeared red (Figure 4-5).

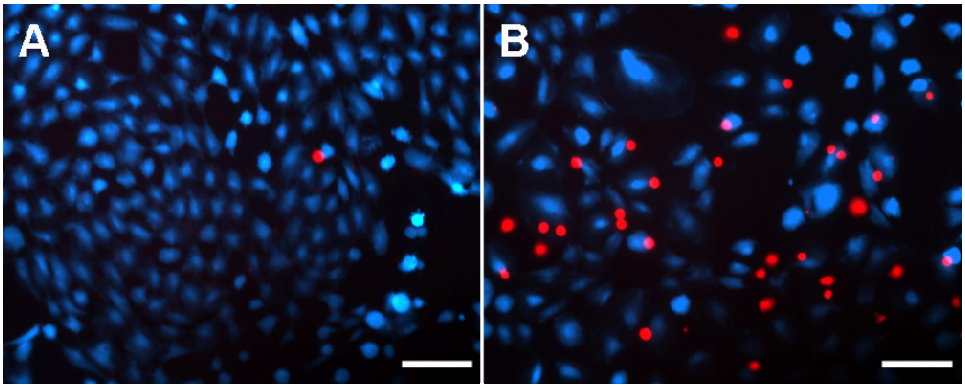

Figure 4–5 Targeted cells (red) adhering to control (A) and PEG-biotin modified (B) cultured cells (blue) in a parallel plate chamber. The scale bar is 100 µm.

The number of targeted cells bound to control treated coverslips (Figure 4-5, A) was significantly less than the number bound to NHS-PEG-biotin treated coverslips (Figure 4-5, B). The total number of cells that adhered to NHS-PEG-biotin treated coverslips was 20 ± 5 per mm^2 as compared to only 1 ± 0.3 per mm^2 for control coverslips (Figure 4-6). These results were found to be significant with $p < 0.005$.

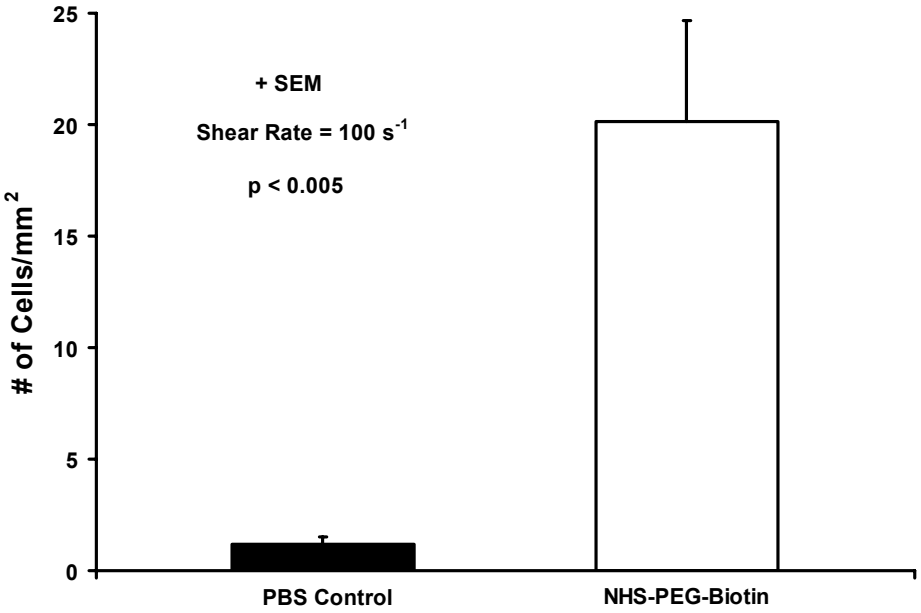

Figure 4–6 Number of adherent PEG-biotin modified cells on control and PEG-biotin treated coverslips following application of NeutrAvidin at 100 s^{-1}. Data is shown +SEM with n = 9–10 and the results are significant with p < 0.005.

4.4 DISCUSSION

These results provide the first validation of the ability of the intravascular modification and biotin and avidin targeting system. NeutrAvidin-coated microspheres were preferentially targeted to PEG-biotin modified cell surfaces as demonstrated by the binding data. Additionally, the data confirmed that NeutrAvidin-coated microspheres could be targeted to modified cell surfaces even at high shear rates of 1,000 s^{-1} data. A shear rate of 1,000 s^{-1} is more than double the shear rates commonly experienced in human coronary arteries. For example, the mean shear rate for humans is 460 s^{-1} and 440 s^{-1} for the left main and right coronary arteries, respectively [221]. Consequently, the microspheres should be able to target to labeled areas of coronary vasculature since the physiologic shear rate is less than half of that evaluated in the parallel plate

perfusion chamber. Furthermore, this demonstrates the robust nature of the biotin and avidin targeting system and its possible application in high flow blood vessels.

At the low shear rates there was a problem of non-specific adherence of the NeutrAvidin-coated microspheres to control as well as the treated surfaces. Consequently, a BlockAid solution from Molecular Probes was employed to inhibit the non-specific adherence. The BlockAid solution consisted of proteins that would adsorb to the polystyrene microsphere to try and limit nonspecific interactions with cell surface molecules. Increasing the shear rate to 1,000 s^{-1} also resulted in a reduction of nonspecific binding. Designed microspheres, liposomes, or vectors would have lower non-specific binding than the polystyrene microspheres employed in this study. The polystyrene microspheres were selected as a model particulate carrier that was easy to track with epi-fluorescence microscopy.

At first glance, the overall ability to deliver microspheres to the PEG-biotin modified cell surface appears mediocre at best. Based on the number of PEG-biotin molecules per cell from the quantitative flow cytometry, one would expect that more of the microspheres would adhere to the sizeable number of target molecules on the cell surface. In similar targeting systems, the results shown here fall in line with other targeted delivery systems. Strategies utilizing microspheres targeted to E- and P-selectin demonstrated significantly worse delivery of only an average of 30 microspheres/mm^2 [78, 222, 223]. NeutrAvidin-coated microsphere adherence to PEG-biotin modified cell surfaces was superior with 4–7 fold higher binding observed. Another targeting strategy focused on targeting ultrasound contrast microbubbles to endothelial receptors upregulated during inflammation [216, 217, 219, 220]. This approach demonstrated adherence of up to 10 microbubbles per cell [216, 217, 219, 220]. When the number of NeutrAvidin-coated microspheres per mm^2 is converted to per cell the microsphere binding is approximately 2 per

cell. It is important to note, however, that the some of the microbubble targeting protocols used particle solutions that were up to 100 times more concentrated [216, 217, 219, 220]. In addition, some of the binding experiments were stagnant incubations and not deposited under flow.

The effectiveness of the intravascular modification and targeting system investigated in this dissertation might be increased by using more concentrated microsphere solutions, repeated injections of microspheres, or re-circulation of microspheres. All of these parameters could be evaluated and modified based on what therapeutic agent is delivered and what quantity is necessary to produce a beneficial effect. Even so, the ability to deliver microspheres to modified cell surfaces serves as a model for the targeted administration of particulate drugs, liposomes, or viral vectors for the treatment of various vascular maladies.

The ability of targeting PEG-biotin modified cells in suspension to PEG-biotin modified cell surfaces with NeutrAvidin as a bridge demonstrates the flexibility of the targeting system. Agents can be targeted using a one or two step process and any number of entities could be delivered. Based on the average area occupied by HCAECs in culture, the adhered ECs should occupy approximately 11% of the surface once they firmly adhere and spread. Additional studies would be required to determine if this coverage could produce a therapeutic effect.

Endothelial cell delivery is not as efficient as microsphere targeting. Only about 20 endothelial cells could be delivered per mm^2 of modified vascular tissue whereas 115 to 212 microspheres could be delivered to the same surface. This can most likely be attributed to the large disparity in the size of the microspheres and cells. The microspheres have a well-defined, consistent diameter of 1 μm while the cells can vary between 15-25 μm. This 15 to 25-fold increase in diameter of the particle leads to an increase in the force exerted by the fluid motion on the particle which would tend to pull the particle over the surface and prevent firm adhesion.

A propagation of error analysis provides an estimate of the uncertainty in the calculation of the number of microspheres or cells per mm^2 of the cell surface. The number of microspheres or cells per area is computed from measured quantities that have their own associated error. As a result, the error in the measured quantities carries over into the computed number of microspheres or cells per mm^2 of the cell surface. The procedure for determining the error propagation in the computed quantities based on the error in the measured quantities is illustrated in APPENDIX D. In the case of calculating the number of microspheres or cells per cell surface area, the detailed propagation of error analysis is presented in APPENDIX G. For the parallel plate perfusion chamber, the uncertainty in the calculated number of microspheres and cells per mm^2 cell surface is approximately 3%.

Overall, these results provide a good initial test of the combination of the modification and targeting system under development. However, cultured endothelial cells only represent one model of a vascular surface where the targeting system may be employed. In relation to applicability to intravascular injury treatments, the modification and targeting system must also be able to function on exposed extracellular matrix following endothelial denudation. A more complex system must be utilized to model exposed matrix surfaces following vascular injury and endothelial denudation. The only construct that can replicate the complex multilayer structure of blood vessels are explanted arteries. These along with a more appropriate perfusion apparatus will permit a more thorough evaluation of the intravascular modification and targeting system.

5.0 TARGETED DELIVERY TO PEG-MODIFIED VASCULAR SURFACES

5.1 INTRODUCTION

Explanted vessels provide a more suitable model surface to investigate the efficacy of modifying the surface with a reactive PEG-biotin for the purpose of targeting microspheres and cells to the modified vascular tissue. The endothelial injury and denudation encountered following intravascular procedures, such as balloon angioplasty and endarterectomy, can be approximated by scraping the lumen of explanted vessels [163, 181]. After injury, the vessels were inserted into a tubular perfusion chamber to assess the ability of modifying the injured vascular surface with a reactive PEG-biotin and the subsequent targeting of microspheres and cells to the labeled surface under physiologic conditions. As was described with delivery to PEG-modified cell surfaces, the scrape-damaged bovine carotid arteries will be treated with NHS-PEG-biotin or PBS as a control for a 1 min incubation, which is relevant in clinical applications. After modification, NeutrAvidin-coated microspheres suspended in solution will be perfused over the cell surface to determine if they are targeted to PEG-biotin modified surfaces. NeutrAvidin-coated microspheres should bind to PEG-biotin modified cell surfaces in a one step process. Targeting of PEG-biotin modified cells will require a second incubation of the PEG-biotin modified surface with NeutrAvidin first. PEG-biotin modified cells in suspension ought to bind to PEG-biotin modified cell surfaces using NeutrAvidin as a bridge in a two step process. This

should validate the PEG- biotin modification and biotin/avidin targeted delivery system on a more representative vascular surface. In addition, the explanted vessels allow for reproduction of the exposed extracellular matrix surface following vascular injury and applicability of the modification and targeting system in the treatment of restenosis, which is of great significance in the treatment of ischemic heart disease.

5.2 METHODS

5.2.1 Vessel Preparation and Injury

A carotid artery was obtained from a previously euthanized bovine and placed in PBS. Excess fat and tissue was removed from the artery and then the artery was filleted along its length exposing the lumen of the vessel. Next, the artery was damaged by scraping the lumen with a weighing spatula (Sigma, St. Louis, MO) three times. Once the vessel was damaged, segments measuring 3.0 cm were cut for use in a tubular perfusion chamber [224]. The upper face of the tubular perfusion chamber had a 0.2 cm in diameter cylindrical hole machined along its length and window measuring 0.2 cm wide by 2.5 cm long inserted into the hole to allow for introduction of test surfaces (Figure 5-1) [163, 181, 182, 224]. The lower surface of the tubular perfusion chamber was a plate with a pedestal used to press and secure the sample into the window with clamps (Figure 5-1) [163, 181, 182, 224]. It is assumed that the flow chamber is cylindrical; however, this is only an approximation as the vessel surface exposed through the window in the upper chamber is in all likelihood flat [163]. The radius of the tubular chamber is 0.1 cm and the exposed vessel length is 2.5 cm [163, 181, 182, 224].

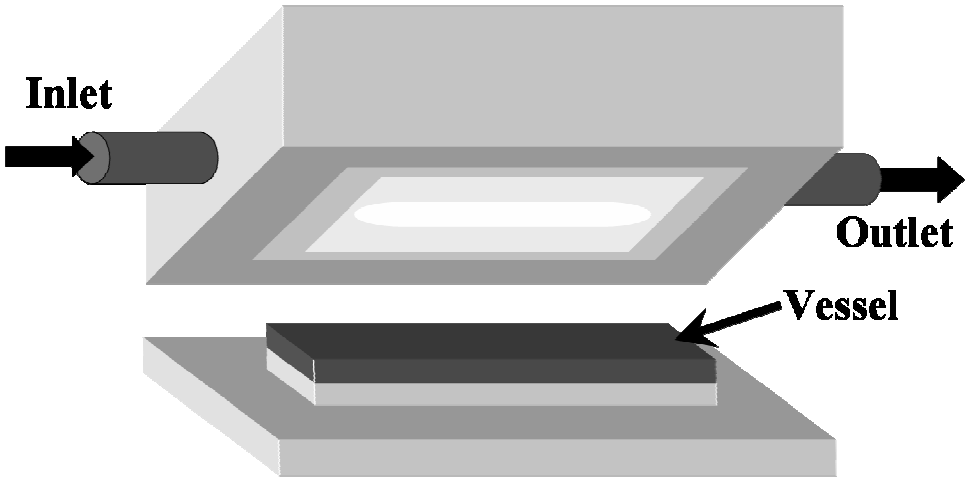

Figure 5–1 Schematic diagram of the tubular perfusion chamber.

Media could be drawn through the chamber at precisely controlled physiologic shear rates using a Harvard PHD 22/200 Infuse/Withdraw Syringe Pump (Harvard Apparatus, Holliston, MA). A detailed derivation of the velocity profile, shear rate, shear stress, volumetric flow rate, and Reynolds number equations for the tubular perfusion chamber appears in APPENDIX H. The shear rate, $\dot{\gamma}$, on the exposed vascular surface can be calculated from the volumetric flow rate, Q, chamber width, w, and chamber height, h, as shown in Equation 5-1.

Equation 5-5-1 Shear Rate for Tubular Perfusion Chamber

$$\dot{\gamma} = \left(\frac{4Q}{\pi R^3} \right)$$

A shear rate of 100 s^{-1} was used for the microsphere and cell targeting experiments.

5.2.2 Microsphere Targeting in a Tubular Perfusion Chamber

For the microsphere targeting experiments, the scrape-damaged bovine carotid artery was loaded into the tubular perfusion chamber and the system was primed with media using the syringe pump. Next, a 1.5 mL solution of 10 mM NHS-PEG-biotin or the vehicle (PBS) control was

injected into the chamber through a stopcock and incubated for 1 min. After the incubation, the artery is perfused with media for 10 min. A $7.28x10^6$ part/mL suspension of Fluospheres NeutrAvidin labeled microspheres is drawn through the chamber at the specified shear rate for 10 min followed immediately by another 10 min was with the media alone. Finally, the number of bound microspheres is counted using epi-fluorescence microscopy.

5.2.3 Cell Targeting in a Tubular Perfusion Chamber

For the cell targeting experiments, HCAECs grown in a BD Falcon 75 cm^2 tissue culture flask were labeled with CellTracker Orange CMTMR, harvested, and modified with NHS-PEG-biotin as described previously. The same perfusate media and perfusion system (Figure 5-1) was employed for these experiments. A shear rate of 100 s^{-1} was used for the cell targeting experiments as calculated utilizing Equation 5-1. The scrape-damaged bovine carotid artery was loaded into the tubular perfusion chamber and the system was primed with media using the syringe pump. Next, a 1.5 mL solution of 10 mM NHS-PEG-biotin or the vehicle (PBS) control was injected into the chamber through a stopcock and incubated for 1 min. After the incubation, the artery is perfused with media for 10 min. Now, a 2 mg/mL solution of NeutrAvidin Biotin-Binding Protein or the vehicle (PBS) control was injected into the chamber through a stopcock for another 1 min incubation. After the incubation, the artery is perfused with media for 10 min. The PEG-biotin modified cell suspension is then drawn through the chamber at the specified shear rate for 10 min followed immediately by another 10 min was with the media alone. This ensures that the cells in suspension adhere to the endothelial surface under shear and not from stagnation or settling resulting from a stoppage in flow. Finally, the number of adherent cells is counted using epi-fluorescence microscopy.

5.2.4 Epi-Fluorescence Microscopy of Samples

Epi-fluorescence microscopy of the samples was completed as previously elucidated in Subsection 4.2.4.

5.2.5 Statistical Analysis

Statistical analysis of the collected data was conducted in the same fashion as described in Subsection 4.2.5.

5.3 RESULTS

5.3.1 Targeted Delivery of Microspheres to Scrape-Damaged Arteries

Epi-fluorescence microscopy was used to visualize the adherent microspheres. The scrape-damaged bovine carotid artery exhibited background auto-fluorescence in green (Figure 5-1). Microspheres were yellow-green fluorescent and easily identified with their intensity over background, but were shown in purple for clarity (Figure 5-2). The number of microspheres bound to untreated bovine carotid arteries (Figure 5-2, A) was significantly less than the number bound to NHS-PEG-biotin treated arteries (Figure 5-2, B). The total number of microspheres that adhered to NHS-PEG-biotin treated bovine carotid arteries was 60 ± 16 per mm^2 as compared to only 11 ± 4 per mm^2 for control arteries (Figure 5-3). These results were found to be significant with $p = 0.01$ (Figure 5-3).

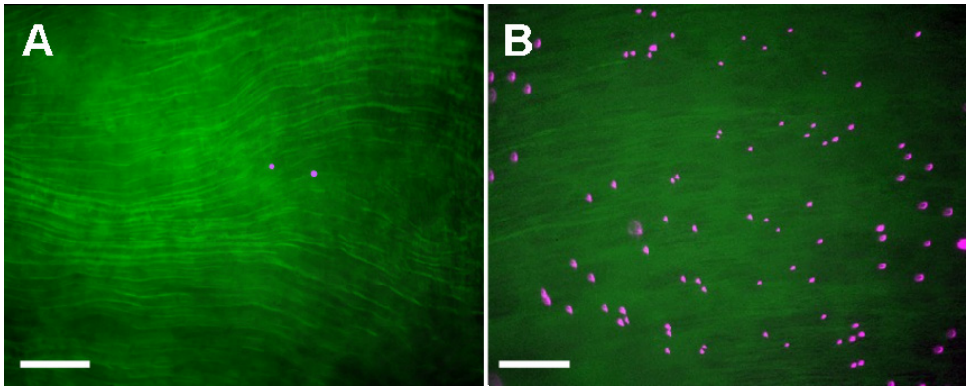

Figure 5–2 Targeted microspheres (purple) adhering to control (A) and PEG-biotin modified (B) scrape-damaged bovine carotid arteries (green) in a tubular perfusion chamber. The scale bar is 100 µm.

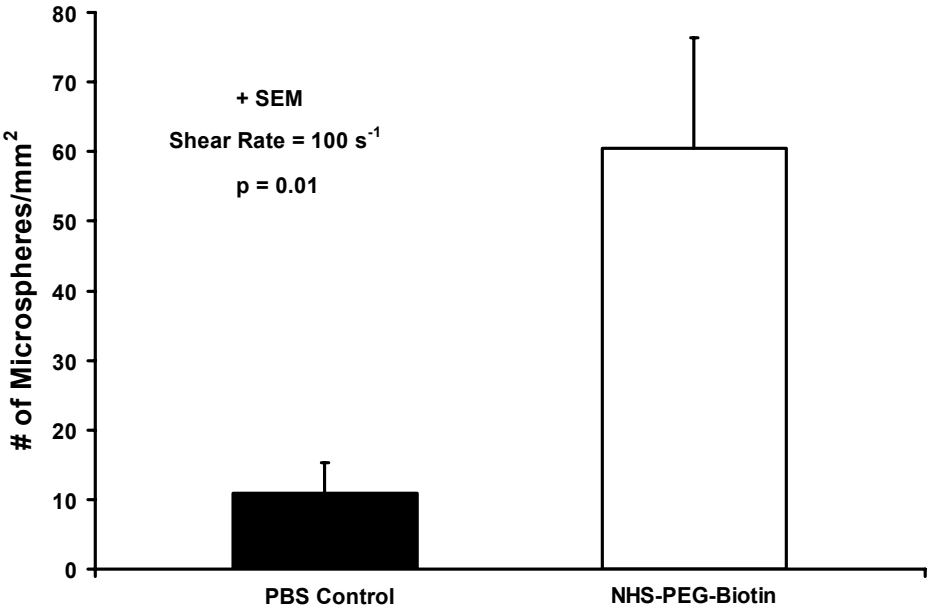

Figure 5–3 Number of adherent NeutrAvidin-coated microspheres on control and PEG-biotin treated scrape-damaged bovine carotid arteries at 100 s^{-1}. Data is shown +SEM with n = 12 and the results are significant with p = 0.01.

5.3.2 Targeted Delivery of Cells to Scrape-Damaged Arteries

Two-color epi-fluorescence microscopy was used to visualize the HCAECs bound to the treated and control scrape-damaged bovine carotid arteries. The scrape-damaged bovine carotid artery

exhibited background auto-fluorescence in green (Figure 5-4). Targeted cells that adhered to the scrape-damaged bovine carotid arteries under shear were labeled with CellTracker Orange CMTMR and appeared red (Figure 5-4). The number of targeted cells bound to control treated bovine carotid arteries (Figure 5-4, A) was significantly less than the number bound to NHS-PEG-biotin treated arteries (Figure 5-4, B).

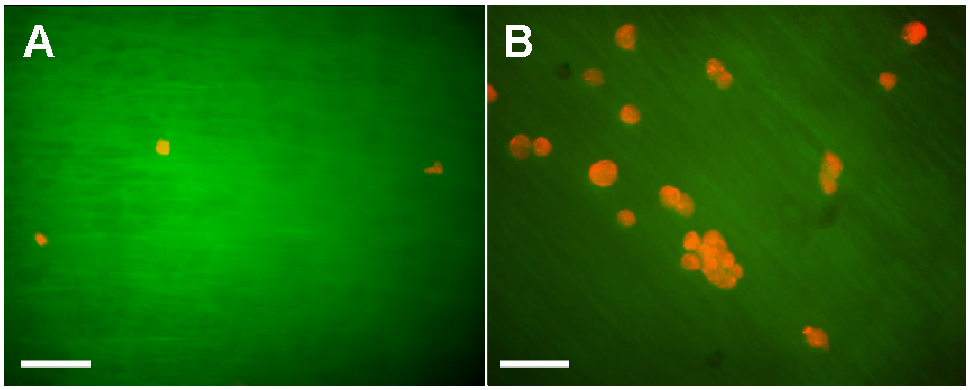

Figure 5–4 Targeted HCAECs (red) adhering to control (A) and PEG-biotin modified (B) scrape-damaged bovine carotid arteries (green) in a tubular perfusion chamber. The scale bar is 100 µm.

The total number of cells that adhered to NHS-PEG-biotin treated bovine carotid arteries was 22 ± 5 per mm^2 as compared to only 6 ± 2 per mm^2 for control arteries (Figure 5-5). These results were found to be significant with $p < 0.01$ (Figure 5-5).

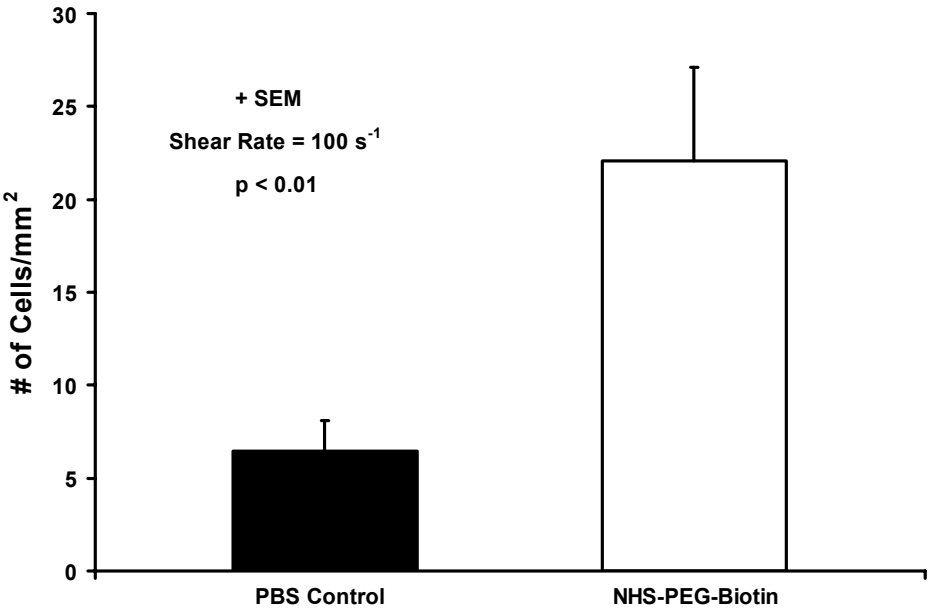

Figure 5–5 Number of adherent PEG-biotin modified cells on control and PEG-biotin treated scrape-damaged bovine carotid arteries with application of NeutrAvidin at 100 s^{-1}. Data is shown +SEM with n = 9 and the results are significant with $p < 0.01$.

5.4 DISCUSSION

The results from this chapter suggest that modification with a protein-reactive PEG and targeted delivery using biotin and avidin is feasible on injured vascular surfaces. Targeted microspheres and cells preferentially adhere to PEG-biotin modified injured vascular surfaces. This makes the procedure pertinent to the prevention of restenosis following intravascular procedures such as angioplasty, stenting, and endarterectomy. Molecular barrier formation, systemic and local delivery of pharmaceutics, and re-endothelialization are all possible strategies to inhibit restenosis following intravascular procedures. The intravascular modification and targeted delivery system developed here is applicable to all three of the aforementioned therapies.

As demonstrated previously in our lab, modification of scrape-damaged placental or balloon injured rabbit femoral arteries with a reactive PEG resulted in a substantial reduction of adhered and activated platelets on the modified vascular surfaces following contact with blood [163, 181, 182]. The decrease in platelet deposition on the injured, thrombogenic vascular surfaces can be attributed to formation of a molecular shield masking the adhesive ligands that bind and activate platelets [162-164, 181, 182]. Formation of a molecular barrier inhibiting platelet deposition, by itself, is advantageous in preventing restenosis following intravascular procedures. However, this benefit could be further augmented by targeting pharmaceuticals or assisting with re-endothelialization.

A number of targeting strategies have been developed to deliver pharmaceuticals or vectors to sites of vascular injury in an attempt to inhibit thrombosis and restenosis. An in depth discussion of targeted pharmacological therapy and gene therapy appears in the Treatments Subsection 1.4.2 on restenosis. One such treatment of neointimal hyperplasia involved using anti-restenotic agents conjugated to antibodies against cross-linked heparin, which is deposited at the site of arterial injury [75]. Targeting heparin or low molecular weight heparin using this technique was shown to reduce neointima formation [75]. Unlike this method, our targeting molecule formed a molecular barrier to try and inhibit restenosis. In addition, further therapeutic benefit is possible through the targeted delivery of NeutrAvidin-coated microspheres. Furthermore, the system utilizing antibodies to cross-linked fibrin will only work at sites of vascular injury; whereas, the protein-reactive PEG we employed can modify healthy endothelium or exposed matrix following injury allowing for the treatment of more conditions.

Again, the overall ability to deliver microspheres to PEG-biotin modified scrape-damaged vascular surfaces appears limited. However, the results presented in this dissertation fall in line

with other targeted delivery systems. Strategies utilizing microspheres targeted to E- and P-selectin demonstrated significantly worse delivery of only an average of 30 microspheres/mm^2 [78, 222, 223]. The number of NeutrAvidin-coated microspheres adhering to PEG-biotin modified vascular surfaces was double that found with selectin-modified microspheres. Another targeting strategy focused on targeting ultrasound contrast microbubbles to endothelial receptors upregulated during inflammation [216, 217, 219, 220]. This approach demonstrated adherence of up to 10 microbubbles per cell [216, 217, 219, 220]. It is important to note, however, that the some of the microbubble targeting protocols used particle solutions that were up to 100 times more concentrated [216, 217, 219, 220]. In addition, some of the binding experiments were stagnant incubations and not deposited under flow.

The effectiveness of the intravascular modification and targeting system investigated in this dissertation might be increased by using more concentrated microsphere solutions, repeated injections of microspheres, or re-circulation of the microsphere solution. All of these parameters could be evaluated and modified based on what therapeutic agent is delivered and what quantity is necessary to produce a beneficial effect. Even so, the ability to deliver microspheres to PEG-biotin modified damaged vascular surfaces serves as a model for the targeted administration of particulate drugs, liposomes, or viral vectors for the treatment of various vascular maladies.

Another approach to inhibit restenosis following vascular injury employs expedited or assisted re-endothelialization to heal injured vessels [137, 141, 144, 225]. Disruption of the endothelial layer following many intravascular procedures is thought to be a major factor in thrombotic occlusions and neointima formation [137]. Replacing the endothelial layer might abrogate thrombus formation thereby reducing restenosis. An in depth discussion of re-endothelialization appears in the Treatments Subsection 1.4.2 on restenosis. One study injected

endothelial progenitor cells intravenously after injury to inhibit neointima formation [144]. The cells were not targeted to the site of vascular injury as was possible with our protein-reactive PEG-biotinylated surfaces and cells using NeutrAvidin as a bridge. Other studies have focused on harvesting endothelial progenitors and incubating them inside the vessel following injury [137, 141, 225]. However, attachment of the endothelial progenitors took upwards of 20 min, which is not well-suited to time sensitive procedures such as balloon angioplasty.

NHS-PEG-biotin covalently links to cell membranes or matrix proteins in a much shorter time frame (1 min). The cells can then be infused intravenously and should preferentially adhere to the modified surfaces. This ability to assist in re-endothelialization is supported by the experiments demonstrating attachment of PEG-biotin labeled HCAECs to PEG-biotin modified scrape-damaged bovine carotid arteries using NeutrAvidin. Based on the average area occupied by HCAECs in culture, the adhered ECs should occupy approximately 13% of the surface once they firmly adhere and spread. Additional studies would be required to determine if this coverage could produce a therapeutic effect.

As mentioned previously, PEG modification is commonly used to prevent protein and cell adhesion on surfaces. Consequently, the ability of the PEG-biotin labeled endothelial cells to firmly adhere, spread, and proliferate following binding to PEG-biotin modified vascular is a major concern. On endothelial cell surfaces, PEG-biotin is quickly eliminated as demonstrated by the PEG-biotin modification persistence data presented in Chapter 3. The loss of PEG-biotin modification from the endothelial surface should abrogate its ability to resist cell adhesion and enable cells to firmly adhere and spread. This hypothesis was tested by applying PEG-biotin labeled rat heart microvessel endothelial cells (RHMVECs) on PEG-biotin modified scrape-damaged rat aortas using NeutrAvidin as a bridge. The RHMVECs were able to firmly adhere,

spread, and proliferate on the modified vascular surface over a period of 6 days (APPENDIX I). Thus, endothelial cells labeled with PEG-biotin should be able to adhere, spread, and proliferate upon targeted delivery to PEG-biotin modified injured vascular surfaces to assist in re-endothelialization.

Endothelial cell delivery is not as efficient as microsphere targeting. Only about 22 endothelial cells could be delivered per mm^2 of modified vascular tissue whereas 60 microspheres could be delivered to the same surface. This can most likely be attributed to the large disparity in the size of the microspheres and cells. The microspheres have a well-defined, consistent diameter of 1 μm while the cells can vary between 15-25 μm. This 15 to 25-fold increase in diameter of the particle leads to an increase in the force exerted by the fluid motion on the particle which would tend to pull the particle over the surface and prevent firm adhesion.

A propagation of error analysis provides an estimate of the uncertainty in the calculation of the number of microspheres or cells per mm^2 of the cell surface. The number of microspheres or cells per area is computed from measured quantities that have their own associated error. As a result, the error in the measured quantities carries over into the computed number of microspheres or cells per mm^2 of the cell surface. The procedure for determining the error propagation in the computed quantities based on the error in the measured quantities is illustrated in APPENDIX D. In the case of calculating the number of microspheres or cells per cell surface area, the detailed propagation of error analysis is presented in APPENDIX G. For the tubular perfusion chamber, the uncertainty in the calculated number of microspheres and cells per mm^2 vascular surface is 2.6% and 1.7%, respectively.

These results provide further validation of the efficacy of the proposed intravascular modification and targeted delivery system. However, the explanted bovine carotid artery in the

tubular perfusion chamber is unable to fully reproduce the physiologic environment and constraints of clinical application. This system does not account for actual balloon inflation injury of vessels. A more rigorous *in vivo* model is necessary to verify the ability to modify balloon injured arteries with a protein-reactive PEG for the targeted delivery of microspheres and cells. Remote injections of the targeted agents, interaction of the components with blood, and physiologic flow conditions are all possible obstacles to the applicability of the proposed modification and targeted delivery system as a treatment following intravascular injury.

6.0 *IN VIVO* MODIFICATION OF BLOOD VESSELS WITH PEG

6.1 INTRODUCTION

The *in vitro* experiments completed thus far have provided insight into the capacity and management of modifying cell and exposed matrix proteins on vascular surfaces. However, further examination in a more clinically applicable setting is required to validate the *in vitro* results and demonstrate its usefulness as a treatment modality following intravascular procedures in the clinic. This chapter focuses on modification of balloon injured vascular surfaces with a protein-reactive PEG in the hopes of blocking thrombosis and providing a site for the targeted delivery of therapeutics and cells to inhibit restenosis. N-hydroxysuccinimide-polyethylene glycol (NHS-PEG) is used to covalently modify vascular surfaces in an *in vivo* rabbit femoral artery model of vascular injury. The NHS reactive group covalently links with primary amines, with the most accessible being the epsilon amine of found on the amino acid lysine [183]. A stable amide bond is formed covalently linking the protein-reactive polymer with a primary amine of a protein on a vascular surface [151, 202]. Previous research demonstrated that modification of vascular surfaces with a protein-reactive PEG forms a molecular barrier preventing platelet and leukocyte adhesion [181, 182]. For evaluating the delivery technique, degree of modification, and duration of the polymer, a reactive NHS-PEG-fluorescein was

utilized, which allowed for direct measurement of the fluorescence intensity of the modifying polymer on an epi-fluorescent microscope.

6.2 METHODS

6.2.1 Surgical Procedure

The animal studies were completed following a protocol approval by the Institutional Animal Care & Use Committee of the University of Pittsburgh. This study employed a rabbit femoral artery model to evaluate the proposed modification and targeting system [182]. Female New Zealand White rabbits (Myrtle's Rabbitry, Inc., Thompson Station, TN) with an average weight of 4.25 kg were anesthetized with an intramuscular injection of 40 mg/kg ketamine (Webster Veterinary, Sterling, MA) and 5 mg/kg xylazine (Webster Veterinary, Sterling, MA) and sustained on 1.5-2.5% isoflurane (Webster Veterinary, Sterling, MA) administered endotracheally. An ear vein of the rabbit was cannulated with a 22 G x 1 in JELCO IV catheter (Webster Veterinary, Sterling, MA) to provide intravenous access. Fluids were provided with a slow drip of Lactated Ringers (Webster Veterinary, Sterling, MA) through a Venoset Microdrip IV set (Webster Veterinary, Sterling, MA).

An incision was made in the skin exposing the underlying muscle. The muscle was carefully dissected exposing the common femoral, saphenous, and popliteal arteries. Minor side branches off the common femoral artery were ligated and removed. In addition, the saphenous artery was ligated near the knee of the rabbit. SUNDT Slim-Line aneurysm clips (Codman, Raynham, MA)

were placed on the common femoral artery just proximal to the deep femoral artery branch and on the popliteal artery (Figure 6-1).

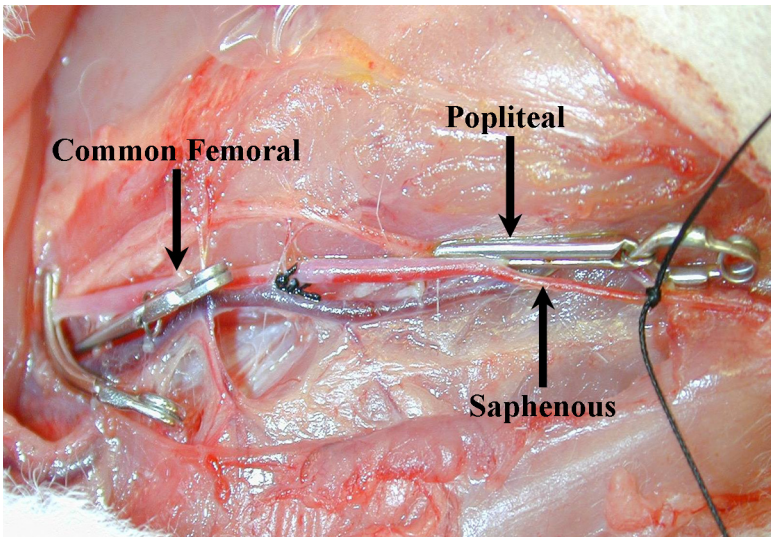

Figure 6–1 Common femoral, popliteal, and saphenous arteries. Clamps are placed on the common femoral and popliteal arteries and the saphenous artey ligated.

An arteriotomy was made in the saphenous artery to allow access to the lumen of the common femoral artery. Only one leg was used in survival studies to minimize trauma to the animal and allow for adequate mobility for water and food intake. In acute studies, the same procedure was repeated on the other leg of the animal to minimize the number of animals required for statistically significant results.

6.2.2 Balloon Injury

A 2F Fogarty embolectomy catheter (Edwards Lifesciences, Irvine, CA) was inserted through the arteriotomy in the saphenous artery until it reached the clamp on the common femoral artery. The balloon was then inflated with air using a 1 mL BD slip-tip disposable tuberculin syringe (Fisher Scientific, Pittsburgh, PA) until the vessel distension was observed (Figure 6-2).

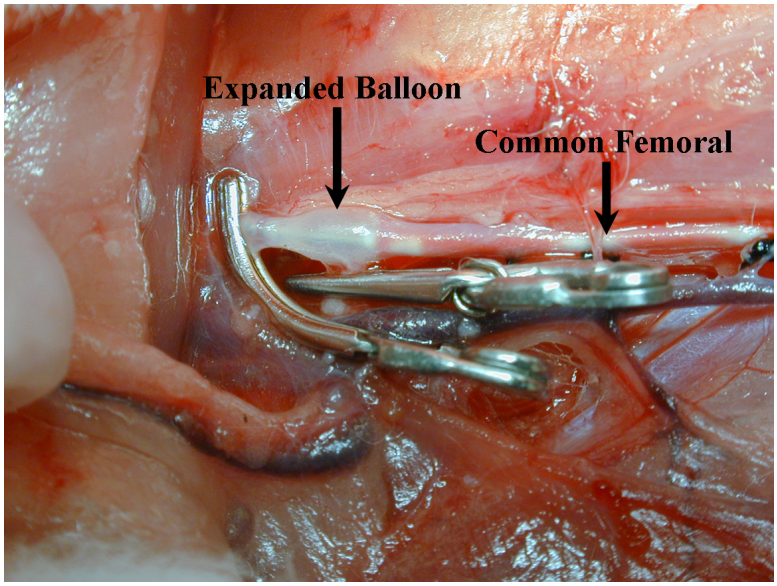

Figure 6–2 Inflated 2F Fogarty embolectomy catheter in the common femoral artery.

Next, the inflated balloon was withdrawn from the vessel until it reached the branch where the popliteal and saphenous emerge from the common femoral artery. At this point, the balloon was deflated, re-inserted to the clamp on the common femoral artery, and the procedure repeated two additional times to ensure vascular injury [226, 227]. Finally, the 2F Fogarty embolectomy catheter was left deflated after the third pass and carefully removed from the saphenous artery through the arteriotomy.

6.2.3 Assessment of Balloon Denudation

Denudation of the endothelial layer and vascular injury resulting from the passage of the embolectomy catheter was confirmed using Evans blue dye [228]. Evans blue is an azo dye that binds with circulating albumin [228]. An intact endothelium would serve as a barrier to this protein-dye complex, but the complex adsorbs onto denuded arterial segments staining the surface a royal blue color [228]. Following arterial injury with a 2F Fogarty embolectomy

catheter, a small group of rabbits were given an intravenous dose of 10 mg/kg Evans blue dye two hours prior to sacrifice [228]. The uninjured common femoral artery in the other leg was harvested as a control.

6.2.4 PEG Modification of Balloon Injured Vessels

Modification of the arteries was accomplished using either a .025 in outer diameter Micro-Renathane tubing (Braintree Scientific, Braintree, MA) or 2.5 mm Remedy channeled drug delivery balloon catheter (Boston Scientific, Natick, MA). The tube or drug delivery balloon catheter was introduced into the common femoral artery through the arteriotomy in the saphenous artery (Figure 6-3) and threaded until the tip reached the clamp. An aliquot of Phosphate Buffered Saline (PBS) (Cambrex, Walkersville, MD) was added to a pre-weighed sample of NHS-PEG-biotin MW 3,400 or NHS-PEG-fluorescein MW 5,000 (Nektar Therapeutics, San Carlos, CA) to make 1 mL of a 10 mM solution. The solution was mixed until the solid dissolved and then loaded into a 1 mL BD slip-tip disposable tuberculin syringe. Next, the syringe was connected to the port on the drug delivery balloon catheter or to a 27 G x ½ in BD PrecisionGlide needle (Fisher Scientific, Pittsburgh, PA) inserted into the end of the tube to allow for addition of the polymer for modification of the vessel.

The polymer was continuously flushed through the lumen of the common femoral artery for a period of 45 s. After addition of the polymer, the Micro-Renathane tubing or Remedy channeled drug delivery balloon catheter was withdrawn from the common femoral through the arteriotomy. Once the tube or catheter was removed from the saphenous artery, a previously placed ligature (Figure 6-3) was tightened where the saphenous artery branches off the femoral artery to prevent bleeding from the arteriotomy. When the total incubation time for the polymer

in the artery reached 1 min, the aneurysm clips were removed from the popliteal and common femoral arteries to restore blood flow through the femoral and remove any un-reacted polymer. Control arteries were treated in an identical manner except that the vehicle, PBS, was added instead of the reactive polymer.

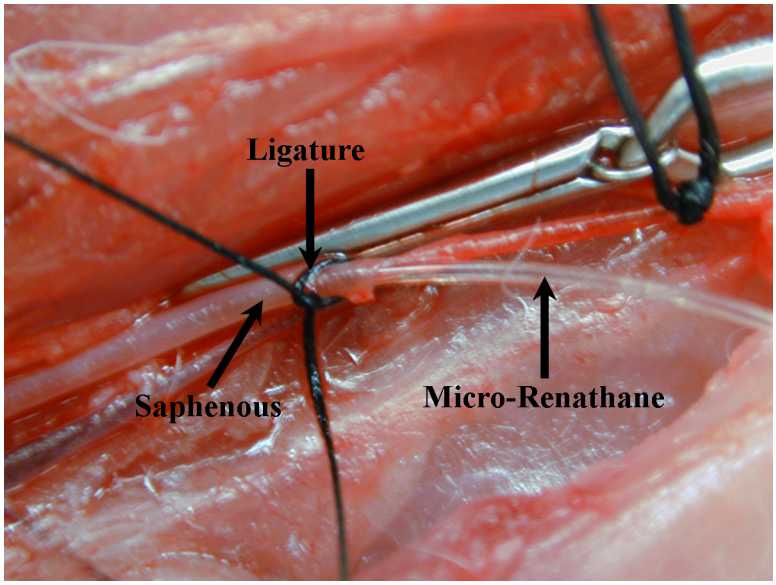

Figure 6–3 Image of the Micro-Renathane tube inserted into the common femoral artery through the arteriotomy in the saphenous artery. The Remedy drug delivery balloon catheter is introduced into the common femoral artery in a similar manner. Once the tube or catheter is withdrawn, the ligature is tightened.

6.2.5 Acute Studies

The open surgical site was covered with a 4 x 4 in Fisherbrand gauze sponge (Fisher Scientific, Pittsburgh, PA) saturated in 0.9% sodium chloride irrigation solution (Fisher Scientific, Pittsburgh, PA) to keep the site moist until final disposition of the animal and harvest of the vessels.

6.2.6 Survival Studies

For measurements collected at 24, 48, and 72 hrs, the surgical sites were closed and the animals recovered. 2-0 Ethicon coated Vicryl sutures with taper point needles were used to close the muscle and for subcutaneous closure of the skin. Once the wound was closed, the anesthesia was discontinued and the rabbits were monitored until they regained consciousness and returned to their housing. Rabbits were given intramuscular injections of 1 mg/kg ketoprofen (Webster Veterinary, Sterling, MA) and 100 mg cefazolin (Webster Veterinary, Sterling, MA) twice a day for a maximum of three days or until the second procedure was performed.

6.2.7 PEG Modification to Prevent Restenosis

In order to study the effects of PEG modification on restenosis after balloon injury, a number of five week survival studies were initiated. After modification of balloon injured vessels with NHS-PEG-biotin, the surgical sites were closed and the animals recovered. 2-0 Ethicon coated Vicryl sutures with taper point needles were used to close the muscle and for subcutaneous closure of the skin. Once the wound was closed, the anesthesia was discontinued and the rabbits were monitored until they regained consciousness and returned to their housing. Rabbits were given intramuscular injections of 1 mg/kg ketoprofen (Webster Veterinary, Sterling, MA) and 100 mg cefazolin (Webster Veterinary, Sterling, MA) for three days following the surgical procedure. After five weeks, the animals were anesthetized and the manipulated vessels were obtained and processed as described in the Vessel Harvest and Preparation Subsection 6.2.8.

6.2.8 Vessel Harvest and Preparation

Animals were maintained on 2.5% isoflurane. A midline incision was made from below the rib cage to the pelvic region. Next, the vena cava and aorta were isolated from the surrounding tissue. At this point, the isoflurane was increased to 5% and the animals euthanized with a supersaturated potassium chloride (KCl) solution (Sigma, St. Louis, MO). The aorta was cannulated with an 18 G x 1 in JELCO IV catheter (Webster Veterinary, Sterling, MA) and the hind limb portion of the animals was flushed with 100 mL of Lactated Ringers through a Venoset IV set (Webster Veterinary, Sterling, MA). The vena cava was severed to allow the excess blood and fluid to drain from the hind limb region. After the blood was flushed, 100 mL of Shandon Glyo-Fixx (Thermo Electron Corporation, Waltham, MA) was administered through a Venoset IV set to pressure fix the arteries for examination. Experimental and control femoral arteries were explanted from the rabbit after fixation along with some carotid arteries, which served as another control in some instances. The explanted vessels were placed in a labeled 6 well tissue culture plate (Fisher Scientific, Pittsburgh, PA) and transported back to the lab for processing.

For epi-fluorescence microscopy studies, excess tissue was removed from the exterior of the arteries and the vessel wall was cut along its length to enable exposure of the lumen. Minutien pins (Fine Science Tools, Foster City, CA) were used to secure the edges of the vessel to pink dental wax (Electron Microscopy Sciences, Hatfield, PA) with the lumen side facing upwards. After securing the vessel to the wax, the sample was placed back into the 6 well tissue culture plate overnight before evaluation using epi-fluorescence microscopy.

Contrastingly, the vessels were prepared differently for the five week restenosis studies. Excess tissue was removed from the exterior of the arteries and they were loaded into cassettes

for paraffin processing and embedding. After embedding in paraffin, cross-sections of the vessel wall were prepared by making three equidistant cuts along the vessel length yielding five segments. The orientation of the vessel segments was maintained from the end where the popliteal and saphenous arteries branched from the common to the common just proximal to the deep femoral branch. Thin cross-sections of the vessel segments were cut and slides prepared. The slides were then stained with hematoxylin and eosin visualized on an epi-fluorescent microscope.

6.2.9 Epi-Fluorescence Microscopy of Explanted Vessels

A Zeiss Axiovert 35 Epi-Fluorescence Microscope (Carl Zeiss, Inc., Thornwood, NY) with a MicroMAX 5 MHz CCD Camera (Princeton Instruments, Trenton, NJ), Mac G4 computer (Apple, Cupertino, CA), and IP Lab software (Scanalytics, Inc., Billerica, MA) were used to capture images from the vessels. Fluorescent micrographs were taken of the rabbit femoral arteries for the polymer modification and restenosis experiments. However, different protocols were used for each application.

For the polymer modification experiments, the IP Lab software was utilized for measuring fluorescence intensity on the vessel lumen. Micrographs of the explanted vessels were taken at 1 mm increments starting where the saphenous and popliteal arteries branched from the femoral and ending at the site of the clamp on the common femoral artery. The fluorescent polymer was labeled with fluorescein, which has a maximum absorption of 490 nm and emission of 514 nm. Using the same filter and exposure settings, the fluorescence intensity of the polymer was measured over the course of 72 hrs and the persistence of the polymer modification determined.

Fluorescent micrographs of rabbit femoral artery cross-sections were collected using IP Lab. An image of each vessel segment was acquired noting its location and orientation. Fluorescent micrographs of the vessel cross-sections were possible due to the auto-fluorescence of the tissue. Furthermore, the demarcation between the neointima and media of balloon injured rabbit femoral arteries was especially noticeable when using epi-fluorescence microscopy. Restenosis experiment vessels were compared using a ratio of the neointima area to media area, $A_{N/M}$, as shown in Equation 6-1.

Equation 6-1 Neointima/Media Area

$$A_{N/M} = \frac{A_N}{A_M}$$

The area of the neointima, A_N, and the media, A_M, were calculated by drawing regions in the image analysis software MetaMorph (Molecular Devices Corporation, Downington, PA) and then dividing the two areas to obtain the ratio.

6.2.10 Statistical Analysis

Statistical analysis of the data acquired from the vessel images was performed using the Analysis Toolpak in Microsoft Excel. Data points are represented as mean values plus or minus their standard deviation (St Dev) or standard error of the mean (SEM) as denoted in the figures. Differences between control and treated groups at all time points were evaluated using a two-factor ANOVA with replication to determine statistical significance.

6.3 RESULTS

6.3.1 Verification of Balloon Injury

Vascular injury resulting from the passage of the embolectomy catheter was easily confirmed using Evans blue dye [228]. Loss and injury of the endothelium abolishes its protective barrier effects allowing the Evans blue-albumin complex to adsorb onto denuded arterial segments staining the surface a royal blue color [228]. This is apparent in Figure 6-4. Arterial segments injured with an embolectomy catheter appear blue (Figure 6-4, A) while uninjured vascular segments retain their natural color (Figure 6-4, B).

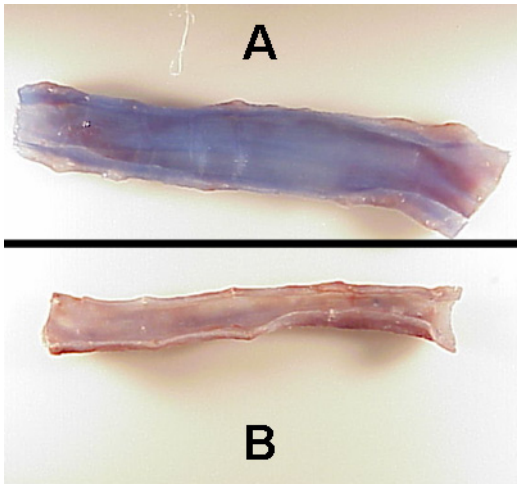

Figure 6–4 Assessment of balloon injury with Evans Blue dye on rabbit femoral arteries (A) injured with an embolectomy catheter and (B) uninjured.

6.3.2 Comparison of PEG Modification Techniques

Modification of the balloon injured rabbit femoral arteries with NHS-PEG-fluorescein was evaluated using a 0.025 in outer diameter Micro-Renathane tube and 2.5 mm Remedy channeled

drug delivery balloon catheter. The background auto-fluorescence was negligible (Figure 6-5, A). A similar pattern of modification was seen with both the Micro-Renathane tubing and the channeled drug delivery balloon catheter (Figure 6-5, B and C). This was further confirmed by measuring the fluorescence intensity of vessel segments modified with the polymer delivered using the Micro-Renathane tubing and Remedy channeled drug delivery balloon catheter. Modification of balloon injured arteries with NHS-PEG-fluorescein resulted in nearly identical fluorescence intensities with a mean of 1241 for the tube and 1230 for the channeled balloon catheter (Figure 6-6). Control vessels showed little to no auto-fluorescence with a mean fluorescence intensity of only 69 (Figure 6-6).

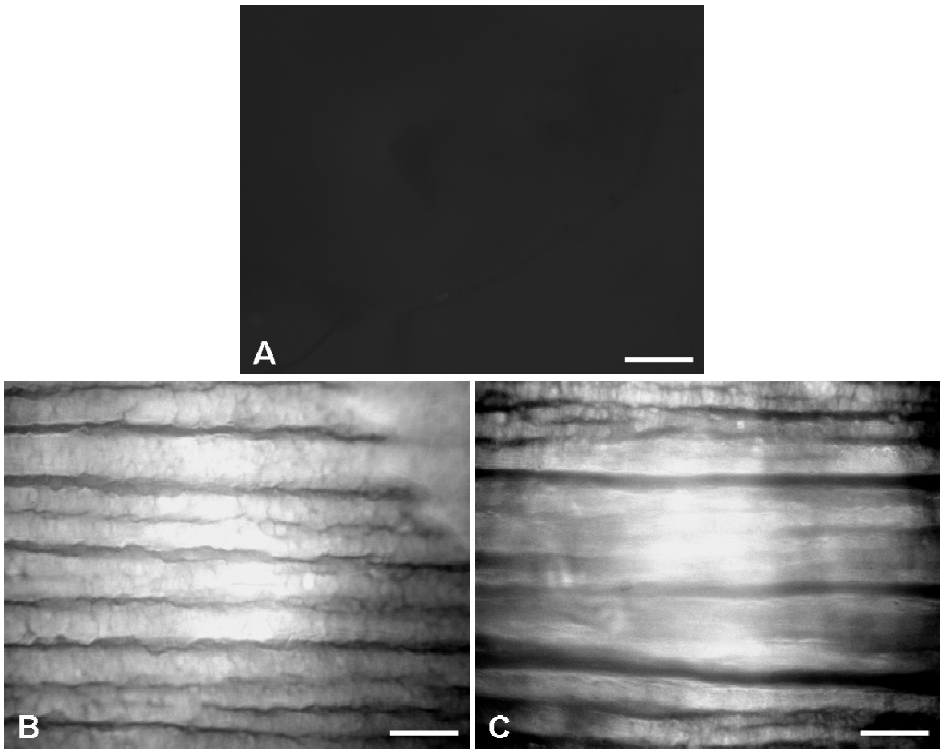

Figure 6–5 Fluorescent micrographs of different modification techniques with reactive PEG-fluorescein: (A) Vehicle (PBS) control, (B) Micro-Renathane tubing, and (C) Remedy channeled drug delivery balloon catheter. Scale bar is 100 μm.

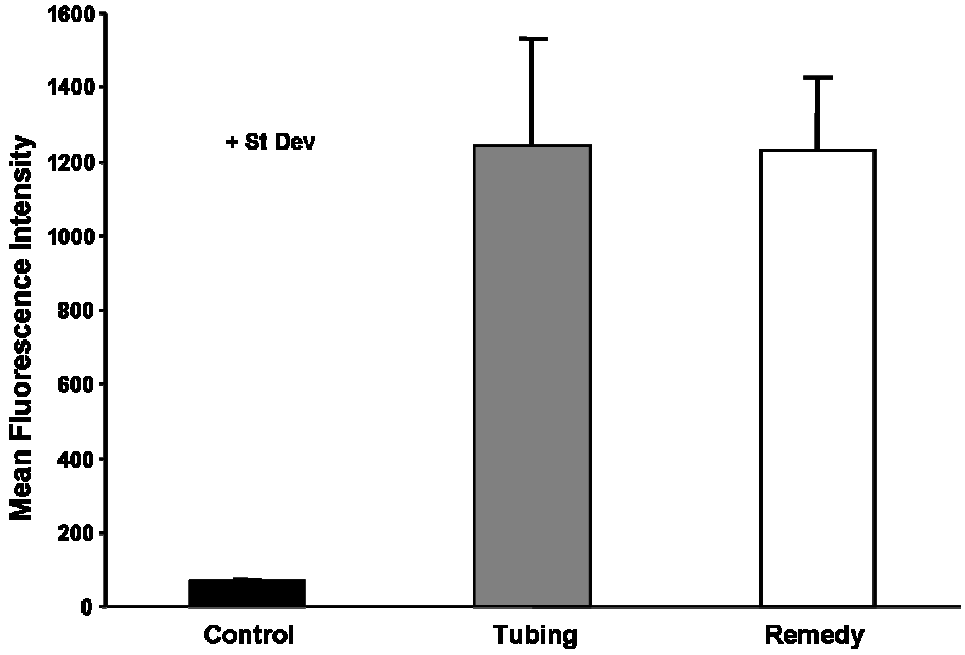

Figure 6–6 Mean fluorescence intensity comparing the vehicle, Micro-Renathane tubing, and Remedy channeled drug delivery balloon catheter delivery methods. Data is shown as MESF +St Dev with n = 3.

There was no difference in modification of balloon injured arteries regardless of whether the Micro-Renathane tubing or Remedy drug delivery catheter were used for administration of the reactive PEG. Since there was no difference in the ability to deliver the polymer with either technique, subsequent experiments evaluating the duration of the polymer in the vessel or ability to target microspheres to the polymer were completed using the Micro-Renathane tubing. The Micro-Renathane tubing was selected because of its smaller size in comparison to the Remedy channeled drug delivery balloon catheter, which allowed for easier introduction into the rabbit saphenous artery with fewer complications.

6.3.3 Duration of PEG Modification

In order to assess the ability of the polymeric barrier to inhibit thrombosis and as a site for the targeted delivery of therapeutics, it was important to establish the maintenance of the polymer on

the vascular surface post-modification. Again, the balloon injured rabbit femoral arteries were modified with NHS-PEG-fluorescein or the vehicle, PBS, as a control administered through the Micro-Renathane tubing. Modifying the balloon injured arteries with a fluorescent PEG allowed for evaluation of the polymer coverage using epi-fluorescence microscopy. After modification of the balloon injured rabbit femoral arteries, blood flow was re-established and the vessels were harvested at 0, 24, 48, and 72 hrs. At each time point, images of the vessels were acquired and processed to measure the fluorescence intensity of the remaining polymer on the surface to determine the maintenance of the polymeric barrier on the vessel surface over time.

It was apparent that the polymer coverage decreased over time, but remained on balloon injured vessels for the entire evaluation period of 72 hrs (Figure 6-7).

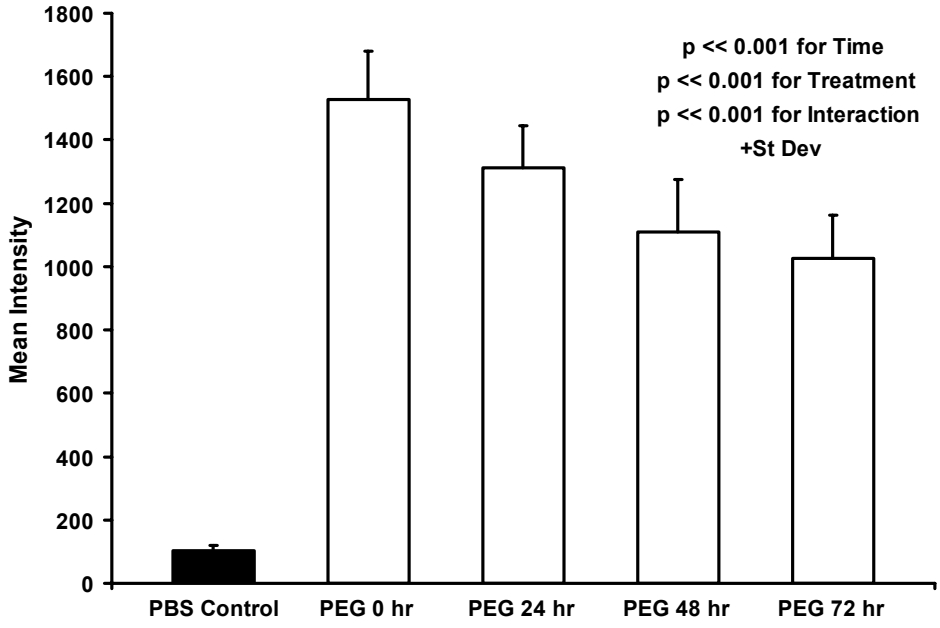

Figure 6–7 Duration of PEG-fluorescein on balloon injured rabbit femoral arteries after modification at 0, 24, 48, and 72 hrs. Data is shown as MESF +St Dev with n = 4 at all times and treatments and the results are significant with p << 0.001 for the time, treatment, and interaction.

There was little to no background auto-fluorescence associated with control vessels at any time point with a mean fluorescence intensity of only 101 (Figure 6-7). The maximum PEG-fluorescein coverage occurred at 0 hr with a mean intensity of 1,529, which then decreased gradually over the next 72 hrs (Figure 6-7). At 24 hrs, the mean fluorescence intensity dropped to 1,312 and then further decreased to 1,110 and 1,028 at 48 and 72 hrs, respectively (Figure 6-7). Even though the polymer remaining on the balloon injured vessel declined over time, greater than 67% of the original fluorescence was maintained at 72 hrs (Figure 6-7). As a result, the modification of the balloon injured arteries with the polymer would likely be maintained for even longer time than 72 hrs.

The ANOVA performed on the PEG duration data revealed that the mean fluorescence intensity varies with the treatment (control vs. NHS-PEG-fluorescein) as well as the time post-modification (0, 24, 48, and 72 hrs) with a significance value of $p << 0.001$ (Figure 6-7). In addition, the ANOVA demonstrated that there was interaction between the treatment and post-modification time with significance of $p << 0.001$ (Figure 6-7). The fluorescence intensity did not depend upon the post-modification time for the control vessels (Figure 6-7). However, the mean intensity of the NHS-PEG-fluorescein treated femoral arteries decreased as the time post-modification increased (Figure 6-7).

6.3.4 Consistency of PEG Modification

Along with evaluating the maintenance of the polymer, fluorescence intensity data from the images along the entire length of the balloon injured vessels modified with the fluorescent PEG were used to determine the consistency of the polymer coverage. The fluorescence intensity of the vessel segments remained fairly consistent over the entire length for the 0, 24, 48, and 72 hr

time points (Figure 6-8). There was some fluctuation of the mean intensity of the fluorescent polymer over the length of the vessel, but the coverage remained fairly uniform (Figure 6-8). Establishing the consistency of the polymeric coverage along the entire length of the modified vessel was important in evaluating the effectiveness of the barrier to inhibit thrombosis or the signal to deliver targeted therapeutics.

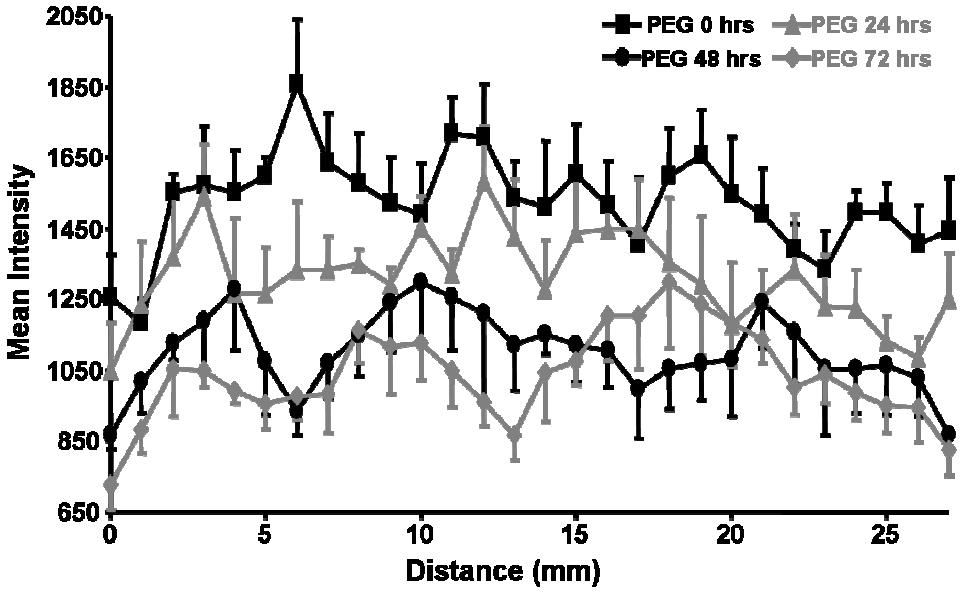

Figure 6–8 Distribution of PEG-fluorescein modified, balloon injured rabbit femoral arteries along the vessel length at 0, 24, 48, and 72 hrs. Data is shown as MESF + or – SEM with n = 4 at all times.

6.3.5 Effects of PEG Modification on Restenosis

Fluorescent micrographs of an uninjured control (Figure 6-9, A) and balloon injured (Figure 6-9, B) rabbit femoral demonstrate the pronounced neointima formation as a result of restenosis. The fluorescent images provided easy identification of the lumen surface, LS, internal elastic membrane, IEM, and external elastic membrane, EEM (Figure 6-10). Once these structures were

identified, regions were drawn on the micrographs using the MetaMorph image analysis software and the areas were calculated.

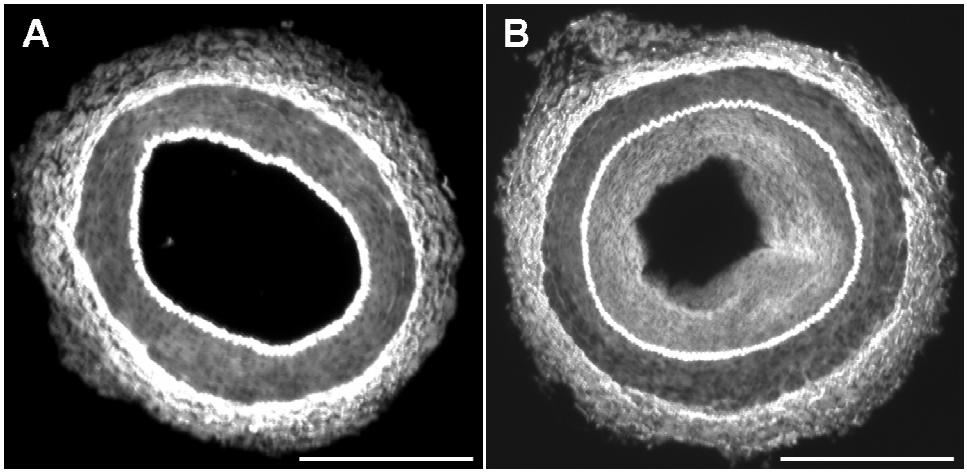

Figure 6–9 Fluorescent micrographs of rabbit femoral arteries. Rabbit femoral arteries were (A) un-manipulated or (B) balloon injured (B) and harvested after 5 weeks. The scale bar is 1 mm.

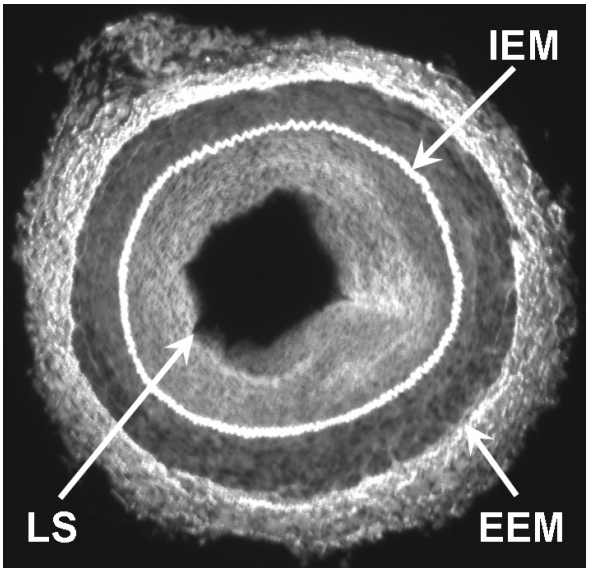

Figure 6–10 Fluorescent micrograph of a balloon injured rabbit femoral artery. The lumen surface, LS, internal elastic membrane, IEM, and external elastic membrane, EEM, are identified.

Subtracting the EEM area, A_{EEM}, from the IEM area, A_{IEM}, yielded the media area, A_M (Equation 6-2).

Equation 6-2 Media Area

$$A_M = A_{EEM} - A_{IEM}$$

In a similar fashion, the neointima area, A_N, is obtained by subtracting the lumen surface area, A_{LS}, from the IEM area, A_{IEM} (Equation 6-3).

Equation 6-3 Neointima Area

$$A_N = A_{IEM} - A_{LS}$$

Finally, the neointima to media area is computed utilizing Equation 6-1.

Comparing the neointima to media ratios for untreated balloon injured and PEG-biotin treated balloon injured rabbit femoral arteries would ascertain if the PEG-biotin modification alone could inhibit restenosis following intravascular injury. The ratio of neointima to media area for untreated balloon injured and PEG-biotin treated balloon injured rabbit femoral arteries is exhibited in Figure 6-11.

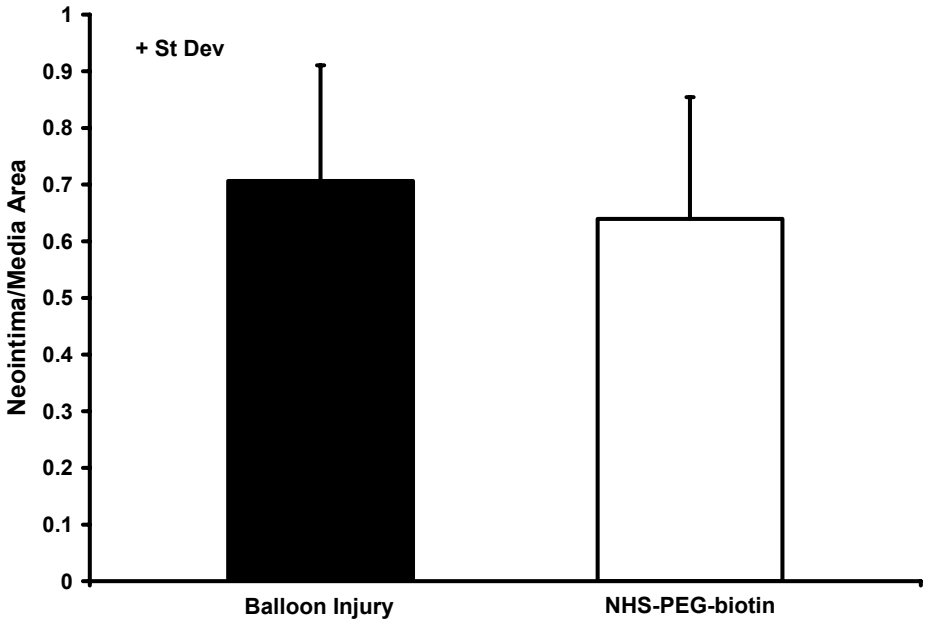

Figure 6–11 Ratio of the neointima to media area as a measure of neointima formation following injury. Data is shown + StDev with n = 5.

PEG-biotin modified balloon injured femoral arteries exhibited only a slightly reduced mean neointima to media ratio than control injured arteries (Figure 6-11). However, the difference in the mean neointima to media ratios was not significant. Consequently, PEG-biotin modification of balloon injured vascular surfaces demonstrated no substantial effect in inhibiting restenosis after balloon injury.

6.4 DISCUSSION

The results presented in this chapter demonstrate the ability of protein-reactive PEG to modify balloon injured vascular surfaces in a clinical setting. Modification of injured vascular surfaces was confirmed using epi-fluorescence microscopy and a fluorescent protein-reactive PEG. Significant modification of the balloon injured femoral arteries was possible at physiologic pH and temperature and with short reaction of times of no more than 1 min. This is especially relevant for time-sensitive intravascular procedures. In addition, the protein-reactive PEG was easily applied to vascular surfaces using a small diameter tube or channeled drug delivery catheter. Both the small diameter tube and channeled catheter produced comparable modification of the vessel. Modification of the vascular surface with the reactive PEG was maximal immediately following application and declined over time.

The *in vivo* studies, the PEG barrier seems to be more durable than on cell surfaces. After 72 hrs, 67% of the original amount of PEG remained on the balloon injured surface. However, over half of the original modification was lost after 24 hrs in the EC modification studies. This is likely due to the fact that the denuded matrix is decellularized so there is not and active endocytotic cycle removing the polymer modification from the surface. Removal of PEG from

the matrix surfaces will likely be delayed until infiltration of the surface by endothelial, monocyte, or smooth muscle cells degrade the polymer. This may permit a longer barrier effect and extended opportunity to target agents.

A number of studies have endeavored to block thrombosis and recurrent restenosis at the site of vascular injury using a number of different strategies. Coatings have been applied to injured vascular surfaces to physically inhibit platelet deposition. Another tactic is to use a hydrogel to prevent platelet deposition by creating a barrier and for sustained release of therapeutics. Furthermore, local intravascular drug or gene delivery has been employed to curb intimal hyperplasia. Drug-eluting stents are still yet another avenue aimed at preventing restenosis following angioplasty of stenosed vessels. Modification of vascular surfaces with a reactive PEG as described in this study is applicable to all of the current strategies under investigation.

Nanocoatings of hyaluron and chitosan deposited onto damaged vascular surfaces have been used to inhibit platelet deposition [123]. One of the drawbacks of the hyaluron and chitosan nanocoatings is that formation of a suitable barrier requires multiple administrations of the polyelectrolytes [123]. Another study focused on concealing extracellular matrix ligands with a PEGylated fibronectin, which interacts with fibrillar collagens, to reduce platelet recognition and binding [125]. However, this method of camouflaging ligands associated with platelet recognition and binding with PEGylated fibronectin required 30 min to cover the injured vascular surface [125]. Both the hyaluron and chitosan nanocoatings and PEGylated fibronectin systems for inhibiting intravascular thrombosis require extended application periods or repeated administrations, which may be detrimental in time-sensitive procedures. The protein-reactive PEG employed to in our system rapidly modifies vascular surfaces (less than 1 min) with only a single application required. Modification of biomaterials with a protein-reactive PEG has been

shown to reduce platelet deposition on biomaterial surfaces [181]. Furthermore, the reactive PEG has demonstrated an ability to inhibit platelet deposition on injured vascular surfaces [162, 182]. The molecular barrier thickness could easily be controlled by changing the Molecular Weight (MW) or branching of the polymer molecule still applied in a single treatment.

Hydrogel barriers formed by photopolymerization have also demonstrated an ability to inhibit thrombosis and reduce intimal thickening on injured vascular surfaces [126, 127]. The hydrogel establishes a barrier preventing blood from contacting the injured vessel wall, which would prevent platelet adhesion [126]. Formation of the hydrogel barriers using photopolymerization requires additional steps such as adsorption of a photoinitiator on the injured vessel surface, flushing of excess initiator, administration of the hydrogel precursors, and adequate illumination (external or internal) to form the gel [126, 127]. In our study, the protein reactive PEG can be applied to the vascular surface in one step while angioplasty is being performed at the site using a channeled drug delivery catheter. PEG hydrogels have also been synthesized to release nitric oxide (NO) or YC-1, a benzyl indazole derivative, as therapeutic agents to reduce platelet adhesion and smooth muscle cell proliferation after vascular injury [128, 129]. It is believed that therapeutics such as these and others could be delivered to PEG-modified vascular sites using the targeting strategy under investigation in this dissertation in a clinical setting.

Previously, our lab demonstrated that reactive PEG possessed the capability of inhibiting platelet deposition on injured vascular surfaces [162, 182]. However, the benefit of PEG modification in the first long term (5 week) evaluation of its ability to prevent restenosis was not evident. Neointima formation was similar in PEG modified and balloon injured controls. It is

important to note that there was a high incidence of complete vessel occlusion in the restenosis studies, which limited the sample size for statistical comparison.

A number of factors may have contributed to the inability of the PEG modification to inhibit restenosis. First, the solution concentrations of the reactive PEG in this dissertation was significantly less than that employed in previous studies that demonstrated an effect [162, 182]. Lower solution concentrations were used because of concerns over the increased osmolarity of the 20% (w/v) reactive PEG solutions and its effect upon cells (APPENDIX B). However, this should not be a major concern on denuded vascular surfaces with exposed extracellular matrix and few cells. Increasing the modifying solution concentrations could increase the PEG coverage on the vascular surface and might improve its ability to inhibit restenosis.

The conformation of the PEG chains on the vascular surface is another factor that could have affected its ability to inhibit restenosis. From the cell modification studies, it was estimated that most of the PEGs were likely in a mushroom conformation (APPENDIX C). The density of the covalently grafted PEGs on the surface needed to be increased in order for the chains to interact with one another and extend farther from the surface (APPENDIX C). A thicker PEG layer extending from the vascular surface should provide increased protection from protein and platelet deposition, which may increase its ability to inhibit restenosis. This relates to the concentration of the reactive PEG solutions. More concentrated reactive PEG solutions should lead to denser coverage and a thicker barrier layer. The actual number and density of PEG molecules reacted onto injured vascular surfaces is unknown so it is difficult to speculate on the density and thickness of the polymer layer.

Another possibility that may have affected the PEG layers ability to inhibit restenosis is the balloon injury model utilized in these studies. As mentioned, there was a high incidence of

complete vessel occlusion in the restenosis studies. Perhaps this was an indication that the embolectomy catheter balloon injury model employed here was too severe to evaluate the effects of PEG modification on preventing restenosis. Further studies are necessary to provide more insight into the factors that limited the ability of the PEG modification to inhibit restenosis.

In summary, protein-reactive PEG could be used to modify balloon injured vascular surfaces in a clinical setting. Substantial modification is possible at physiologic pH and temperature with brief incubation periods, important for time-sensitive intravascular procedures. Furthermore, the protein-reactive PEG could be easily applied to vascular surfaces using a channeled drug delivery catheter, which could perform angioplasty of an occluded vessels and delivery of the polymer simultaneously. Modification of balloon injured vascular surfaces with reactive PEG alone did not show a marked reduction in restenosis; however, this ability could be augmented by delivery of pharmaceutics or cells to the injured surface. The next chapter investigates the ability of the PEG-biotin modification to serve as a target for the site-specific delivery of microspheres and endothelial cells.

7.0 *IN VIVO* TARGETING TO PEG-MODIFIED VESSELS

7.1 INTRODUCTION

In addition to blocking thrombosis at sites of vascular injury, it would be advantageous to have a means of targeting intravenously injected agents to labeled vascular segments for further therapeutic benefit. Modifying vascular surfaces with a reactive PEG could serve various functions. The reactive PEG could be employed to form a molecular barrier on damaged vascular surfaces to inhibit platelet deposition [162, 182]. In addition, vascular surfaces labeled with a reactive PEG could be utilized as a site-specific target to deliver agents to the modified locations. A tag, such as biotin, on one end of the PEG molecule could facilitate the capture of therapeutic agents conjugated to avidin or one of its derivatives. PEG-biotin modified surfaces could provide a target for the delivery of proteins, drugs, microspheres, or cells. It would be beneficial to deliver anti-mitotic or anti-inflammatory therapeutics to sites of vascular injury such as those found after balloon angioplasty, carotid endarterectomies, and anastomoses. Furthermore, it might be possible to deliver chemotherapeutic agents to PEG-biotin modified tumor vasculature. The data presented in this paper demonstrate the ability of modifying healthy and injured vascular tissue with a protein-reactive polymer for site-specific delivery of microspheres in a clinical setting.

7.2 METHODS

7.2.1 Surgical Procedure

The animal studies were completed following a protocol approval by the Institutional Animal Care & Use Committee of the University of Pittsburgh as described in Subsection 6.2.1.

7.2.2 Balloon Injury

Balloon injury was accomplished in the same manner as elucidated in Subsection 6.2.1.

7.2.3 PEG Modification of Balloon Injured Vessels

Modification of the arteries was accomplished using the same procedure as found in Subsection 6.2.3 except for the cell targeting experiments. For the cell targeting experiments, the 0.025 in outer diameter Micro-Renathane tubing was left in the vessel lumen following administration of the reactive PEG or vehicle. The 1 mL BD slip-tip disposable tuberculin syringe was replaced with a 3 mL BD Luer Lock syringe (Fisher Scientific, Pittsburgh, PA) filled with PBS. When the total incubation time for the polymer or vehicle in the artery reached 1 min, the un-reacted polymer or vehicle was flushed from the artery. Now, 1 mL sample of a 2 mg/mL sample of NeutrAvidin was loaded into a 1 mL BD slip-tip disposable tuberculin syringe. Next, the syringe was connected to the 27 G x ½ in BD PrecisionGlide needle inserted into the end of the tube to allow for addition of NeutrAvidin to bridge the PEG-biotin modified vessel surface and EPCs.

The NeutrAvidin solution was continuously flushed through the lumen of the common femoral artery for a period of 45 s. After addition of the NeutrAvidin, the Micro-Renathane tubing was withdrawn from the common femoral through the arteriotomy. Once the tube was

removed from the saphenous artery, a previously placed ligature was tightened where the saphenous artery branches off the femoral artery to prevent bleeding from the arteriotomy. When the total incubation time for the NeutrAvidin in the artery reached 1 min, the aneurysm clips were removed from the popliteal and common femoral arteries to restore blood flow through the femoral and remove any excess NeutrAvidin. Control arteries were treated in an identical manner except that the vehicle, PBS, was added instead of the NeutrAvidin.

7.2.4 Acute Studies

Acute studies were completed as described in Subsection 6.2.4.

7.2.5 Survival Studies

Survival studies were completed as described in Subsection 6.2.5.

7.2.6 PEG Modification of Uninjured Vessels

In the case of modifying healthy vasculature, the tip of a 30 G x ½ in BD PrecisionGlide needle (Fisher Scientific, Pittsburgh, PA) was bent to make a curved 90º angle and inserted into the common femoral artery lumen near the clamp for injection of the polymer for vessel modification. Again, an aliquot of PBS was added to a pre-weighed sample of NHS-PEG-biotin to make 1 mL of a 10 mM solution. The solution was mixed until the solid dissolved and then loaded into a 1 mL BD slip-tip disposable tuberculin syringe. Next, the syringe was connected to the curved needle and inserted into the lumen of the common femoral artery just before the aneurysm clip with the bevel facing toward the saphenous and popliteal branches. The polymer

was continuously flushed through the lumen of the vessel and out the site of the arteriotomy in the saphenous artery for a period of 45 s.

After addition of the polymer, the needle was carefully withdrawn from the common femoral artery and a small amount of Avitene Flour (Davol, Inc., Cranston, RI), a microfibrillar collagen hemostat, was placed at site of access to control bleeding. In addition, a previously placed ligature was tightened where the saphenous artery branches off the femoral artery. When the total incubation time for the polymer in the artery reached 1 min, the aneurysm clips were removed from the popliteal and common femoral arteries to restore blood flow through the femoral and remove any un-reacted polymer. Control arteries were treated in an identical manner except that the vehicle, PBS, was added instead of the reactive polymer.

7.2.7 *In Vivo* Microsphere Targeting

In the case of the 0 hr time point, intravenous access was already established at the beginning of the surgical procedure, which permitted administration of the microspheres. For the extended time points, the animals were anesthetized and an ear vein catheterized as described previously in the Surgical Procedure section. A bolus of 4.80×10^8 particles of yellow-green fluorescent Fluospheres NeutrAvidin labeled microspheres (Molecular Probes, Eugene, OR) in 1 mL of PBS was loaded into a 1 mL BD slip-tip disposable tuberculin syringe. An 18 G x 1 ½ in BD PrecisionGlide needle (Fisher Scientific, Pittsburgh, PA) was placed on the tip of the syringe and the needle inserted into an access port on the Venoset Microdrip IV set. The entire solution of microspheres was injected into the rabbit over a period of 30 s and then flushed with Lactated Ringers solution. The microspheres were allowed to circulate in the bloodstream of the rabbit for 1 hr before the vessels were harvested.

7.2.8 Isolation of EPCs

Endothelial Progenitor Cells (EPCs) were isolated from the bone marrow of euthanized rabbits [229]. Bone marrow was extracted from the hind limbs of rabbits and collected in a 50 mL conical tube (Fisher Scientific, Pittsburgh, PA). The bone marrow was then centrifuged at 220g for 5 min at room temperature and the supernatant removed. 20 mL of DMEM was added to the conical tube to mechanically disperse pellet. At this point, the dispersed cell suspension was passed through a 70 μm Cell Strainer (Fisher Scientific, Pittsburgh, PA) into a new 50 mL conical. Again, the bone marrow was centrifuged at 220g for 5 min at room temperature and the supernatant removed.

15 mL of HISTOPAQUE-1077 (Fisher Scientific, Pittsburgh, PA) was added to a new 50 mL conical tube. The marrow cell pellet was dispersed in 15 mL of DMEM and slowly added on top of the HISTOPAQUE-1077. The mixture was centrifuged at 400g for 30 minutes at room temperature. After completion, the opaque interface containing the mononuclear cells was transferred to a new conical tube and resuspended in 20 mL of DMEM. The bone marrow was centrifuged at 220g for 5 min at room temperature and the supernatant removed. Again, 20 mL of DMEM was used to resuspend the cell pellet, the suspension was centrifuged, and the supernatant removed. Next, the mononuclear cells were resuspended in 12 mL of EPC growth media and plated in a BD Falcon 75 cm^2 tissue culture flask for 1 hr to remove any differentiated, adhesive cells. After 1 hr, the non-adhered cells suspended in the media were removed from the flask and plated in a new BD Falcon 75 cm^2 tissue culture flask coated with 2 mL of a 50 μg/mL solution of fibronectin (Fisher Scientific, Pittsburgh, PA).

7.2.9 Modification of EPCs with PEG-biotin

Rabbit endothelial progenitor cells from bone marrow (REPCBM) grown in a BD Falcon 75 cm^2 tissue culture flask were labeled with a 5 μM CellTracker Orange CMTMR solution in EGM-2 media for 45 min in the incubator. After the incubation, the CellTracker Orange CMTMR solution was replaced with fresh EGM-2 media. Cells grown in the BD Falcon 75 cm^2 flask were removed from the flask using ReagentPack with trypsin and collected in a BD Falcon BlueMax Jr. 15 mL Graduated tube (Fisher Scientific, Pittsburgh, PA). The tube was then centrifuged at 220g for 5 min in a Sorvall Legend RT and the supernatant removed. The cell pellet was dispersed and modified with 1 mL of a 10 mM NHS-PEG-biotin solution for 1 min. After modification, 9 mL of PBS was added to the cell suspension and the tube vortexed. Again, the cell suspension was centrifuged at 220g for 5 min and the supernatant removed. Next, the cells were resuspended in 1 mL of PBS.

7.2.10 *In Vivo* Cell Targeting

In the case of the 0 hr time point, intravenous access was already established at the beginning of the surgical procedure, which permitted administration of the EPCs. A bolus of 2 million EPCs labeled with CellTracker Orange CMTMR in 1 mL of PBS was loaded into a 1 mL BD slip-tip disposable tuberculin syringe. An 18 G x 1 ½ in BD PrecisionGlide needle (Fisher Scientific, Pittsburgh, PA) was placed on the tip of the syringe and the needle inserted into an access port on the Venoset Microdrip IV set. The entire cell suspension was injected into the rabbit over a period of 30 s and then flushed with Lactated Ringers solution. The cells were allowed to circulate in the bloodstream of the rabbit for 1 hr before the vessels were harvested.

7.2.11 Vessel Harvest and Preparation

Vessel harvest and preparation protocols are the same as those found in Subsection 6.2.8.

7.2.12 Epi-Fluorescence Microscopy of Explanted Vessels

Epi-fluorescence microscopy evaluation of the explanted vessels was conducted in a similar fashion as that described in Subsection 6.2.9. The Fluospheres NeutrAvidin labeled microspheres were yellow-green fluorescent with excitation/emission spectra of 505 nm and 515 nm, respectively.

7.2.13 Statistical Analysis

Statistical analysis of the data acquired from the vessel images was performed using the Analysis Toolpak in Microsoft Excel. Data points are represented as mean values plus or minus their standard deviation (St Dev) as denoted in the figures. For the acute microsphere targeting studies, the control and treated groups were compared using an unpaired, two-sample Student's *t*-test assuming unequal variances using the two-tailed distribution and the p values calculated to determine significant variations. However, for the microsphere delivery experiments at 0, 24, 48, and 72 hrs, differences between control and treated groups at all time points were evaluated using a two-factor ANOVA with replication to determine statistical significance.

7.3 RESULTS

7.3.1 Targeted Delivery of Microspheres to Balloon Injured Vessels

The 1 μm diameter fluorescent microspheres were easily identifiable using epi-fluorescent microscopy and appear as the bright dots (Figure 7-1). Virtually no microspheres were observed binding to a remote un-manipulated carotid artery (Figure 7-1, A). The number of microspheres bound to untreated balloon injured (Figure 7-1, B) was significantly less than the number bound to NHS-PEG-biotin treated balloon injured (Figure 7-1, C) rabbit femoral arteries. However, there is a fair amount of non-specific binding of NeutrAvidin-coated microspheres adhering to untreated balloon injured rabbit femoral arteries (Figure 7-1, B).

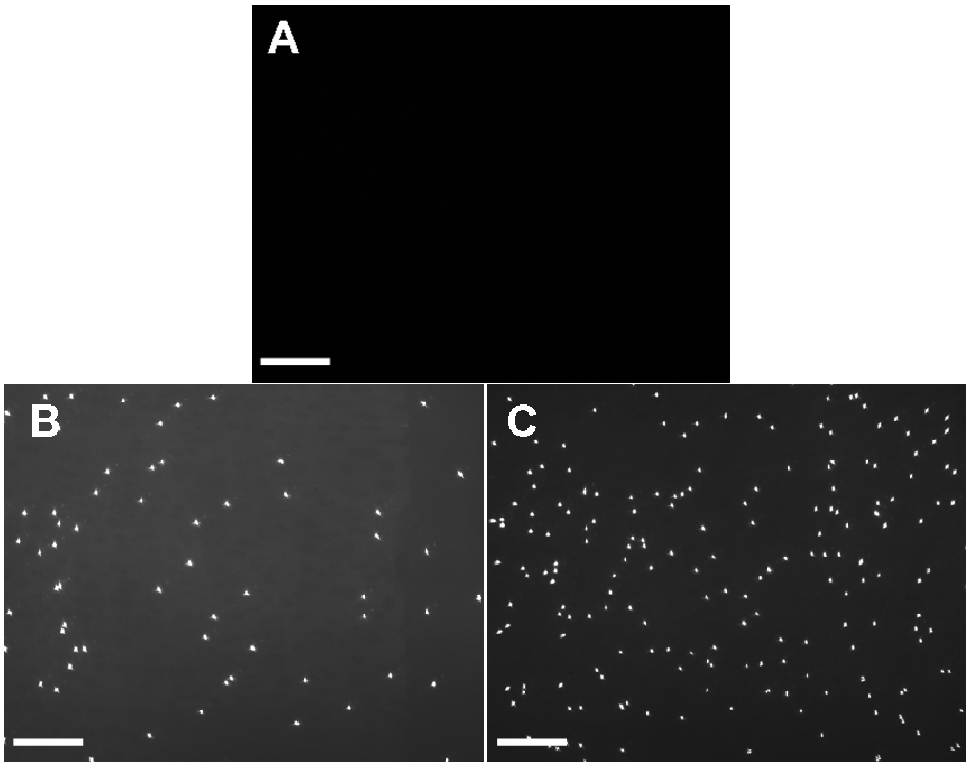

Figure 7–1 Micrographs of targeted microspheres adhering to (A) un-manipulated carotid, (B) balloon injured control femoral artery, and (C) PEG-biotin modified balloon injured femoral arteries at 0 hr. The scale bar is 100 μm.

Microsphere binding was quantified using an epi-fluorescent microscope to count the number of fluorescent microspheres per micrograph and normalizing the quantity to the number per mm^2 of vessel treated with the reactive PEG-biotin or the vehicle control. The microsphere binding data for acute delivery of NeutrAvidin-coated microspheres are summarized in Figure 7-2.

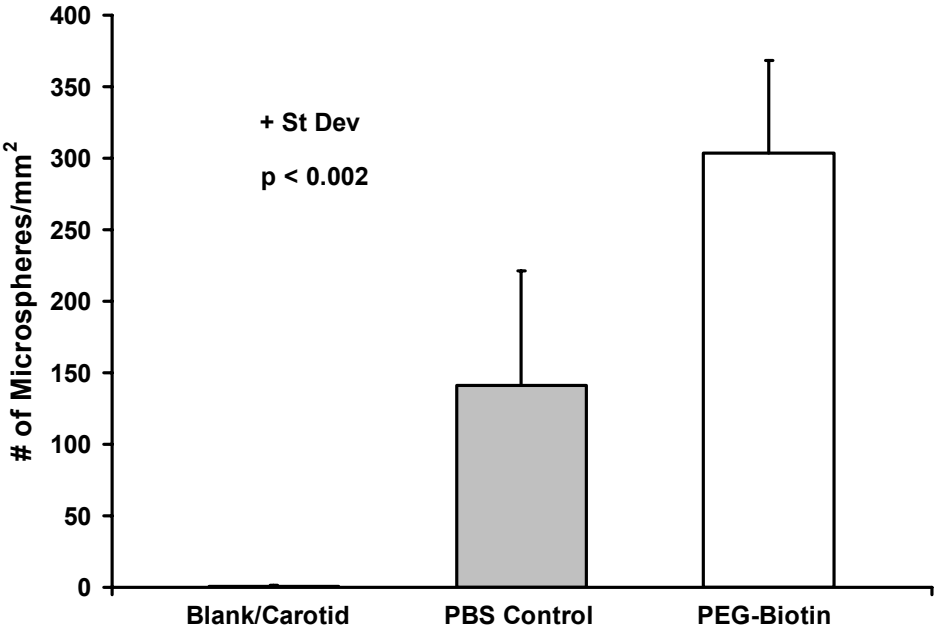

Figure 7–2 Number of targeted microspheres adhering to control and PEG-biotin treated balloon injured rabbit femoral arteries *in vivo at* 0 hrs. Data is shown +St Dev with n = 9 and the results are significant with p = 0.002.

It is evident that the microspheres are preferentially targeted to vascular tissue modified with the polymer as opposed to the uninjured and un-modified vascular surfaces. The microsphere binding to damaged arteries labeled with the polymer target was more than double that of the damaged, un-modified arteries. Microsphere binding to PEG-biotin modified, damaged arteries is 304 microspheres per mm^2 as compared to 113 microspheres per mm^2 for the damaged, un-modified control and only about 1 microsphere per mm^2 for an undamaged, un-modified artery.

All of the results are significant with $p < 0.002$. It is evident that the microspheres are preferentially targeted to vascular tissue modified with the polymer as opposed to the uninjured and un-modified vascular surfaces. However, there was a fair amount of non-specific binding of the microspheres to un-modified, but injured vascular surfaces.

Chapter 6 established that the polymeric coverage was maintained for a minimum of 72 hrs on the balloon injured vascular surface. As a result, it would be desirable to evaluate if targeted microspheres could be delivered to the polymer over the same time frame. This would enable continuous or repeated administration of the pharmacologic agents or vectors to the site of vascular injury for increased therapeutic benefit.

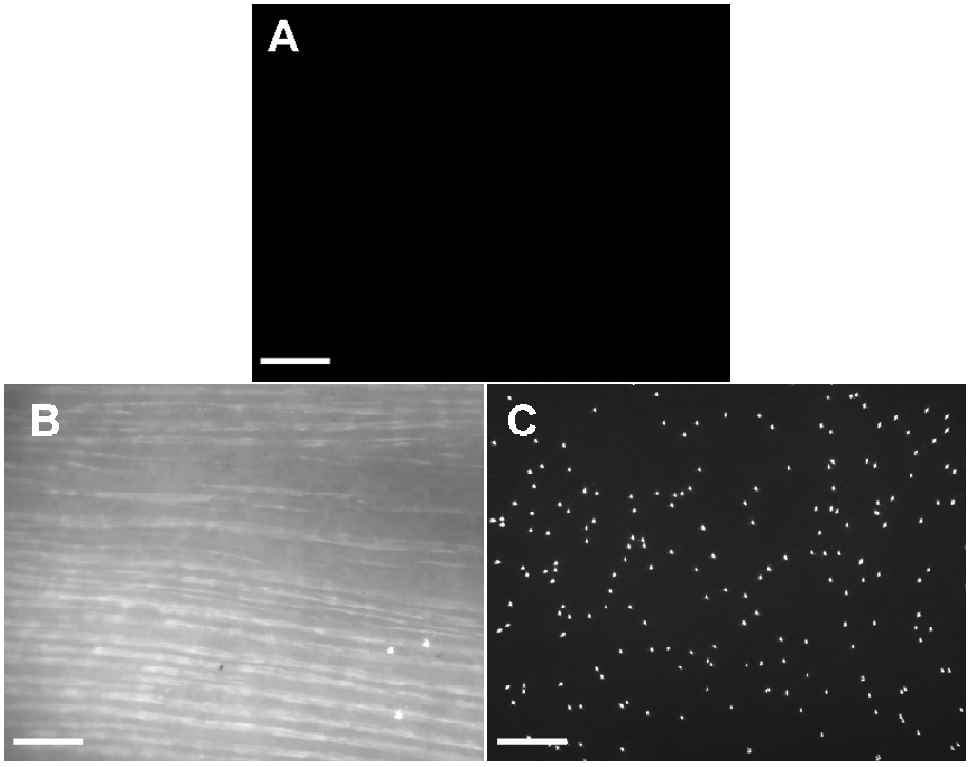

Figure 7–3 Micrographs of targeted microspheres adhering to (A) un-manipulated carotid, (B) balloon injured control femoral artery, and (C) PEG-biotin modified balloon injured femoral arteries at 0 hr. The scale bar is 100 μm.

Figure 7-3 shows some representative micrographs of NeutrAvidin-coated microsphere binding to control and PEG-biotin treated rabbit femoral arteries at extended times (24, 48, and 72 hrs). Again, practically no microspheres were observed binding to a remote un-manipulated carotid artery (Figure 7-3, A). The number of microspheres bound to untreated balloon injured (Figure 7-3, B) was significantly less than the number bound to NHS-PEG-biotin treated balloon injured (Figure 7-3, C) rabbit femoral arteries. At extended times, the non-specific binding to balloon injured rabbit femoral arteries (Figure 7-3, B) was substantially reduced as compared to the acute data (Figure 7-1, B). At all time points, the number of NeutrAvidin-coated microspheres adhering to PEG-biotin treated balloon injured femoral arteries was greater than the quantity binding to untreated balloon injured femoral arteries (Figure 7-4).

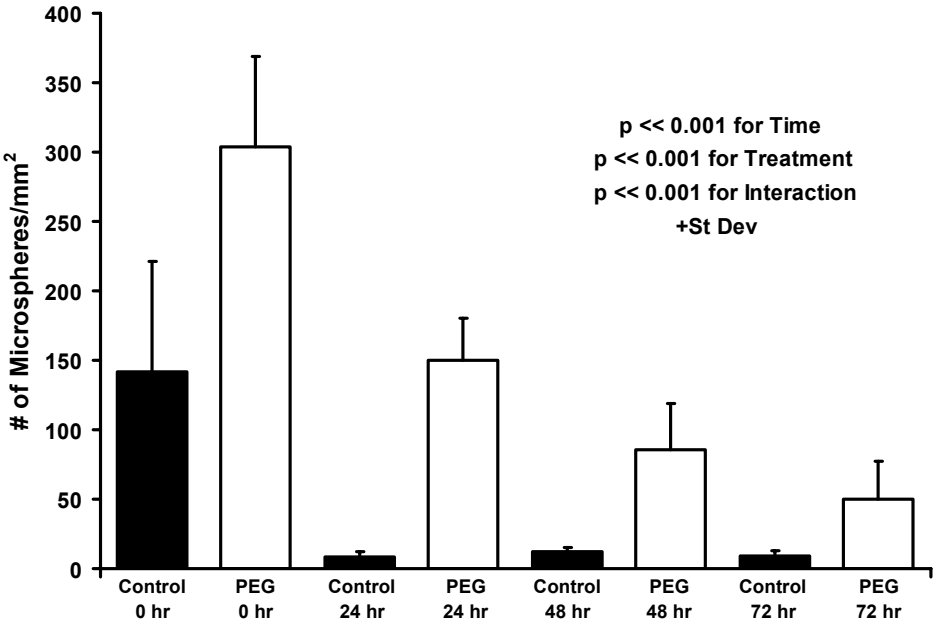

Figure 7–4 Number of targeted microspheres adhering to control and PEG-biotin treated, balloon injured rabbit femoral arteries *in vivo* at 0, 24, 48, and 72 hrs post-modification. Data is shown +St Dev with n = 4 at all times and treatments and the results are significant with p << 0.001 for the delivery time, treatment, and interaction.

As mentioned before, a total of 304 microspheres per mm^2 bound to PEG-biotin modified balloon injured femoral arteries as compared to 113 microspheres per mm^2 for the injured, un-modified control at 0 hrs (Figure 7-4). Some non-specific binding of NeutrAvidin-coated microspheres to injured, un-modified femoral arteries was observed at 0 hrs (Figure 7-4). The total number of adherent microspheres to PEG-biotin modified, balloon injured arteries decreased as the time post-modification increased (Figure 7-4). However, the ability to target NeutrAvidin-coated microspheres was maintained for a minimum of 72 hrs (Figure 7-4). At 24 hrs, the number of adherent microspheres to PEG-biotin modified, balloon injured arteries was 150 per mm^2 (Figure 7-4). This number further decreased to 86 at 48 hrs and 50 at 72hrs (Figure 7-4). In comparison, the non-specific binding of NeutrAvidin-coated microspheres diminished sharply to an average of 10 microspheres per mm^2 at all times greater than 0 hrs (Figure 7-4). This data confirmed that the NeutrAvidin-coated microspheres were preferentially targeted to PEG-biotin modified as opposed to control balloon injured rabbit femoral arteries. In addition, the ability to target microspheres to the polymer modified vascular surfaces was maintained for a minimum of 72 hrs.

The ANOVA performed on the microsphere targeting data revealed that the mean number of microspheres per mm^2 varied with the treatment (untreated vs. NHS-PEG-biotin) as well as the delivery time post-modification (0, 24, 48, and 72 hrs) with a significance value of $p << 0.001$ (Figure 7-4). In addition, the ANOVA demonstrated that there was interaction between the treatment and delivery time with a significance of $p << 0.001$ (Figure 7-4). The number of adherent microspheres per mm^2 decreased sharply from 0 to 24 hrs and then remained constant out to 72 hrs for untreated injured (Figure 7-4). Furthermore, the number of microspheres per

mm^2 binding to the NHS-PEG-biotin treated femoral arteries decreased as the time before targeted delivery of the microspheres increased (Figure 7-4).

7.3.2 Targeted Delivery of Microspheres to Uninjured Vessels

In addition to targeting pharmaceuticals to sites of vascular injury, we evaluated the ability of using the same targeting strategy to target agents to healthy vascular tissue, which would be applicable for delivering chemotherapeutics to tumor vasculature. This application was evaluated by addition of the reactive polymer or vehicle control to uninjured rabbit femoral arteries as described in the Materials and Methods section. As was the case with targeting to balloon injured arteries, the NeutrAvidin-coated microspheres were preferentially targeted to uninjured rabbit femoral arteries modified with the polymer as opposed to the un-modified arteries (Figure 7-5).

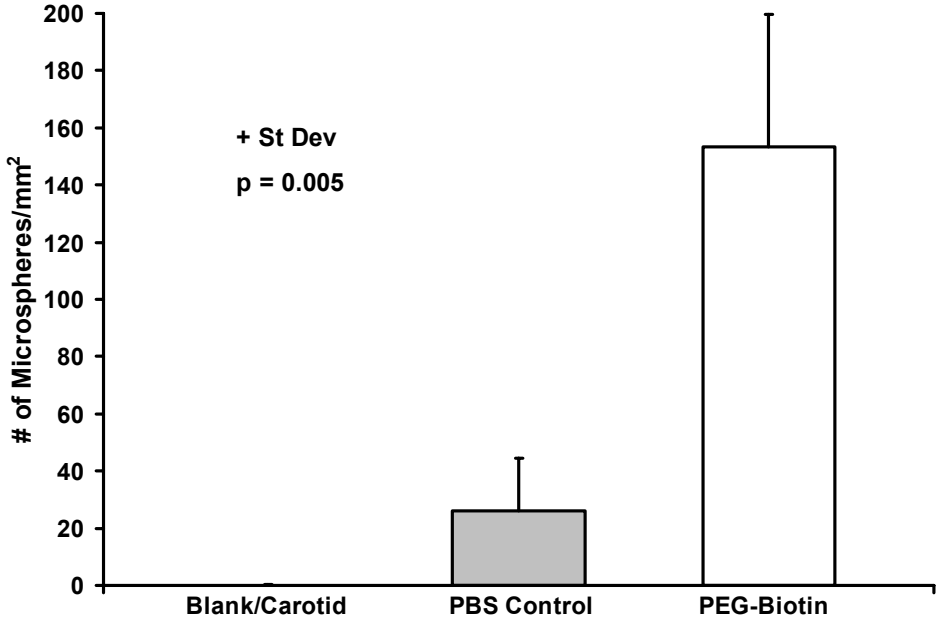

Figure 7–5 Number of targeted microspheres binding to control (vehicle) and PEG-biotin treated uninjured rabbit femoral arteries *in vivo* at 0 hrs. Data is shown +St Dev with n = 5 and the results are significant with p = 0.005.

A total of 153 microspheres per mm^2 bound to PEG-biotin modified uninjured femoral arteries as opposed to only 26 microspheres per mm^2 for the un-modified control at 0 hrs ($p = 0.005$) (Figure 7-5). The total number of microspheres adhering to PEG-biotin modified uninjured rabbit femoral arteries at 0 hr (Figure 7-5) was less than that seen with the PEG-biotin modified, balloon injured arteries (Figure 7-2). However, the difference in targeting between the control and polymer modified vessel surfaces was greater for the uninjured (Figure 7-5) as opposed to the balloon injured femoral arteries (Figure 7-2).

7.3.3 Targeted Delivery of Cells to Balloon Injured Vessels

No EPCs were evident on control or PEG-biotin modified balloon injured rabbit femoral arteries after intravenous injection of REPCBM for a 1 hr circulation period (Figure 7-6, A). This experiment was repeated additional times with no success. As a result, PEG-biotin labeled REPCBM were injected into the vessel lumen using the Micro-Renathane tube for a stagnant 1 min incubation following the NeutrAvidin incubation and rinse with 3 mL of PBS to see if the cells were able to adhere. Following the stagnant incubation, the majority of the femoral artery surface was covered with REPCBM; however, blood reflow through the femoral artery was not reestablished in this instance (Figure 7-6, B). Once blood reflow was restored 1 hr following a stagnant 1 min incubation with the PEG-biotin modified REPCBM, few, if any, EPCs remained on the artery surface (Figure 7-6, C). The EPCs were unable to withstand the shear force caused by the fluid flow through the femoral artery. Thus, initial attempts at targeted EPC delivery to modified vascular surfaces *in vivo* proved unsuccessful.

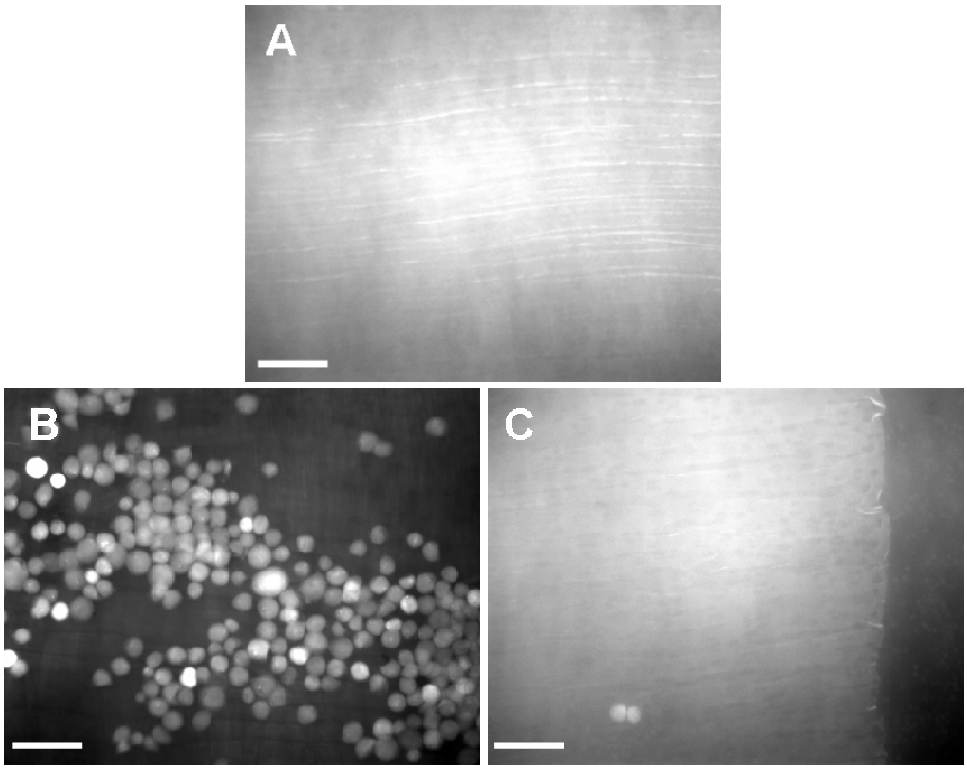

Figure 7–6 Micrographs of targeted EPCs adhering after (A) intravenous injection, (B) stagnant incubation, and (C) 1 hr of blood reflow following a stagnant incubation on PEG-biotin modified balloon injured femoral arteries. The scale bar is 100 µm.

7.4 DISCUSSION

The results presented in this chapter confirmed that the proposed intravascular modification and targeted delivery system was clinically applicable. Modification of vascular surfaces with the protein-reactive PEG was demonstrated in the preceding chapter. These data verified that targeted microspheres were preferentially delivered to vascular sites labeled with PEG-biotin following intravenous administration. Furthermore, this ability to deliver agents to PEG-biotin modified vascular surfaces was retained for a minimum of 72 hrs. Additional studies showed that the microspheres were targeted to uninjured vascular endothelium as well.

The overall ability to deliver microspheres to PEG-biotin modified balloon injured rabbit femoral arteries appears limited. However, the results presented in this dissertation fall in line with other targeted delivery systems. Strategies utilizing microspheres targeted to E- and P-selectin demonstrated significantly worse delivery of only an average of 30 microspheres/mm^2 [78, 222, 223]. The number of NeutrAvidin-coated microspheres adhering to PEG-biotin modified vascular surfaces was up to 10 times that found with selectin-modified microspheres. Another targeting strategy focused on targeting ultrasound contrast microbubbles to endothelial receptors upregulated during inflammation [216, 217, 219, 220]. This approach demonstrated adherence of up to 10 microbubbles per cell [216, 217, 219, 220]. It is important to note, however, that the some of the microbubble targeting protocols used particle solutions that were up to 100 times more concentrated [216, 217, 219, 220]. In addition, some of the binding experiments were stagnant incubations and not deposited under flow.

The effectiveness of the intravascular modification and targeting system investigated in this dissertation might be increased by using more concentrated microsphere solutions or continuous or multiple administration of the microspheres. Furthermore, the generality of the targeted delivery system would permit delivery of multiple agents simultaneously or on a defined schedule due to the extended ability to target. All of these parameters could be evaluated and modified based on what therapeutic agent is delivered and what quantity is necessary to produce a beneficial effect. Even so, the ability to deliver microspheres to PEG-biotin modified damaged vascular surfaces serves as a model for the targeted administration of particulate drugs, liposomes, or viral vectors for the treatment of various vascular maladies.

A propagation of error analysis provides an estimate of the uncertainty in the calculation of the number of microspheres per mm^2 of vascular surface. The number of microspheres per area

is computed from measured quantities that have their own associated error. As a result, the error in the measured quantities carries over into the computed number of microspheres or cells per mm^2 of the vascular surface. The procedure for determining the error propagation in the computed quantities based on the error in the measured quantities is illustrated in APPENDIX D. In the case of calculating the number of microspheres or cells per vascular surface area, the detailed propagation of error analysis is presented in APPENDIX G. For the *in vivo* animal studies, the uncertainty in the calculated number of microspheres per mm^2 vascular surface is 3.0%.

The intravascular modification and targeted delivery system under investigation in this dissertation is applicable to local administration of pharmaceutics or vectors to injured vascular surfaces to inhibit thrombosis and restenosis. Local delivery of drugs, and vectors can be accomplished using specialized drug delivery catheters that employ passive, pressure-driven, electrically, or mechanically enhanced diffusion for delivery [84, 230, 231]. The protein-reactive PEG investigated here could be delivered with one of these specialized drug delivery balloon catheters. However, the polymer coating should act as a barrier, preventing platelet deposition, as well as providing a site for the targeted delivery of intravenously administered therapeutics over extended times. Using the drug delivery catheters for direct delivery of the agents only allows for one application. Another approach used delivery of losatran from fibrin glue applied at the site of vascular injury to prevent restenosis [124]. The difficulties with using fibrin glue are that elution of the entrapped agent occurred very rapidly preventing long-term delivery and the technique cannot be used with angioplasty because it requires vessel access [124].

Local delivery of therapeutics is also possible by targeting the molecules or using targeted carriers to direct the therapy to specific vascular segments. One such method targets heparin or

low molecular weight heparin conjugated to antibodies against cross-linked heparin, which is deposited at the site of arterial injury, to reduce neointima formation [75]. Another method targets microspheres or particles to selected vascular sites using antibodies to exposed surface markers. Hyaluron microspheres conjugated to antibodies against E- and P-selectin preferentially adhered to inflammatory vascular sites and successfully delivered plasmid DNA [81]. Similarly, biodegradable particles conjugated to antibodies for E- and P-selectin, ICAM-1, and VCAM-1 also showed targeting to inflamed endothelium [78]. Unlike the methods described here, our targeting molecule forms a molecular barrier to initially inhibit platelet deposition [182]. In addition, we can target therapeutic agents to specific vascular segments using a tag on the end of the polymer molecule. Using the protein-reactive PEG as described in our system permits modification of healthy endothelium or exposed matrix following vascular injury. This allows for the treatment of more conditions and is not dependent upon the expression and availability of specific surface markers that are up-regulated in certain disease states, but still commonly found at various levels in healthy vasculature.

The sirolimus (CYPHER, Cordis J&J) and paclitaxel (TAXUS, Boston-Scientific) drug-eluting stents have demonstrated significant promise in preventing restenosis. Randomized-controlled trials have demonstrated a reduction in the need for repeat revascularization after coronary interventions by 60-80% when using drug-eluting stents [52]. However, long-term results of the effects of drug-eluting stents are still unknown and some complications and reservations have surfaced. As the drug-eluting stents are applied to more complex lesions, there have been increasing occurrences of late stent thrombosis [56, 58]. The polymer substrate for delivery of the drug has also come under scrutiny. There are numerous reports suggesting a possible hypersensitivity reaction to the polymer coating on the stents resulting in extensive

inflammation of the vessel wall [56, 58, 59]. Modification of injured vascular surfaces with our protein-reactive polymer provides another strategy that could even be used in conjunction with drug-eluting stents to further improve outcomes of coronary interventions.

Initial attempts to deliver EPCs were unsuccessful. No EPCs were found at modified vascular sites following intravenous administration and locally administered EPCs did not remain after reestablishment of blood flow. Further investigation is required to determine if a more suitable cell source or delivery protocol could assist in targeting and adherence of endothelial cells to assist in re-endothelialization of the injured vascular surface.

In conclusion, the data presented in this chapter establish the efficacy of the proposed intravascular modification and targeted delivery system examined in this dissertation. Furthermore, the successful delivery of microspheres to PEG-biotin modified vascular surfaces *in vivo* provides direct evidence of its clinical applicability. The results confirmed that targeted microspheres are preferentially delivered to vascular sites labeled with PEG-biotin following intravenous administration. Furthermore, the ability to deliver agents to PEG-biotin modified vascular surfaces is retained for a minimum of 72 hrs. Additional studies showed that microspheres could be targeted to uninjured vascular endothelium modified with PEG-biotin as well. Unfortunately, intravenously or locally administered EPCs could not be delivered or retained on PEG-biotin modified surfaces *in vivo*.

8.0 SUMMARY

8.1 CONCLUSIONS

Platelet deposition and restenosis are common problems associated with intravascular procedures such as anastomoses, balloon angioplasty, and carotid endarterectomies. As a result, it would be beneficial to have a treatment following these types of procedures that could protect the damaged vascular surface from thrombus formation, deliver a site-specific therapeutic agent, re-endothelialize the denuded surface, or any combination of these at the site of injury. Reactive PEG modification of vascular surfaces has already been shown to inhibit platelet deposition on injured vascular surfaces. Additionally, delivery of targeted pharmaceuticals or vectors to the injured vessel could provide local anticoagulation, anti-mitotic activity, or gene therapy further inhibiting vascular thrombosis and restenosis at the injury site until re-endothelialization occurs naturally. Furthermore, the targeting system could be exploited to deliver endothelial cells to the denuded vascular wall speeding re-endothelialization of the injured surface to expedite the healing process and assist in preventing re-occlusion.

In conclusion, we demonstrated that a protein-reactive PEG could be used to covalently modify healthy and injured vascular tissue. On a damaged vascular surface, the PEG creates a molecular barrier that inhibits platelet deposition [181, 182]. The ability of PEG modification to inhibit restenosis in the injured vessel still needs further investigation. Furthermore, by attaching

a specific tag molecule (biotin) at the terminus of the polymer, we were able to target microspheres and cells to the labeled vascular tissue. The microspheres represent a model drug carrier that could be loaded with various agents to treat numerous maladies. In the case of vascular injury, such as with balloon angioplasties or carotid endarterectomies, anti-thrombotic or anti-mitotic agents could be delivered to inhibit neointimal hyperplasia. In addition, since the targeting strategy labeled healthy endothelium as well, it might be used to target chemotherapeutic agents to tumor vasculature. Finally, the targeting strategy might also be employed to speed re-endothelialization at the site of vascular injury by targeting harvested endothelial or endothelial progenitors to the injured site following an intravascular procedure.

8.2 FUTURE WORK

Additional studies are needed to investigate the polymeric barrier and attempt to quantify the extent of modification *in vivo* to enable a better understanding of the surface coverage. Perhaps using longer MW or branched reactive PEGs would provide a more effective and durable barrier that could help reduce neointima formation in the long term. Just recently Nektar Therapeutics began production of NHS-PEG-biotin MW 5,000. All previous formulations of NHS-PEG-biotin that were used in this dissertation were MW 3,400. In addition, it would be beneficial and provide further support to the targeting concept if the ability to deliver pharmaceutical agents or vectors could be demonstrated *in vivo*. Such an approach might ultimately produce more favorable results in restenosis experiments.

Reactive PEG modification as a molecular barrier or targeting system has broader applications than just intravascular procedures such as anastomoses, angioplasty, and

endarterectomies. PEG modification of tumor vasculature could be used as a target for the delivery of chemotherapeutic agents to decrease systemic toxicity. In addition, PEG modification might be used to prevent rejection of organs or cells following transplantation. PEG modification could provide a molecular barrier temporarily masking antigenic determinants. Moreover, the reactive PEG could also be employed to target anti-rejection agents to the transplanted cells or organs and reduce systemic immunosuppression, which leads to an increased risk of infection and specific forms of cancer. The applicability of the intravascular modification and targeting strategy developed here should be evaluated as possible therapeutic avenues in the treatment of malignant neoplasms or cell, tissue, and organ rejection.

APPENDIX A

NOMENCLATURE

Abbreviations

ACE	Angiotensin-converting enzyme
ACS	Acute Coronary Syndromes
ADA	Adenosine Deaminase
bFGF	Basic Fibroblast Growth Factor
BM	Bone Marrow
BSA	Bovine Serum Albumin
CABG	Coronary Artery Bypass Grafting
CEA	Carotid Endarterectomies
CMAC	7-amino-4-chloromethylcoumarin
CMTMR	5-(and -6)-(((4-chloromethyl)benzoyl)amino) tetramethylrhodamine
CTB	CellTracker Blue CMAC
CTO	CellTracker Orange CMTMR
DES	Drug-Eluting Stents
DMEM	Dulbecco's Modified Eagle's Medium
EBM	Endothelial Basal Media

EC	Endothelial Cell
ECM	Extracellular Matrix
EDTA	Ethylenediaminetetraacetate
EEM	External Elastic Membrane
EGM	Endothelial Growth Media
EPC	Endothelial Progenitor Cell
FACS	Fluorescence-Activated Cell Sorting
FBS	Fetal Bovine Serum
FDA	Food and Drug Administration
FITC	Fluorescein Isothiocyanate
Fl	Fluorescein
F/P	Fluorescence to Protein
G-CSF	Granulocyte Colony-Stimulating Factor
GM-CSF	Granulocyte-Macrophage Colony-Stimulating Factor
HBSS	Hank's Balanced Salt Solution
HCAEC	Human Coronary Artery Endothelial Cell
IEM	Internal Elastic Membrane
IFN	Interferon
IgG	Immunoglobulin G
LDL	Low-Density Lipoprotein
LDL-C	Low-Density Lipoprotein-Cholesterol
LIMA	Left Internal Mammary Artery
LMWH	Low Molecular Weight Heparin

ln	Natural Logarithm
LS	Lumen Surface
M	Media
MESF	Molecules of Equivalent Soluble Fluorophore
MI	Myocardial Infarction
MMP	Matrix Metalloproteinase
MW	Molecular Weight
N	Neointima
n	Sample Size
NADH	Nicotinamide Adenine Dinucleotide
NHS	N-Hydroxysuccinimide
NO	Nitric Oxide
PBS	Phosphate Buffered Saline
PCI	Percutaneous Coronary Intervention
PEG	Polyethylene Glycol
PSGL	P-Selectin Glycoprotein Ligand
PTCA	Percutaneous Transluminal Coronary Angioplasty
R^2	Coefficient of Determination
REPCBM	Rabbit Endothelial Progenitor Cells from Bone Marrow
RGD	Arginine(Arg)-Glycine(Gly)-Aspartic Acid(Asp)
RHMVEC	Rat Heart Microvessel Endothelial Cell
SCID	Severe Combined Immunodeficiency Disease
SEM	Standard Error of the Mean

SMC	Smooth Muscle Cell
StDev	Standard Deviation
t	Time
T-E	Trypsin/EDTA
TIA	Transient Ischemic Attack
TNS	Trypsin Neutralizing Solution
VEGF	Vascular Endothelial Growth Factor
VSMC	Vascular Smooth Muscle Cell
(w/v)	Weight per Volume

Units

Å	Angstrom
cm	Centimeter
cp	Centipoise
dL	Deciliter
dyne	Dyne
g	Gram
hr	Hour
kg	Kilogram
L	Liter
min	Minute
mL	Milliliter
mM	Millimolar

mm Millimeter

mOsm Milliosmoles

N Newton

nm Nanometer

p Poise

pN PicoNewton

s Second

μL Microliter

μM Micromolar

μm Micrometer

Symbols

α Alpha

β Beta

$\dot{\gamma}$ Shear Rate

τ Shear Stress

τ_{ij} Stress in j Direction on a Face Normal to the i axis

μ Viscosity

ρ Density

π Pi

∞ Infinity

A Area

C_1 Arbitrary Constant

C_2	Arbitrary Constant
Ca	Calcium
D	Diameter
f(i)	Function of i
h	Height
L, l	Length
ℓ	Monomer Length
N	Degree of Polymerization
p	Pressure
Δp	Pressure Gradient
Q	Volumetric Flow Rate
R	Radius
R_f	Flory Radius
Re	Reynolds Number
S	Surface
s	Distance Between Polymer Graft Sites
V	Volume
v_i	Velocity in the i Direction
w	Width

APPENDIX B

OSMOLARITY OF PEG SOLUTIONS

Previous modification studies, completed in our lab, routinely employed protein-reactive PEG solution concentrations of 20% (weight, w/volume, v) or 0.2 g/mL [162-164, 181, 182]. However, we experienced difficulties when trying to use that concentration on cultured ECs. A large number of cells would shrivel and detach from the 12 well tissue culture plate before completion of the experiment. As a result, there were not enough cell counts to analyze using quantitative flow cytometry. It was postulated that the observed cell changes were a result of increased osmolarity associated with the protein-reactive PEG solutions as compared to the vehicle (PBS) when incubated on the cultured cells.

The extracellular fluid has a profound effect on the cell volume of animal cells [2, 184]. When a cell is placed in an isotonic (isosmotic) solution, there is no net change in water movement across the cell membrane and the cell volume remains constant (Figure B-1, B) [2, 184]. If a cell is placed in a hypertonic (hyperosmotic) solution, one that has a greater osmotic concentration than the cell, there is a net flow of water out of the cell causing the cell to shrivel (crenate), which can possibly lead to cell death (Figure B-1, A) [2, 184]. Contrastingly, when a cell is placed in a hypotonic (hyposomotic) solution, one that has a lower osmotic concentration than the cell, there is a net influx of water into the cell causing the cell to swell (Figure B-1, C)

[2, 184]. In hypotonic solutions, cell membranes may burst (lyse) when the water buildup inside the cell is excessive due to the difference in osmolarity of the cell and the solution (Figure B-1, C) [2, 184].

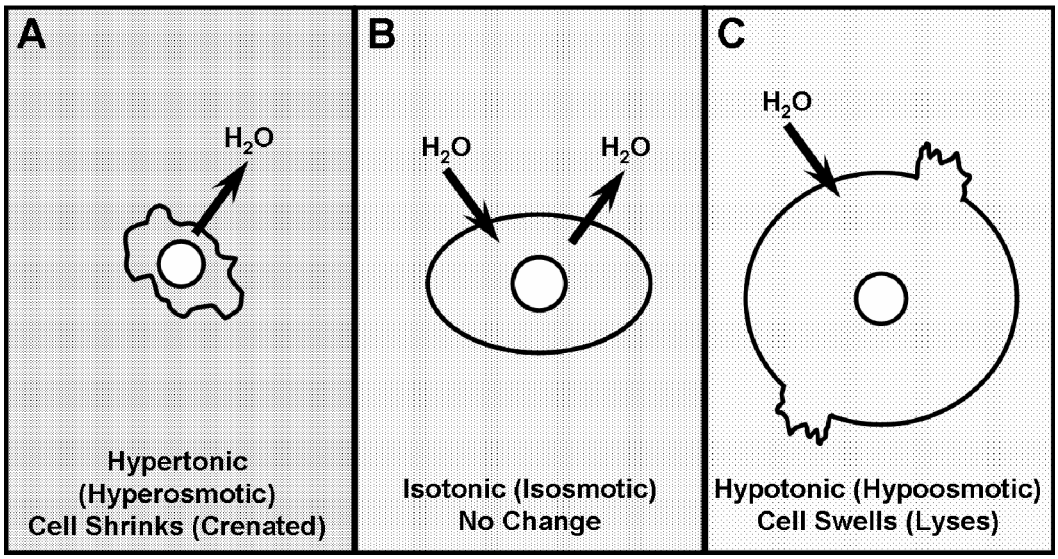

Figure B–1 Cell volume changes as a result of different extracellular fluid environments. (A) Cells shrink in a hypertonic, (B) remain unchanged in an isotonic, and (C) swell or lyse in a hypotonic environment.

Varying solution concentrations of NHS-PEG-biotin were prepared by dissolving the protein-reactive polymer in PBS. The osmolarity of the various solutions were determined by analysis on an Osmette II Osmometer (Fisher Scientific, Pittsburgh, PA) and the results given as milliosmoles (mOsm)/kg of H_2O or liter (L). The normal osmolarity of intracellular fluid is 280 mOsm/L [2]. NHS-PEG-biotin solutions of 0, 0.78, 1, 5, and 10% (w/v) were prepared by dissolving pre-weighed samples of the protein-reactive polymer with PBS. Aliquots of 0.5 mL of each concentration were loaded into the Osmette II Osmometer to determine the osmolarity of each solution concentration tested. A 20% (w/v) sample was not tested because of the cost

associated with that large a quantity of the polymer. The results are presented in Table B-1 displaying the osmolarity of the particular solution concentrations.

Table B–1 Osmolarity of NHS-PEG-biotin Solutions

Solution Concentration (w/v %)	Solution Concentration (mM)	Osmolarity (mOsm/L)
0	0	275
0.78	2.29	285
1	2.94	288
5	14.7	386
10	29.4	725

It is apparent that even at 10% (w/v), one-half the normal concentration used in previous studies [162-164, 181, 182], the solution is exceptionally hypertonic with an osmolarity more than 2.5 times normal. A 20% (w/v) solution would have an even greater osmolarity. A hypertonic NHS-PEG-biotin solution as demonstrated here (Table B-1) placed on cultured cells would cause an outflow of water from the cell leading to shrinkage and detachment of the cells from the tissue culture plates. These results confirmed that NHS-PEG-biotin solution concentrations, as employed previously, were extremely hypertonic, which would explain the difficulties experienced in completing the concentration studies. Consequently, all of the experiments completed in this dissertation utilized NHS-PEG-biotin solution concentrations of 10 mM (3.4 %) to minimize the effects of the osmolarity of the polymer solutions on cell surfaces.

APPENDIX C

PEG CHAIN CONFORMATION

The structure of PEG molecules covalently linked to surfaces varies depending upon the distance between the attachment sites and the surface properties [153, 214, 232]. The three basic structures, pancake, mushroom, and brush, are demonstrated in Figure C-1 [153, 214, 232].

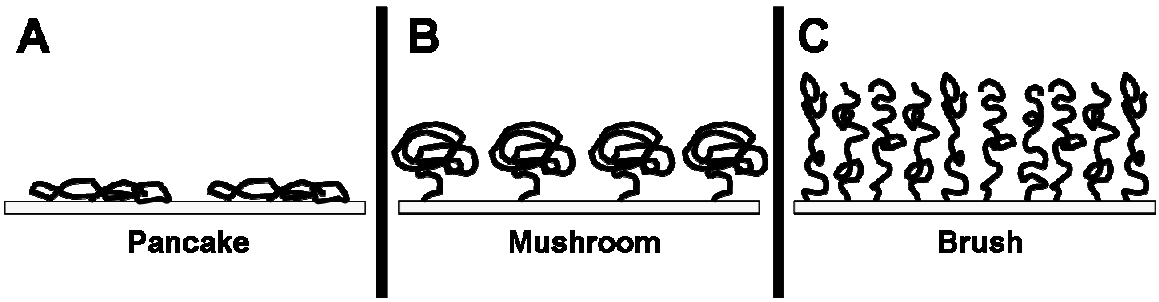

Figure C–1 Cell Illustrations of possible PEG structures, (A) pancake, (B) mushroom, and (C) brush, grafted onto surfaces.

The pancake structure (Figure C-1, A) represents PEG molecules grafted onto extremely hydrophilic surfaces [232]. However, in the case of PEG attachment to lipid bilayers in a good solvent, such as the aqueous environment extracellular fluids, the PEG molecules will most likely extend away from the surface into the solvent in a mushroom (Figure C-1, B) or brush (Figure C-1, C) conformation [153, 214, 232].

If the PEG linkage sites are disperse, then the PEG molecules will not interact with one another and the molecules will take on the mushroom conformation (Figure C-1, B) [153, 214, 232]. In the mushroom regime, the size of the PEG molecule is given by the Flory radius (mushroom or half-sphere radius), which is calculated using Equation C-1 [153, 214, 233-235].

Equation C-1 Flory Radius

$$R_f = \ell \times n^{(3/5)}$$

In Equation C-1, the Flory Radius, R_f, is computed by multiplying the monomer length, ℓ, by the degree of polymerization , n, raised to the 0.6 [153, 214, 233-235]. For the molecule of interest, NHS-PEG-biotin MW 3,400, the monomer length, degree of polymerization, and calculated Flory radius appear in Table C-1.

Table C–1 Degree of Polymerization, Monomer Length, and Flory Radius of PEG MW 3,400

	NHS-PEG-Biotin MW 3,400
n	69
ℓ (nm)	0.35
R_f (nm)	4.44

Contrastingly, if the distance between PEG attachment sites is less than the Flory radius, the PEG molecules will interact with one another and the chains will extend away from the surface in a brush regime [153, 214, 232]. For the brush conformation, the distance between the covalently linked PEG molecules is less than the Flory radius and can vary depending upon the density of PEG molecules. In the case of homogeneous surfaces with known attachment sites and modification, the distance between PEG molecules can easily be determined. However, cell membranes present an inhomogeneous surface with lipids, proteins, and polysaccharides. As a result, it is exceedingly difficult to measure the distance between covalently linked PEG

molecules. In addition, the distance between attached PEGs should vary considerably since the protein-reactive PEG modifies cell surface and transmembrane proteins and not the other membrane constituents.

Assessing the distance between grafted PEG molecules on cell surfaces was beyond the scope of this dissertation, but it is possible to estimate the distance. The distance between PEG attachment sites could be estimated by dividing the number of PEG-biotin molecules per cell by the lumen area of the cells. This assumes equal spacing of the PEG molecules over the entire cell surface, which is unlikely due to its inhomogeneity. However, this assumption provides a basis for estimation of the distance between PEG molecules, which is useful for evaluating the probable structure of the PEG molecules, mushroom or brush, the layer thickness, and surface coverage.

Quantitative flow cytometry provided the number of PEG-biotin molecules per cell. The cell area could be approximated by counting the number of cells using a Hausser Bright-Line hemacytometer (Fisher Scientific, Pittsburgh, PA) and dividing by the growth area. For HCAECs, the lumen area per cell was estimated at 5,850 μm^2. The number of PEG-biotin molecules per cell following modification with a 10 mM solution was 7.96×10^7 and 11.0×10^7 for a 1 min and 5 min incubation, respectively. The area per PEG molecule, PEG_{Area}, can be calculated using Equation C-1.

Equation C-2

$$PEG_{Area} = \left(\frac{\text{Cell Area}}{\text{\# PEGs/Cell}} \right)$$

Assuming the PEG molecules projects a circular coverage area on the cell, the radius per PEG molecule, R_{PEG} is computed using Equation C-3.

Equation C-3

$$R_{PEG} = \sqrt{\frac{PEG_{Area}}{\pi}}$$

The distance, s, between PEG molecules is simply twice the radius of the PEG molecules as shown in Equation C-4.

Equation C-4

$$s = 2 \times R_{PEG}$$

Equations C-2, C-3, and C-4 are used to calculate the values for both the 1 and 5 min incubations and the results tabulated in Table C-2.

Table C–2 Area, Radius, and Distance of PEG Molecules

	Incubation Time (min)	
	1	**5**
Cell Area (nm^2)	5.85×10^9	5.85×10^9
# PEGs/Cell	7.96×10^7	11.0×10^7
PEG_{Area} (nm^2)	73.49	53.18
R_{PEG} (nm)	4.84	4.11
s (nm)	9.68	8.22

It is apparent that the distance between PEG molecules at 1 min (Table C-2) is greater than twice the Flory radius (Table C-1) so the PEGs should assume a mushroom conformation and the layer thickness approximates the Flory radius. After a 5 min incubation with the reactive PEG, the distance between covalently linked PEGs (Table C-2) is nearly equal to twice the Flory radius (Table C-1) so the PEGs begin to interact with one another and begin to transform into the brush regime [214]. These calculations assumed equidistant spacing of the PEG molecules, however, in reality, the PEG density could be significantly higher as the covalently linked PEGs are probably clustered on the proteins found on the cell membrane. Consequently, there may be

areas where the separation between neighboring PEG molecules is significantly less than twice the Flory radius and the PEG molecules assume a brush structure instead of the mushroom conformation. In the case of a concentrated PEG brush, the theoretical thickness, L, of the PEG layer can be calculated using Equation C-5 [214, 235].

Equation C-5

$$L = n \times \frac{\ell^{(5/3)}}{s^{(2/3)}}$$

As the distance between attached PEG molecules decreases, the thickness of the PEG layer increases. A thicker PEG layer should increase its effectiveness in preventing protein and cell adhesion.

APPENDIX D

PROPAGATION OF ERROR

Many physical quantities cannot be measured directly, but involve multiple steps to determine their value [236]. Often times one quantity can be calculated based on from other directly measurable quantities [236]. For instance, assume that λ is a computed quantity that can be calculated from α, β, and γ, which are other directly measurable or previously computed quantities. The uncertainty in the calculated or measured variables is given by σ. The basic equation for calculation of the propagation of error is given by Equation D-1.

Equation D-8-1

$$\sigma_\lambda^2 = \left(\frac{d\lambda}{d\alpha}\right)_{\beta,\gamma}^2 \sigma_\alpha^2 + \left(\frac{d\lambda}{d\beta}\right)_{\alpha,\gamma}^2 \sigma_\beta^2 + \left(\frac{d\lambda}{d\gamma}\right)_{\alpha,\beta}^2 \sigma_\gamma^2$$

The differentials in Equation D-1 indicate the effects of changes in α, β, and γ on λ. Equation D-1 can be used to determine the propagation of error for addition, subtraction, multiplication, and division of the measured quantities in the calculation of λ.

In the case of addition, λ can be computed using Equation D-2.

Equation D-8-2

$$\lambda = \alpha + \beta + \gamma$$

Using Equation D-2, the differentials in Equation D-1 are evaluated as follows.

Equation D-8-3

$$\frac{d\lambda}{d\alpha} = \frac{d\lambda}{d\beta} = \frac{d\lambda}{d\gamma} = 1$$

The basic equation for calculation of the propagation of error can be simplified by substituting the results from Equation D-3 into Equation D-1 resulting in Equation D-4.

Equation D-8-4

$$\sigma_\lambda^2 = \sigma_\alpha^2 + \sigma_\beta^2 + \sigma_\gamma^2$$

Subtraction of the measured quantities results in the same final equation because each partial derivative is squared. In conclusion, the total error of a computed quantity is simply the sum of the errors of the measured quantities added or subtracted in the calculation [236].

In the case of multiplication, λ can be computed using Equation D-5.

Equation D-5

$$\lambda = \alpha\beta\gamma$$

Using Equation D-5, the differentials in Equation D-1 are evaluated as follows.

Equation D-6

$$\frac{d\lambda}{d\alpha} = \beta\gamma; \frac{d\lambda}{d\beta} = \alpha\gamma; \frac{d\lambda}{d\gamma} = \alpha\beta$$

The basic equation for calculation of the propagation of error can be simplified by substituting the results from Equation D-6 into Equation D-1 resulting in Equation D-7.

Equation D-7

$$\sigma_\lambda^2 = (\beta\gamma)^2 \sigma_\alpha^2 + (\alpha\gamma)^2 \sigma_\beta^2 + (\alpha\beta)^2 \sigma_\gamma^2$$

Equation D-7 can be further reduced by dividing through by Equation D-8 to yield Equation D-9.

Equation D-8

$$\lambda^2 = \alpha^2\beta^2\gamma^2$$

Equation D-9

$$\%\sigma_{\lambda}^{2} = \%\sigma_{\alpha}^{2} + \%\sigma_{\beta}^{2} + \%\sigma_{\gamma}^{2}$$

The percentage errors are computed as described in Equation D-10.

Equation D-10

$$\%\sigma_{i} = \left(\frac{\sigma_{i}}{i} \right) \times 100\%$$

Division of the measured quantities results in the same final equation because each partial derivative is squared. In conclusion, the total error of a computed quantity is obtained by adding the percentage errors of the measured quantities multiplied or divided in the calculation [236].

APPENDIX E

CALCULATION OF PEG-BIOTIN MOLECULES ERROR ANALYSIS

The number of PEG-biotin molecules per cell can be calculated using Equation E-1.

Equation E-1

$$\#\text{ of PEG - biotin Molecules/Cell} = \left(\frac{\text{Sample MESF - Control MESF}}{\text{Effective F/P Ratio}} \right)$$

The calculated MESF is computed by subtracting the Control MESF from the Sample MESF. Thus, the MESF error can be calculated by adding the errors associated with the Control and Sample MESF as shown in Equation E-2.

Equation E-2

$$\sigma_{MESF}^2 = \sigma_{Sample}^2 + \sigma_{Control}^2$$

The error of the Sample and Control are given in Equation E-3.

Equation E-3

$$\sigma_{Sample} = \sigma_{Control} = 21{,}000$$

Substituting the values from Equation E-3 into Equation E-2 and taking the square root produces Equation E-4.

Equation E-4

$$\sigma_{MESF} = 29{,}700$$

The actual number of PEG-biotin molecules per cell is computed by dividing the calculated MESF by the Effective F/P Ratio as elucidated in Equation E-1. Consequently, the total error in the number of PEG-biotin molecules per cell can be determined by adding the percentage errors for the calculated MESF and the Effective F/P ration as demonstrated in Equation E-5.

Equation E-5

$$\%\sigma^2_{Molecules} = \%\sigma^2_{MESF} + \sigma^2_{F/P}$$

The percentage errors for the MESF and Effective F/P ratio are given in Equation E-6.

Equation E-6

$$\sigma_{MESf} = \left(\frac{29{,}700}{6.1\times10^6}\right)\times100\% = 0.49\%; \sigma_{F/P} = \left(\frac{0.018}{0.20}\right)\times100\% = 9\%$$

Substituting the values from Equation E-6 into Equation E-5 and taking the square root produces Equation E-7.

Equation E-7

$$\%\sigma_{Molecules} = 9.0\%$$

Based on the errors in the measured quantities, calculated MESF and Effective F/P ratio, the expected total error in the calculation of the number of PEG-biotin molecules per cell is 9%.

APPENDIX F

PARALLEL PLATE PERFUSION CHAMBER CALCULATIONS

The parallel plate perfusion chamber is analogous to incompressible viscous flow between fixed, parallel plates with a pressure gradient as illustrated in Figure F-1 [237-239].

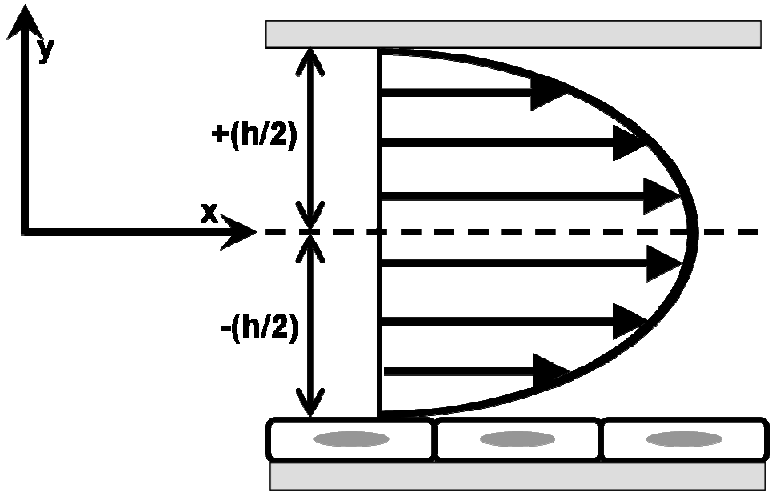

Figure F–1 Incompressible viscous flow between fixed parallel plates with a pressure gradient.

The first step is to solve for the velocity profile of the fluid between the parallel plates by using the x-component of the Navier-Stokes Equation, also known as the Equation of Motion, for a Newtonian fluid with constant density, ρ, and viscosity, μ, in rectangular coordinates (Equation F-1) [237-239].

Equation F-1 Navier-Stokes Equation (x-component) for Constant ρ and μ

$$\rho\left(\frac{\partial v_x}{\partial t}+v_x\frac{\partial v_x}{\partial x}+v_y\frac{\partial v_x}{\partial y}+v_z\frac{\partial v_x}{\partial z}\right)=-\frac{\partial p}{\partial x}+\mu\left(\frac{\partial^2 v_x}{\partial x^2}+\frac{\partial^2 v_x}{\partial y^2}+\frac{\partial^2 v_x}{\partial z^2}\right)+\rho g_x$$

At this point, a number of assumptions permit reduction of the Navier-Stokes Equation to a form that is more easily solved. First, it is assumed that the plates are very wide and long compared to the distance between the plates so the flow is only in the x direction (Equation F-2) and is only a function of y (Equation F-3) [239].

Equation F-2 Fluid Flow in x Direction

$$v_x \neq 0; v_y = v_z = 0$$

Equation F-3 Fluid Velocity a Function of y

$$v_x = f(y)$$

Furthermore, the chamber is always kept parallel to the ground and at constant height so gravity effects can be ignored (Equation F-4).

Equation F-4 Gravity Effects are Negligible

$$g_x = 0$$

Additional assumptions are that the flow is steady (Equation F-5) and laminar.

Equation F-5 Steady State Flow

$$\frac{\partial}{\partial t} = 0$$

Applying Equations F-2, F-3, F-4, and F-5, the Navier-Stokes Equation (Equation F-1) reduces to Equation F-6.

Equation F-6

$$0 = -\frac{\partial p}{\partial x}+\mu\left(\frac{d^2 v_x}{dy^2}\right)$$

The pressure gradient only varies along the x axis and not the y or z axis so the pressure is only a function of x. Equation F-6 can be rearranged to Equation F-7.

Equation F-7

$$\mu\left(\frac{d^2v_x}{dy^2}\right)=\frac{dp}{dx}$$

The pressure gradient, dp/dx, is defined as shown in Equation F-8.

Equation F-8

$$\frac{dp}{dx}=\frac{p(x=L)-p(x=0)}{L-0}=\frac{p(L)-p(0)}{L}$$

In order for the fluid to flow through the chamber, the pressure at the entrance (x = 0) must be greater than at the exit (x = L), which serves as the driving force for fluid movement. Thus, p(x = 0) is greater than p(x = L). The change in pressure, Δp, is defined in Equation F-9.

Equation F-9

$$\Delta p = p(0)-p(L)$$

As a result, the pressure gradient can be written as demonstrated in Equation F-10.

Equation F-10

$$\frac{dp}{dx}=\frac{p(L)-p(0)}{L}=\frac{-\left[p(0)-p(L)\right]}{L}=-\frac{\Delta p}{L}$$

Based on the theory of separation of variables, when one quantity that varies only with y equates to another quantity that varies only with x, the two quantities are both equal to the same constant (Equation F-11) [239].

Equation F-11

$$\mu\left(\frac{d^2v_x}{dy^2}\right)=\frac{dp}{dx}=-\frac{\Delta p}{L}$$

Reorganizing Equation F-11 permits integration (Equation F-12).

Equation F-12

$$\int d\left(\frac{dv_x}{dy}\right) = \int\left(\frac{1}{\mu}\right)\left(-\frac{\Delta p}{L}\right)dy$$

Integration of Equation F-12 yields Equation F-13 where C_1 is an arbitrary constant.

Equation F-13

$$\frac{dv_x}{dy} = -\left(\frac{1}{\mu}\right)\left(\frac{\Delta p}{L}\right)y + C_1$$

Rearranging Equation F-13 permits integration the second time (Equation F-14).

Equation F-14

$$\int dv_x = \int -\left(\frac{1}{\mu}\right)\left(\frac{\Delta p}{L}\right)ydy + \int C_1 dy$$

Integration of Equation F-14 yields Equation F-15 where C_2 is another arbitrary constant.

Equation F-15

$$v_x = -\left(\frac{1}{\mu}\right)\left(\frac{\Delta p}{L}\right)\left(\frac{y^2}{2}\right) + C_1 y + C_2$$

The constants, C_1 and C_2, are determined by applying no-slip boundary conditions at the wall (Equation F-16).

Equation F-16 No-Slip

$$@\, y = \pm\frac{h}{2}; v_x = 0$$

Applying the no-slip boundary conditions at the wall to Equation F-15 generates two equations for evaluation of the constants C_1 (Equation F-17) and C_2 (Equation F-18).

Equation F-17

$$C_1 = 0$$

Equation F-18

$$C_2 = \left(\frac{1}{2\mu}\right)\left(\frac{\Delta p}{L}\right)\left(\frac{h^2}{4}\right)$$

Substituting Equations F-17 and F-18 into Equation F-15 yields the velocity profile, $v_x(y)$, of the fluid in the parallel plate perfusion chamber (Equation F-19).

Equation F-19Velocity Profile, $v_x(y)$

$$v_x(y) = \left(\frac{1}{2\mu}\right)\left(\frac{\Delta p}{L}\right)\left(\frac{h^2}{4} - y^2\right)$$

The velocity profile (Equation F-19) can be used to solve for the fluid velocity at any vertical distance, y, in the chamber.

The volumetric flow rate, Q, can be defined as the volume of fluid, V, that passes through and is normal to surface, S, with area, A as shown in Equation F-20 [239].

Equation F-20 Volumetric Flow Rate

$$Q = \int_S (V \bullet n) dA$$

In the case of the parallel plate chamber, the surface is defined by the width, w, and height, h, of the chamber. Therefore, the elemental area, dA, can be represented as Equation F-21 and the surface integrated from 0 to w and 0 to h.

Equation F-21 Elemental Area

$$dA = dydz$$

The volume of fluid that passes normal to the surface of interest is given by the velocity profile (Equation F-22).

Equation F-22 Volume Normal to the Surface

$$(V \bullet n) = v_x(y) = \left(\frac{1}{2\mu}\right)\left(\frac{\Delta p}{L}\right)\left(\frac{h^2}{4} - y^2\right)$$

Equations F-21 and F-22 can be inserted into Equation F-20 yielding Equation F-23.

Equation F-23 Volumetric Flow Rate

$$Q = \int_0^w \int_{-\frac{h}{2}}^{\frac{h}{2}} \left(\frac{1}{2\mu}\right)\left(\frac{\Delta p}{L}\right)\left(\frac{h^2}{4} - y^2\right) dy dz$$

Integrating Equation F-23 with respect to y and z and evaluating it over the limits of integration results in a simplified equation for computation of the volumetric flow rate (Equation F-24).

Equation F-24 Volumetric Flow Rate

$$Q = \left(\frac{w}{2\mu}\right)\left(\frac{\Delta p}{L}\right)\left(\frac{h^3}{6}\right)$$

The volumetric flow rate is controlled by the syringe pump withdrawal rate so it is a known parameter for the parallel plate perfusion chamber. Consequently, the Volumetric Flow Rate Equation (Equation F-24) can be rearranged to solve for the pressure drop over the length of the chamber, Δp/L (Equation F-25).

Equation F-25 Pressure Drop

$$\left(\frac{\Delta p}{L}\right) = \frac{12\mu Q}{w h^3}$$

Now, the pressure drop (Equation F-25) can be substituted back into the velocity profile (Equation F-19) to produce Equation F-26.

Equation F-26 Velocity Profile, $v_x(y)$

$$v_x(y) = \left(\frac{6Q}{wh}\right)\left(\frac{1}{4} - \frac{y^2}{h^2}\right)$$

In order to assure that the microsphere and cell delivery experiments are conducted under physiologic conditions, it is important to know the shear rate ($\dot{\gamma}$) and shear stress (τ) on the endothelial surface in the parallel plate perfusion chamber. The shear stress of interest is τ_{yx},

which is the shear stress in the x direction on a surface normal to the y axis [237-239]. Stokes' viscosity relation for the shear stress components of a Newtonian fluid in laminar flow gives the following equation in rectangular coordinates (Equation F-27) [237-239].

Equation F-27 Stress Tensor Component for Newtonian Fluids

$$\tau_{yx} = \tau_{xy} = \mu\left(\frac{\partial v_x}{\partial y} + \frac{\partial v_y}{\partial x}\right)$$

There is no velocity in the y direction and the velocity in the x direction is only a function of y; thus, Equation F-27 can be further simplified to Equation F-28.

Equation F-28 Shear Stress

$$\tau_{yx} = \tau_{xy} = \mu\left(\frac{dv_x}{dy}\right)$$

Now, the velocity profile (Equation F-26) can be substituted into the shear stress equation (Equation F-28) as shown in Equation F-29.

Equation F-29 Shear Stress

$$\tau_{yx} = \tau_{xy} = \mu\left(\frac{dv_x}{dy}\right) = \mu\frac{d}{dy}\left[\left(\frac{6Q}{wh}\right)\left(\frac{1}{4} - \frac{y^2}{h^2}\right)\right]$$

Taking the derivative of the velocity profile with respect to y yields the following equation for the shear stress (Equation F-30).

Equation F-30 Shear Stress

$$\tau_{yx} = \tau_{xy} = \left(\frac{6\mu Q}{wh}\right)\left(-\frac{2y}{h^2}\right) = -\left(\frac{12\mu Q}{wh^3}\right)y$$

Of particular interest is the shear stress on the coverslip surface where y = -(h/2). Substituting this value for y into Equation F-30 and simplifying leads to Equation F-31 for the calculation of the shear stress on the coverslip surface as a function of fluid viscosity, volumetric flow rate, width, and height.

Equation F-31 Shear Stress

$$\tau_{yx}\left(-\frac{h}{2}\right)=\frac{6\mu Q}{wh^2}$$

Shear rate ($\dot{\gamma}$) is another useful parameter for comparison of the parallel plate perfusion chamber to physiologic environments. The shear rate is calculated in a similar manner as the shear stress and is shown in Equation F-32.

Equation F-32 Shear Rate

$$\dot{\gamma}_{yx}=\dot{\gamma}_{xy}=\left(\frac{\partial v_x}{\partial y}+\frac{\partial v_y}{\partial x}\right)=\frac{\tau_{yx}}{\mu}=\frac{\tau_{xy}}{\mu}$$

There is no velocity in the y direction and the velocity in the x direction is only a function of y; thus, Equation F-32 can be further simplified to Equation F-33.

Equation F-33 Shear Rate

$$\dot{\gamma}_{yx}=\frac{dv_x}{dy}$$

Now, the velocity profile (Equation F-26) can be substituted into the shear rate equation (Equation F-33) as shown in Equation F-34.

Equation F-34 Shear Rate

$$\dot{\gamma}_{yx}=\frac{d}{dy}\left[\left(\frac{6Q}{wh}\right)\left(\frac{1}{4}-\frac{y^2}{h^2}\right)\right]$$

Taking the derivative of the velocity profile with respect to y yields the following equation for the shear rate (Equation F-35).

Equation F-35 Shear Rate

$$\dot{\gamma}_{yx}=\left(\frac{6Q}{wh}\right)\left(-\frac{2y}{h^2}\right)=-\left(\frac{12Q}{wh^3}\right)y$$

Of particular interest is the shear rate on the coverslip surface where y = -(h/2). Substituting this value for y into Equation F-35 and simplifying leads to Equation F-36 for the calculation of the shear rate on the coverslip surface as a function of flow rate, width, and height.

Equation F-36 Shear Rate

$$\dot{\gamma}_{yx}\left(-\frac{h}{2}\right)=\frac{6Q}{wh^2}$$

One final parameter that is of interest in evaluating the parallel plate perfusion chamber is the Reynolds number. The Reynolds number is employed to determine if the flow is laminar or turbulent [237-239]. The transition from laminar to turbulent flow usually occurs when the Reynolds number is in the region of 2,100 [237-239]. Thus, calculation of the Reynolds number for flow rates utilized in the parallel plate perfusion chamber is important in evaluating whether or not the flow is laminar or turbulent. The derivations in this appendix are based on the assumption of laminar flow so turbulence should be avoided or the derivations are no longer relevant. For parallel flat plates, the Reynolds number, Re, is the product of the fluid density, ρ, characteristic velocity, v, and characteristic length, L, divided by the viscosity, μ (Equation F-37) [237-239].

Equation F-37 Reynolds Number

$$\mathrm{Re}=\frac{\rho v L}{\mu}$$

The chamber dimensions are 2.95 cm long by 0.9 cm wide by 200 μm high [216-220]. The viscosity of DMEM at 37ºC is approximately 0.0089 poise [240, 241]. Using these values, the volumetric flow rate (Equation F-36), shear stress (Equation F-31), and Reynolds number (Equation F-37) can be computed for flow in the parallel plate perfusion chamber for any desired shear rate. Table F-1 shows the computed values for these parameters for various shear rates.

Table F–1 Parameters for the Parallel Plate Perfusion Chamber

Shear Rate, $\dot{\gamma}$ (s^{-1})	Volumetric Flow Rate, Q (cm^3/s)	Shear Stress, τ ($dyne/cm^2$)	Reynolds Number, Re
0	0.000	0.00	0.00
100	0.006	0.89	83.28
200	0.012	1.78	166.56
300	0.018	2.67	249.84
400	0.024	3.56	333.12
500	0.030	4.45	416.40
600	0.036	5.34	499.68
700	0.042	6.23	582.96
800	0.048	7.12	666.24
900	0.054	8.01	749.52
1000	0.060	8.90	832.79

APPENDIX G

MICROSPHERE AND CELL DELIVERY ERROR ANALYSIS

The number of adhered microspheres per mm^2 of vascular surface, Micros/mm^2, can be computed by dividing the microsphere count from an individual micrograph, $Micro_{Count}$, by the micrograph area, $Area_{Field}$ as illustrated in Equation G-1.

Equation G-1 Microsphere Calculation

$$Micros/mm^2 = \left(\frac{Micro_{Count}}{Area_{Field}} \right)$$

Similarly, the number of attached cells per mm^2 of vascular surface, Cells/mm^2, can be computed by dividing the cell count from an individual micrograph, $Cell_{Count}$, by the micrograph area, $Area_{Field}$ as illustrated in Equation G-2.

Equation G-2 Cell Calculation

$$Cells/mm^2 = \left(\frac{Cell_{Count}}{Area_{Field}} \right)$$

All of the fluorescent micrographs were taken with a Zeiss LD Plan Neofluar 20x objective. The 20x objective micrograph field measures 0.68 ± 0.005 mm wide by 0.54 ± 0.005 mm high. Multiplication of the micrograph filed width and height yields the total area. Consequently, the error associated with computation of the micrograph area is calculated by adding the percentage errors of the width and height (Equation G-3).

Equation G-3

$$\%\sigma^2_{Area} = \%\sigma^2_{Width} + \sigma^2_{Height}$$

The percentage error for the width and height is shown in Equation G-4.

Equation G-4

$$\%\sigma_{Width} = \frac{0.005}{0.68} * 100\% = 0.74\%; \%\sigma_{Height} = \frac{0.005}{0.54} * 100\% = 0.93\%$$

Substituting the values from Equation G-4 into Equation G-3 and taking the square root produces Equation G-5.

Equation G-5

$$\%\sigma_{Area} = 1.2\%$$

The percent error of the micrograph area is 1.18% based on the uncertainty in the measurement of the width and height.

The errors in the microsphere and cell counts vary depending upon the system under investigation (parallel plate, tubular, or *in vivo*) and whether microspheres or cells are counted. As a result, calculation of the error propagation differs for each particular agent delivered and the method used for evaluation. In general, the error in the count per mm^2 can be computed utilizing Equation G-6.

Equation G-6

$$\%\sigma^2_{Count/mm^2} = \%\sigma_{Count} + \sigma^2_{Area}$$

The microsphere count error for the parallel plate, tubular, and *in vivo* delivery methods are presented in Table G-1. In addition, the percentage error for the microsphere count and total percentage error of the number of microspheres per mm^2 surface is calculated and presented in Table G-1. There is some variation in the total error of the calculated number of microspheres per area, but it is fairly consistent irregardless of whether the experiment was conducted in the

parallel plate, tubular, or *in vivo* system. The overall error in the number of microspheres per mm^2 is approximately 3% (Table G-1).

Table G–1 Microsphere Delivery Error Analysis

	Microsphere Count Error	% Microsphere Count Error	% Error in the # of Microspheres/mm^2
Parallel	±2	2.6	2.9
Tubular	±0.5	2.3	2.6
In Vivo	±2	2.7	3.0

The cell count error for the parallel plate, tubular, and *in vivo* delivery methods are presented in Table G-2. In addition, the percentage error for the cell count and total percentage error of the number of cells per mm^2 surface is calculated and presented in Table G-2. There is some variation in the total error of the calculated number of cells per area, but it is fairly consistent irregardless of whether the experiment was conducted in the parallel plate, tubular, or *in vivo* system. The overall error in the number of cells per mm^2 ranges from 2-3%.

Table G–2 Cell Delivery Error Analysis

	Cell Count Error	% Cell Count Error	% Error in the # of Cells/mm^2
Parallel	±0.2	2.7	3.0
Tubular	±0.1	1.2	1.7
In Vivo	N/A	N/A	N/A

APPENDIX H

TUBULAR PERFUSION CHAMBER CALCULATIONS

The tubular perfusion chamber is analogous to incompressible viscous flow in a cylindrical tube with a pressure gradient as illustrated in Figure H-1 [237-239]. It is assumed that the flow chamber is cylindrical; however, this is only an approximation as the vessel surface exposed through the window in the upper chamber is in all likelihood flat [163].

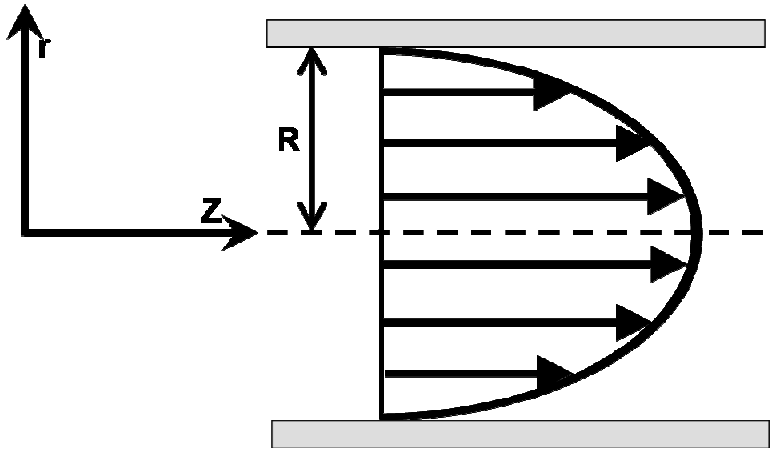

Figure H–1 Incompressible viscous flow in a cylindrical tube with a pressure gradient.

The first step is to solve for the velocity profile of the fluid in the cylindrical tube using the z-component of the Navier-Stokes Equation, also known as the Equation of Motion, for a

Newtonian fluid with constant density, ρ, and viscosity, μ, in cylindrical coordinates (Equation H-1) [237-239].

Equation H-1 Navier-Stokes Equation (z-component) for Constant ρ and μ

$$\rho\left(\frac{\partial v_z}{\partial t}+v_r\frac{\partial v_z}{\partial r}+\frac{v_\theta}{r}\frac{\partial v_z}{\partial \theta}+v_z\frac{\partial v_z}{\partial z}\right)=-\frac{\partial p}{\partial z}+\mu\left(\frac{1}{r}\frac{\partial}{\partial r}\left(r\frac{\partial v_z}{\partial r}\right)+\frac{1}{r^2}\frac{\partial^2 v_z}{\partial \theta^2}+\frac{\partial^2 v_z}{\partial z^2}\right)+\rho g_z$$

At this point, a number of assumptions permit reduction of the Navier-Stokes Equation to a form that is more easily solved. First, it is assumed that the length of the tube is long compared to its radius and the fluid flow is only in the z direction (Equation H-2) [239].

Equation H-2 Fluid Flow in z Direction

$$v_z \neq 0; v_r = v_\theta = 0$$

Another assumption is there is no circumferential or radial variation in the velocity profile and it is only a function of r (Equation H-3) [239].

Equation H-3 Fluid Velocity a Function of y

$$v_z = f(r)$$

Furthermore, the chamber is always kept parallel to the ground and at constant height so gravity effects can be ignored (Equation H-4).

Equation H-4 Gravity Effects are Negligible

$$g_z = 0$$

Additional assumptions are that the flow is steady (Equation H-5) and laminar.

Equation H-5 Steady State Flow

$$\frac{\partial}{\partial t} = 0$$

Applying Equations H-2, H-3, H-4, and H-5, the Navier-Stokes Equation (Equation H-1) reduces to Equation H-6.

Equation H-6

$$0 = -\frac{\partial p}{\partial z} + \frac{\mu}{r}\frac{d}{dr}\left(r\frac{dv_z}{dr}\right)$$

The pressure gradient only varies along the z axis and not the r or θ axis so the pressure is only a function of z. Equation H-6 can be rearranged to Equation H-7.

Equation H-7

$$\frac{\mu}{r}\frac{d}{dr}\left(r\frac{dv_z}{dr}\right) = \frac{dp}{dz}$$

The pressure gradient, dp/dz, is defined as shown in Equation H-8.

Equation H-8

$$\frac{dp}{dz} = \frac{p(z=L) - p(z=0)}{L-0} = \frac{p(L) - p(0)}{L}$$

In order for the fluid to flow through the chamber, the pressure at the entrance (z = 0) must be greater than at the exit (z = L), which serves as the driving force for fluid movement. Thus, p(z = 0) is greater than p(z = L). The change in pressure, Δp, is defined in Equation H-9.

Equation H-9

$$\Delta p = p(0) - p(L)$$

As a result, the pressure gradient can be written as demonstrated in Equation H-10.

Equation H-10

$$\frac{dp}{dz} = \frac{p(L) - p(0)}{L} = \frac{-\left[p(0) - p(L)\right]}{L} = -\frac{\Delta p}{L}$$

Based on the theory of separation of variables, when one quantity that varies only with y equates to another quantity that varies only with x, the two quantities are both equal to the same constant (Equation H-11) [239].

Equation H-11

$$\frac{\mu}{r}\frac{d}{dr}\left(r\frac{dv_z}{dr}\right)=\frac{dp}{dz}=-\frac{\Delta p}{L}$$

Reorganizing Equation H-11 permits integration (Equation H-12).

Equation H-12

$$\int d\left(r\frac{dv_z}{dr}\right)=\int\left(\frac{1}{\mu}\right)\left(-\frac{\Delta p}{L}\right)rdr$$

Integration of Equation H-12 yields Equation H-13 where C_1 is an arbitrary constant.

Equation H-13

$$r\frac{dv_z}{dr}=-\left(\frac{1}{\mu}\right)\left(\frac{\Delta p}{L}\right)\left(\frac{r^2}{2}\right)+C_1$$

Rearranging Equation H-13 and dividing through by r permits integration the second time (Equation H-14).

Equation H-14

$$\int dv_z=\int-\left(\frac{1}{2\mu}\right)\left(\frac{\Delta p}{L}\right)rdr+\int\frac{C_1}{r}dr$$

Integration of Equation H-14 yields Equation H-15 where C_2 is another arbitrary constant.

Equation H-15

$$v_z=-\left(\frac{1}{2\mu}\right)\left(\frac{\Delta p}{L}\right)\left(\frac{r^2}{2}\right)+C_1\ln(r)+C_2$$

The constants, C_1 and C_2, are determined by applying boundary conditions. At the wall, the no-slip boundary condition applies (Equation H-16).

Equation H-16 No-Slip

$$@\,r=R;v_z=0$$

The second boundary condition stipulates that the velocity profile must be finite at all positions in the r direction. This boundary condition relates to the natural logarithm, ln, of the radius as it nears 0. In the limit as the radius approaches 0, the natural logarithm, ln(r), goes to negative infinity, -∞. Applying the boundary condition of finite flow at all values of r requires that C_1 equal 0 (Equation H-17).

Equation H-17 Finite Velocity

$$C_1 = 0$$

Now, the no-slip boundary condition at the wall (Equation H-16) and finite fluid velocity (Equation H-17) can be inserted into Equation H-15 to evaluate C_2 (Equation H-18).

Equation H-18

$$C_2 = \left(\frac{1}{2\mu}\right)\left(\frac{\Delta p}{L}\right)\left(\frac{R^2}{2}\right)$$

Substituting Equations H-17 and H-18 into Equation H-15 yields the velocity profile, $v_z(r)$, of the fluid in the tubular perfusion chamber (Equation H-19).

Equation H-19Velocity Profile, $v_z(r)$

$$v_z(r) = \left(\frac{1}{4\mu}\right)\left(\frac{\Delta p}{L}\right)\left(R^2 - r^2\right)$$

The velocity profile (Equation H-19) can be used to solve for the fluid velocity at any radius, r, in the chamber.

The volumetric flow rate, Q, can be defined as the volume of fluid, V, that passes through and is normal to surface, S, with area, A as shown in Equation H-20 [239].

Equation H-20 Volumetric Flow Rate

$$Q = \int_S (V \bullet n) dA$$

In the case of the tubular chamber, the surface is defined by the circumference of the cylinder, 2πr, and the differential radius, dr. Therefore, the elemental area, dA, can be represented as Equation H-21 and the surface integrated from 0 to R.

Equation H-21 Elemental Area

$$dA = 2\pi r dr$$

The volume of fluid that passes normal to the surface of interest is given by the velocity profile (Equation H-22).

Equation H-22 Volume Normal to the Surface

$$(V \bullet n) = v_z(r) = \left(\frac{1}{4\mu}\right)\left(\frac{\Delta p}{L}\right)\left(R^2 - r^2\right)$$

Equations H-21 and H-22 can be inserted into Equation H-20 yielding Equation H-23.

Equation H-23 Volumetric Flow Rate

$$Q = \int_0^R \left(\frac{1}{4\mu}\right)\left(\frac{\Delta p}{L}\right)\left(R^2 - r^2\right)2\pi r dr$$

Integrating Equation H-23 with respect to r and evaluating it over the limits of integration results in a simplified equation for computation of the volumetric flow rate (Equation H-24).

Equation H-24 Volumetric Flow Rate

$$Q = \left(\frac{\pi R^4}{8\mu}\right)\left(\frac{\Delta p}{L}\right)$$

The volumetric flow rate is controlled by the syringe pump withdrawal rate so it is a known parameter for the parallel plate perfusion chamber. Consequently, the Volumetric Flow Rate Equation (Equation H-24) can be rearranged to solve for the pressure drop over the length of the chamber, Δp/L (Equation H-25).

Equation H-25 Pressure Drop

$$\left(\frac{\Delta p}{L}\right)=\frac{8\mu Q}{\pi R^4}$$

Now, the pressure drop (Equation H-25) can be substituted back into the velocity profile (Equation H-19) to produce Equation H-26.

Equation H-26Velocity Profile, $v_z(r)$

$$v_z(r)=\left(\frac{2Q}{\pi R^2}\right)\left(1-\frac{r^2}{R^2}\right)$$

In order to assure that the microsphere and cell delivery experiments are conducted under physiologic conditions, it is important to know the shear rate ($\dot{\gamma}$) and shear stress (τ) on the vascular surface in the tubular perfusion chamber. The shear stress of interest is τ_{rz}, which is the shear stress in the z direction on a surface normal to the r axis [237-239]. Stokes' viscosity relation for the shear stress components of a Newtonian fluid in laminar flow gives the following equation in cylindrical coordinates (Equation H-27) [237-239].

Equation H-27 Stress Tensor Component for Newtonian Fluids

$$\tau_{rz}=\tau_{zr}=-\mu\left(\frac{\partial v_z}{\partial r}+\frac{\partial v_r}{\partial z}\right)$$

There is no velocity in the r direction and the velocity in the z direction is only a function of r; thus, Equation H-27 can be further simplified to Equation H-28.

Equation H-28 Shear Stress

$$\tau_{rz}=\tau_{zr}=-\mu\left(\frac{dv_z}{dr}\right)$$

Now, the velocity profile (Equation H-26) can be substituted into the shear stress equation (Equation H-28) as shown in Equation H-29.

Equation H-29 Shear Stress

$$\tau_{rz} = \tau_{zr} = \mu\left(\frac{dv_z}{dr}\right) = -\mu\frac{d}{dr}\left[\left(\frac{2Q}{\pi R^2}\right)\left(1-\frac{r^2}{R^2}\right)\right]$$

Taking the derivative of the velocity profile with respect to r yields the following equation for the shear stress (Equation H-30).

Equation H-30 Shear Stress

$$\tau_{rz} = \tau_{zr} = -\left(\frac{2\mu Q}{\pi R^2}\right)\left(\frac{-2r}{R^2}\right) = \left(\frac{4\mu Q}{\pi R^4}\right)(r)$$

Of particular interest is the shear stress on the vascular surface where r = R. Substituting this value for r into Equation H-30 and simplifying leads to Equation H-31 for the calculation of the shear stress on the vascular surface as a function of fluid viscosity, volumetric flow rate, and radius.

Equation H-31 Shear Stress

$$\tau_{rz}(R) = \frac{4\mu Q}{\pi R^3}$$

Shear rate ($\dot{\gamma}$) is another useful parameter for comparison of the parallel plate perfusion chamber to physiologic environments. The shear rate is calculated in a similar manner as the shear stress and is shown in Equation H-32.

Equation H-32 Shear Rate

$$\dot{\gamma}_{rz} = \dot{\gamma}_{zr} = -\left(\frac{\partial v_z}{\partial r} + \frac{\partial v_r}{\partial z}\right) = \frac{\tau_{rz}}{\mu} = \frac{\tau_{zr}}{\mu}$$

There is no velocity in the r direction and the velocity in the z direction is only a function of r; thus, Equation H-32 can be further simplified to Equation H-33.

Equation H-33 Shear Rate

$$\dot{\gamma}_{rz} = -\frac{dv_z}{dr}$$

Now, the velocity profile (Equation H-26) can be substituted into the shear rate equation (Equation H-33) as shown in Equation H-34.

Equation H-34 Shear Rate

$$\dot{\gamma}_{rz} = -\frac{d}{dr}\left[\left(\frac{2Q}{\pi R^2}\right)\left(1-\frac{r^2}{R^2}\right)\right]$$

Taking the derivative of the velocity profile with respect to r yields the following equation for the shear rate (Equation H-35).

Equation H-35 Shear Rate

$$\dot{\gamma}_{rz} = -\left(\frac{2Q}{\pi R^2}\right)\left(\frac{-2r}{R^2}\right) = \left(\frac{4Q}{\pi R^4}\right)(r)$$

Of particular interest is the shear rate on the vascular surface where r = R. Substituting this value for r into Equation H-35 and simplifying leads to Equation H-36 for the calculation of the shear rate on the vascular surface as a function of flow rate and radius.

Equation H-36 Shear Rate

$$\dot{\gamma}_{rz}(R) = \frac{4Q}{\pi R^3}$$

One final parameter that is of interest in evaluating the tubular perfusion chamber is the Reynolds number. The Reynolds number is employed to determine if the flow is laminar or turbulent [237-239]. The transition from laminar to turbulent flow usually occurs when the Reynolds number is in the region of 2,000 - 2,300 [237-239]. Thus, calculation of the Reynolds number for flow rates utilized in the tubular perfusion chamber is important in evaluating whether or not the flow is laminar or turbulent. The derivations in this appendix are based on the

assumption of laminar flow so turbulence should be avoided or the derivations are no longer relevant. For cylindrical tubes, the Reynolds number, Re, is the product of the fluid density, ρ, characteristic velocity, v, and characteristic length, L, divided by the viscosity, μ (Equation H-37) [237-239]. In the case of fluid flow in a cylindrical tube, the characteristic length is the diameter of the cylinder, D, or twice the radius, 2R [237-239].

Equation H-37 Reynolds Number

$$\mathrm{Re} = \frac{\rho v L}{\mu} = \frac{\rho v D}{\mu}$$

The radius of the tubular chamber is 0.1 cm and the exposed vessel length is 2.5 cm [163, 181, 182, 224]. The viscosity of DMEM at 37ºC is approximately 0.0089 poise [240, 241]. Using these values, the volumetric flow rate (Equation H-36), shear stress (Equation H-31), and Reynolds number (Equation H-37) can be computed for flow in the tubular perfusion chamber for any desired shear rate. Table H-1 shows the computed values for these parameters for various shear rates.

Table H–1 Parameters for the Tubular Perfusion Chamber

Shear Rate, $\dot{\gamma}$ (s^{-1})	Volumetric Flow Rate, Q (cm^3/s)	Shear Stress, τ ($dyne/cm^2$)	Reynolds Number, Re
0	0.00	0.00	0.00
100	0.08	0.89	56.46
200	0.16	1.78	112.92
300	0.24	2.67	169.38
400	0.31	3.56	225.84
500	0.39	4.45	282.30
600	0.47	5.34	338.76
700	0.55	6.23	395.22
800	0.63	7.12	451.69
900	0.71	8.01	508.15
1000	0.79	8.90	564.61

APPENDIX I

RE-ENDOTHELIALIZATION OF INJURED RAT AORTA

Frozen ampules of rat heart microvessel endothelial cells (RHMVECs) (VEC Technologies, Inc., Rensselaer, NY) were thawed and placed into BD Falcon 75 cm^2 tissue culture flasks (Fisher Scientific, Pittsburgh, PA). RHMVECs were grown in MCDB-131C complete media (VEC Technologies, Inc., Rensselaer, NY). Cell cultures were grown in a Thermo Forma (Thermo Electron Corporation, Waltham, MA) water jacketed CO_2 incubator maintained at 37°C with 5% CO_2 in a humidified environment. Standard aseptic cell culture techniques were utilized [203]. Upon reaching 70-90% confluence, the RHMVECs were subcultured into additional BD Falcon 75 cm^2 tissue culture flasks using ReagentPack containing Hank's Balanced Salt Solution (HBSS), trypsin/EDTA (T/E), and trypsin neutralizing solution (TNS) (Cambrex, Walkersville, MD). The EC subculture procedure was completed as instructed in Clonetics Endothelial Cell Systems – Instructions for Use (Cambrex, Walkersville, MD). Confluent BD Falcon 75 cm^2 tissue culture flasks were used in the re-endothelialization study.

RHMVECs grown in a BD Falcon 75 cm^2 tissue culture flask were labeled with a 5 μM CellTracker Orange CMTMR (Molecular Probes, Eugene, OR) solution in MCDB-131C complete media for 45 min in the incubator. After the incubation, the CellTracker Orange CMTMR solution was replaced with fresh MCDB-131C complete media. Cells grown in the BD

Falcon 75 cm^2 flask were removed from the flask using ReagentPack with trypsin and collected in a BD Falcon BlueMax Jr. 15 mL Graduated tube (Fisher Scientific, Pittsburgh, PA). The tube was then centrifuged at 220g for 5 min in a Sorvall Legend RT and the supernatant removed. The cell pellet was dispersed and modified with 1 mL of a 10 mM NHS-PEG-biotin solution for 1 min. After modification, 9 mL of PBS was added to the cell suspension and the tube vortexed. Again, the cell suspension was centrifuged at 220g for 5 min and the supernatant removed. Next, the cells were resuspended in 12 mL of MCDB-131C complete media and kept at 37°C in a Fisher Isotemp Economy water bath (Fisher Scientific, Pittsburgh, PA).

A segment of aorta was obtained from a previously euthanized rat and placed in PBS. Excess fat and tissue was removed from the aorta and it was cut along its length exposing the lumen of the vessel. Next, the aorta was damaged by scraping the lumen with a weighing spatula (Sigma, St. Louis, MO) three times. Once the aorta was damaged, the vessel was cut into six segments measuring 0.5 cm in length. Minutien pins (Fine Science Tools, Foster City, CA) were used to secure the edges of the aorta to pink dental wax (Electron Microscopy Sciences, Hatfield, PA) with the lumen side facing upwards. After securing the vessel to the wax, the samples were placed into a 6 well tissue culture plate with MCDB-131C complete media.

The scrape-damaged rat aortas were modified with the protein-reactive PEG. First, the MCDB-131C complete media was removed from the aorta segments in the 6 well tissue culture plate. Next, a 1.5 mL solution of 10 mM NHS-PEG-biotin was applied to the aorta segments and incubated for 1 min. After the incubation, the vessel segments were rinsed with 3 mL of DMEM three times. Now, a 2 mg/mL solution of NeutrAvidin Biotin-Binding Protein was applied to the aorta segments for another 1 min incubation. After the incubation, the vessel segments were rinsed with 3 mL of DMEM three times. At this point, the PEG-biotin modified RHMVEC

suspension is incubated on the aorta segments for 1 min. After the cell incubation, the vessel segments were rinsed with 3 mL of DMEM three times. Finally, the vessel segments were removed from the 6 well tissue culture plate and observed on an epi-fluorescent microscope after the initial attachment and then at 1, 2, 3, 4, 5, and 6 days. Fluorescent micrographs of the aorta segments at the specified time points were collected and examined to look for RHMVEC attachment, spreading, and proliferation.

Representative fluorescent micrographs of PEG-biotin labeled RHMVECs on scrape-damaged PEG-biotin modified rat aortas using NeutrAvidin as a bridge at 0, 2, 4, and 6 days are shown in Figure I-1.

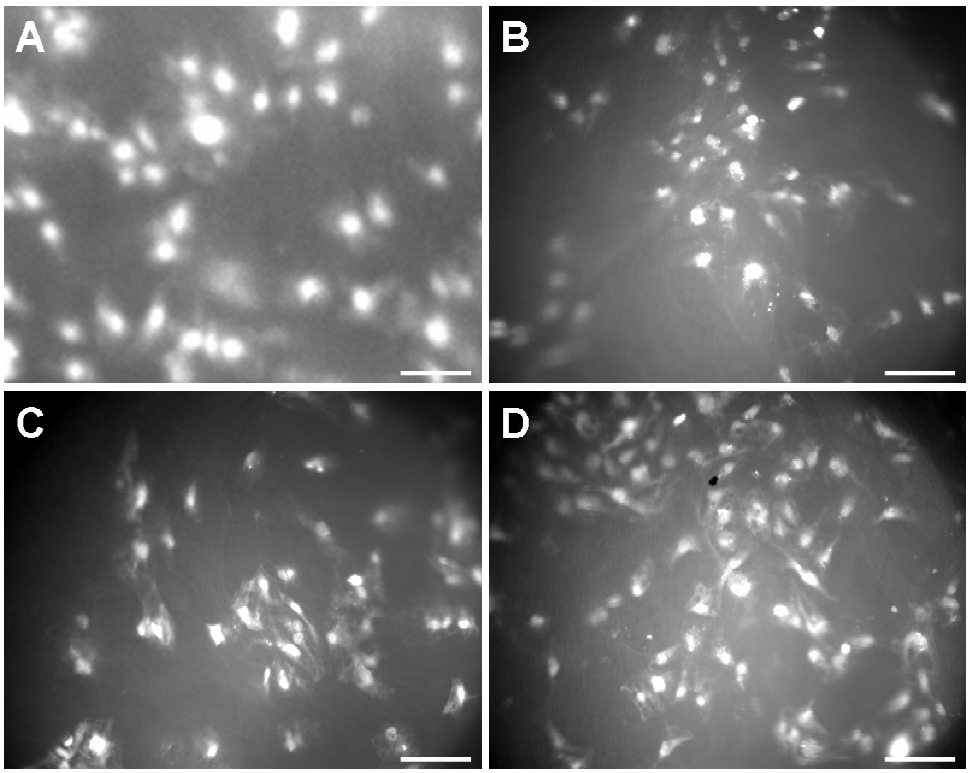

Figure I–1 PEG-biotin labeled RHMVECs on PEG-biotin modified scrape-damaged rat aortas using NeutrAvidin as a bridge on (A) Day 0, (B) Day 2, (C) Day 4, and (D) Day 6. The scale bar is 100 µm.

After initial seeding the cells remain mostly spherical as they have not had a chance to firmly adhere to the vascular surface (Figure I-1, A). At time points past Day 0, it is evident that the cells firmly adhere and spread on the vascular surface (Figure I-1, B, C). In addition, it is evident that coverage of the vascular surface with the RHMVECs increases over time with approximately 70% coverage surface by Day 6 (Figure I-1, D). There was even evidence of cell division in some of the micrographs. In conclusion, PEG-biotin modification of cell and vascular shows no sign of interfering with re-endothelialization on injured vascular surfaces following cell delivery. Thus, endothelial cells labeled with PEG-biotin should be able to adhere, spread, and proliferate upon targeted delivery to PEG-biotin modified injured vascular surfaces to assist in re-endothelialization in a clinical setting.

BIBLIOGRAPHY

1. Aaronson, P.I., J.P.T. Ward, and C.M. Wiener, *The cardiovascular system at a glance*. 2nd ed. 2004, Malden, Mass.: Blackwell Pub. 127.

2. Guyton, A.C. and J.E. Hall, *Textbook of medical physiology*. 9th ed. 1996, Philadelphia: W.B. Saunders. xliii, 1148.

3. Ganong, W.F., *Review of medical physiology*. 13th ed. 1987, Norwalk, Conn.: Appleton & Lange. 665.

4. Haller, H., F. Cosentino, and T.F. Luscher, *Endothelial dysfunction, hypertension and atherosclerosis. A review of the effects of lacidipine.* Drugs R D, 2002. **3**(5): p. 311-23.

5. Dzau, V.J., R.C. Braun-Dullaeus, and D.G. Sedding, *Vascular proliferation and atherosclerosis: new perspectives and therapeutic strategies.* Nat Med, 2002. **8**(11): p. 1249-56.

6. Davignon, J. and P. Ganz, *Role of endothelial dysfunction in atherosclerosis.* Circulation, 2004. **109**(23 Suppl 1): p. III27-32.

7. Bonetti, P.O., L.O. Lerman, and A. Lerman, *Endothelial dysfunction: a marker of atherosclerotic risk.* Arterioscler Thromb Vasc Biol, 2003. **23**(2): p. 168-75.

8. Mullenix, P.S., C.A. Andersen, and B.W. Starnes, *Atherosclerosis as inflammation.* Ann Vasc Surg, 2005. **19**(1): p. 130-8.

9. Lyon, C.J., R.E. Law, and W.A. Hsueh, *Minireview: adiposity, inflammation, and atherogenesis.* Endocrinology, 2003. **144**(6): p. 2195-200.

10. Raines, E.W., *The extracellular matrix can regulate vascular cell migration, proliferation, and survival: relationships to vascular disease.* Int J Exp Pathol, 2000. **81**(3): p. 173-82.

11. Galis, Z.S. and J.J. Khatri, *Matrix metalloproteinases in vascular remodeling and atherogenesis: the good, the bad, and the ugly.* Circ Res, 2002. **90**(3): p. 251-62.

12. Owens, G.K., M.S. Kumar, and B.R. Wamhoff, *Molecular regulation of vascular smooth muscle cell differentiation in development and disease.* Physiol Rev, 2004. **84**(3): p. 767-801.

13. Arias, E., et al., *Deaths: final data for 2001.* Natl Vital Stat Rep, 2003. **52**(3): p. 1-115.

14. Hoyert, D.L., H.C. Kung, and B.L. Smith, *Deaths: preliminary data for 2003.* Natl Vital Stat Rep, 2005. **53**(15): p. 1-48.

15. Kochanek, K.D., et al., *Deaths: final data for 2002.* Natl Vital Stat Rep, 2004. **53**(5): p. 1-115.

16. Minino, A.M., et al., *Deaths: final data for 2000.* Natl Vital Stat Rep, 2002. **50**(15): p. 1-119.

17. Voet, D. and J.G. Voet, *Biochemistry*. 1990, New York: Wiley. xvii, 1223.

18. Antman, E.M. and M. Cohen, *Newer antithrombin agents in acute coronary syndromes.* Am Heart J, 1999. **138**(6 Pt 2): p. S563-9.

19. Wootton, D.M., et al., *A mechanistic model of acute platelet accumulation in thrombogenic stenoses.* Ann Biomed Eng, 2001. **29**(4): p. 321-9.

20. Antoniucci, D., L. Bolognese, and G.M. Santoro, *Advances in antithrombotic therapy of acute myocardial infarction.* Am Heart J, 1999. **138**(2 Pt 2): p. S171-176.

21. Gensini, G.F., M. Comeglio, and M. Falai, *Advances in antithrombotic therapy of acute myocardial infarction.* Am Heart J, 1999. **138**(2 Pt 2): p. S171-6.

22. Jennings, L.K., *The Pharmacodynamics of Anti-Platelet Therapies for Treatment of Acute Coronary Syndromes.* BMES Bulletin, 2001. **25**(2): p. 3-7.

23. Deutsch, E., *The emerging role of low-molecular-weight heparin and antiplatelet therapies in the cardiac catheterization laboratory.* Am Heart J, 1999. **138**(6 Pt 2): p. S577-85.

24. Reeder, G.S., *Contemporary diagnosis and management of unstable angina.* Mayo Clin Proc, 2000. **75**(9): p. 953-7.

25. White, H.D., *Newer antiplatelet agents in acute coronary syndromes.* Am Heart J, 1999. **138**(6 Pt 2): p. S570-6.

26. Abrams, J., *Beneficial actions of nitrates in cardiovascular disease.* The American Journal of Cardiology, 1996. **77**(13): p. C31-C37.

27. Satwani, S., G.W. Dec, and J. Narula, *Beta-adrenergic blockers in heart failure: review of mechanisms of action and clinical outcomes.* J Cardiovasc Pharmacol Ther, 2004. **9**(4): p. 243-55.

28. Schachter, M., *Chemical, pharmacokinetic and pharmacodynamic properties of statins: an update.* Fundamental and Clinical Pharmacology, 2005. **19**(1): p. 117-125.

29. Cundiff, D.K., *Coronary artery bypass grafting (CABG): reassessing efficacy, safety, and cost.* MedGenMed, 2002. **4**(2): p. 7.

30. Amodeo, V.J., et al., *The hybrid approach to coronary artery revascularization: minimally invasive direct coronary artery bypass with percutaneous coronary intervention.* Angiology, 2002. **53**(6): p. 665-9.

31. Mark, D.B. and M.A. Hlatky, *Medical economics and the assessment of value in cardiovascular medicine: Part II.* Circulation, 2002. **106**(5): p. 626-30.

32. Mark, D.B. and M.A. Hlatky, *Medical economics and the assessment of value in cardiovascular medicine: Part I.* Circulation, 2002. **106**(4): p. 516-20.

33. Maziarz, D.M. and T.C. Koutlas, *Cost considerations in selecting coronary artery revascularization therapy in the elderly.* Am J Cardiovasc Drugs, 2004. **4**(4): p. 219-25.

34. Harris, W.O., et al., *Use of coronary artery bypass surgical procedure and coronary angioplasty in treatment of coronary artery disease: changes during a 10-year period at Mayo Clinic Rochester.* Mayo Clin Proc, 1996. **71**(10): p. 927-35.

35. Shah, P.B. and C.M. Lilly, *Interventional therapy for coronary artery disease.* Am J Respir Crit Care Med, 2002. **166**(6): p. 791-6.

36. Windecker, S. and B. Meier, *Intervention in coronary artery disease.* Heart, 2000. **83**(4): p. 481-90.

37. Schofield, P.M., *Indications for percutaneous and surgical revascularisation: how far does the evidence base guide us?* Heart, 2003. **89**(5): p. 565-70.

38. Badimon, J.J., et al., *Different response to balloon angioplasty of carotid and coronary arteries: effects on acute platelet deposition and intimal thickening.* Atherosclerosis, 1998. **140**(2): p. 307-14.

39. Ferns, G.A. and T.Y. Avades, *The mechanisms of coronary restenosis: insights from experimental models.* Int J Exp Pathol, 2000. **81**(2): p. 63-88.

40. Welt, F.G. and C. Rogers, *Inflammation and restenosis in the stent era.* Arterioscler Thromb Vasc Biol, 2002. **22**(11): p. 1769-76.

41. Garas, S.M., P. Huber, and N.A. Scott, *Overview of therapies for prevention of restenosis after coronary interventions.* Pharmacol Ther, 2001. **92**(2-3): p. 165-78.

42. Bauters, C. and J.M. Isner, *The biology of restenosis.* Prog Cardiovasc Dis, 1997. **40**(2): p. 107-16.

43. Ratner, B.D., *Biomaterials science : an introduction to materials in medicine*. 1996, San Diego: Academic Press. xi, 484.

44. Amoroso, G., et al., *Pathophysiology of vascular endothelium and circulating platelets: implications for coronary revascularisation and treatment.* Int J Cardiol, 2001. **79**(2-3): p. 265-75.

45. Bennett, M.R., *In-stent stenosis: pathology and implications for the development of drug eluting stents.* Heart, 2003. **89**(2): p. 218-24.

46. Garza, L., Y.W. Aude, and J.F. Saucedo, *Can we prevent in-stent restenosis?* Curr Opin Cardiol, 2002. **17**(5): p. 518-25.

47. Fattori, R. and T. Piva, *Drug-eluting stents in vascular intervention.* Lancet, 2003. **361**(9353): p. 247-9.

48. Babapulle, M.N. and M.J. Eisenberg, *Coated stents for the prevention of restenosis: Part II.* Circulation, 2002. **106**(22): p. 2859-66.

49. Babapulle, M.N. and M.J. Eisenberg, *Coated stents for the prevention of restenosis: Part I.* Circulation, 2002. **106**(21): p. 2734-40.

50. Beyar, R., *Novel approaches to reduce restenosis.* Ann N Y Acad Sci, 2004. **1015**: p. 367-78.

51. Laroia, S.T. and A.T. Laroia, *Drug-eluting stents. A review of the current literature.* Cardiol Rev, 2004. **12**(1): p. 37-43.

52. Hodgson, J.M., et al., *Drug-eluting stent task force: final report and recommendations of the working committees on cost-effectiveness/economics, access to care, and medicolegal issues.* Catheter Cardiovasc Interv, 2004. **62**(1): p. 1-17.

53. Faxon, D.P., *Bringing reality to drug-eluting stents.* Circulation, 2004. **109**(2): p. 140-2.

54. Grube, E. and L. Buellesfeld, *Paclitaxel-eluting stents: current clinical experience.* Am J Cardiovasc Drugs, 2004. **4**(6): p. 355-60.

55. Virmani, R., F.D. Kolodgie, and A. Farb, *Drug-eluting stents: are they really safe?* Am Heart Hosp J, 2004. **2**(2): p. 85-8.

56. Virmani, R., et al., *Drug-eluting stents: caution and concerns for long-term outcome.* Coron Artery Dis, 2004. **15**(6): p. 313-8.

57. Colombo, A., et al., *Preliminary observations regarding angiographic pattern of restenosis after rapamycin-eluting stent implantation.* Circulation, 2003. **107**(17): p. 2178-80.

58. Bhatia, V., R. Bhatia, and M. Dhindsa, *Drug-eluting stents: new era and new concerns.* Postgrad Med J, 2004. **80**(939): p. 13-8.

59. Mitka, M., *Drug-eluting stents show promise: but experts warn against enthusiasm outpacing science.* Jama, 2004. **291**(6): p. 682-3.

60. Katritsis, D.G., E. Karvouni, and J.P. Ioannidis, *Meta-analysis comparing drug-eluting stents with bare metal stents.* Am J Cardiol, 2005. **95**(5): p. 640-3.

61. Bettmann, M.A., et al., *Carotid stenting and angioplasty: a statement for healthcare professionals from the Councils on Cardiovascular Radiology, Stroke, Cardio-Thoracic and Vascular Surgery, Epidemiology and Prevention, and Clinical Cardiology, American Heart Association.* Stroke, 1998. **29**(1): p. 336-8.

62. Bailes, J.E., *Carotid endarterectomy.* Neurosurgery, 2002. **50**(6): p. 1290-5.

63. Earnshaw, J.J., *Carotid endarterectomy-the evidence.* J R Soc Med, 2002. **95**(4): p. 168-70.

64. Mullenix, P.S., et al., *Carotid endarterectomy remains the gold standard.* Am J Surg, 2002. **183**(5): p. 580-3.

65. Eastcott, H.H., G.W. Pickering, and C.G. Rob, *Reconstruction of internal carotid artery in a patient with intermittent attacks of hemiplegia.* Lancet, 1954. **267**(6846): p. 994-6.

66. Faxon, D.P., W. Coats, and J. Currier, *Remodeling of the coronary artery after vascular injury.* Prog Cardiovasc Dis, 1997. **40**(2): p. 129-40.

67. Conde, I.D. and N.S. Kleiman, *Arterial thrombosis for the interventional cardiologist: from adhesion molecules and coagulation factors to clinical therapeutics.* Catheter Cardiovasc Interv, 2003. **60**(2): p. 236-46.

68. Campbell, J.H., C.L. Han, and G.R. Campbell, *Neointimal formation by circulating bone marrow cells.* Ann N Y Acad Sci, 2001. **947**: p. 18-24; discussion 24-5.

69. Han, C.I., G.R. Campbell, and J.H. Campbell, *Circulating bone marrow cells can contribute to neointimal formation.* J Vasc Res, 2001. **38**(2): p. 113-9.

70. Durand, E., et al., *Time courses of apoptosis and cell proliferation and their relationship to arterial remodeling and restenosis after angioplasty in an atherosclerotic rabbit model.* J Am Coll Cardiol, 2002. **39**(10): p. 1680-5.

71. Pasterkamp, G. and P.C. Smits, *Imaging of atherosclerosis. Remodelling of coronary arteries.* J Cardiovasc Risk, 2002. **9**(5): p. 229-35.

72. Wheeldon, N. and D. Cumberland, *Pharmacologic prevention of acute ischemic complications of coronary angioplasty.* Cathet Cardiovasc Diagn, 1997. **42**(3): p. 249-56.

73. Lefkovits, J. and E.J. Topol, *Pharmacological approaches for the prevention of restenosis after percutaneous coronary intervention.* Prog Cardiovasc Dis, 1997. **40**(2): p. 141-58.

74. Li, J.M., et al., *Recombinant human thrombomodulin inhibits arterial neointimal hyperplasia after balloon injury.* J Vasc Surg, 2004. **39**(5): p. 1074-83.

75. Thomas, A.C. and J.H. Campbell, *Targeted delivery of heparin and LMWH using a fibrin antibody prevents restenosis.* Atherosclerosis, 2004. **176**(1): p. 73-81.

76. Gupta, A.S., et al., *RGD-modified liposomes targeted to activated platelets as a potential vascular drug delivery system.* Thromb Haemost, 2005. **93**(1): p. 106-14.

77. Lestini, B.J., et al., *Surface modification of liposomes for selective cell targeting in cardiovascular drug delivery.* J Control Release, 2002. **78**(1-3): p. 235-47.

78. Sakhalkar, H.S., et al., *Leukocyte-inspired biodegradable particles that selectively and avidly adhere to inflamed endothelium in vitro and in vivo.* Proc Natl Acad Sci U S A, 2003. **100**(26): p. 15895-900.

79. Smirnov, M.D., et al., *Type I and III collagens as a possible target for drug delivery to the injured sites of vascular bed.* Biochem Biophys Res Commun, 1983. **116**(1): p. 99-105.

80. Smirnov, V.N., et al., *Carrier-directed targeting of liposomes and erythrocytes to denuded areas of vessel wall.* Proc Natl Acad Sci U S A, 1986. **83**(17): p. 6603-7.

81. Yun, Y.H., et al., *Hyaluronan microspheres for sustained gene delivery and site-specific targeting.* Biomaterials, 2004. **25**(1): p. 147-57.

82. Bailey, S.R., *Mechanisms of delivery and local drug delivery technologies.* Semin Interv Cardiol, 1996. **1**(1): p. 17-23.

83. Bailey, S.R., *Local drug delivery: current applications.* Prog Cardiovasc Dis, 1997. **40**(2): p. 183-204.

84. Alfke, H., et al., *Local intravascular drug delivery: in vitro comparison of three catheter systems.* Cardiovasc Intervent Radiol, 1998. **21**(1): p. 50-6.

85. Brieger, D. and E. Topol, *Local drug delivery systems and prevention of restenosis.* Cardiovasc Res, 1997. **35**(3): p. 405-13.

86. Gonschior, P., *Local Drug Delivery for Restenosis and Thrombosis N Progress?* J Invasive Cardiol, 1998. **10**(8): p. 528-532.

87. Gottsauner-Wolf, M., et al., *Quantitative evaluation of local drug delivery using the InfusaSleeve catheter.* Cathet Cardiovasc Diagn, 1997. **42**(1): p. 102-8.

88. Herdeg, C., et al., *Local drug delivery with porous balloons in the rabbit: assessment of vascular injury for an improvement of application parameters.* Cathet Cardiovasc Diagn, 1997. **41**(3): p. 308-14.

89. Barath, P., et al., *Infiltrator Angioplasty Balloon Catheter: a device for combined angioplasty and intramural site-specific treatment.* Cathet Cardiovasc Diagn, 1997. **41**(3): p. 333-41.

90. Fletcher, D.A., et al., *Intravascular drug delivery with a pulsed liquid microjet.* Arch Ophthalmol, 2002. **120**(9): p. 1206-8.

91. Pavlides, G.S., et al., *Intramural drug delivery by direct injection within the arterial wall: first clinical experience with a novel intracoronary delivery-infiltrator system.* Cathet Cardiovasc Diagn, 1997. **41**(3): p. 287-92.

92. Reed, M.L., et al., *Micromechanical devices for intravascular drug delivery.* J Pharm Sci, 1998. **87**(11): p. 1387-94.

93. Mitchel, J.F., et al., *Local urokinase delivery with the Channel balloon: device safety, pharmacokinetics of intracoronary drug delivery, and efficacy of thrombolysis.* Cathet Cardiovasc Diagn, 1997. **41**(3): p. 254-60.

94. Mitchel, J.F., et al., *Catheter-based local thrombolysis with urokinase: comparative efficacy of intraluminal clot lysis with conventional urokinase infusion techniques in an in vivo porcine thrombus model.* Cathet Cardiovasc Diagn, 1997. **41**(3): p. 293-302.

95. Guzman, L.A., et al., *Local intraluminal infusion of biodegradable polymeric nanoparticles. A novel approach for prolonged drug delivery after balloon angioplasty.* Circulation, 1996. **94**(6): p. 1441-8.

96. Oberhoff, M., et al., *Time course of smooth muscle cell proliferation after local drug delivery of low-molecular-weight heparin using a porous balloon catheter.* Cathet Cardiovasc Diagn, 1997. **41**(3): p. 268-74.

97. Oberhoff, M., et al., *Local and systemic delivery of low molecular weight heparin following PTCA: acute results and 6-month follow-up of the initial clinical experience with the porous balloon (PILOT-study). Preliminary Investigation of Local Therapy Using Porous PTCA Balloons.* Cathet Cardiovasc Diagn, 1998. **44**(3): p. 267-74.

98. Mitchel, J.F., et al., *Localized delivery of heparin to angioplasty sites with iontophoresis.* Cathet Cardiovasc Diagn, 1997. **41**(3): p. 315-23.

99. Fram, D.B., et al., *Local delivery of heparin to balloon angioplasty sites with a new angiotherapy catheter: pharmacokinetics and effect on platelet deposition in the porcine model.* Cathet Cardiovasc Diagn, 1997. **41**(3): p. 275-86.

100. Bartorelli, A.L., et al., *Local heparin delivery prior to coronary stent implantation: acute and six-month clinical and angiographic results.* Cathet Cardiovasc Diagn, 1997. **42**(3): p. 313-20.

101. Baumbach, A., et al., *Efficacy of low-molecular-weight heparin delivery with the Dispatch catheter following balloon angioplasty in the rabbit iliac artery.* Cathet Cardiovasc Diagn, 1997. **41**(3): p. 303-7.

102. Baumbach, A., et al., *Local delivery of a low molecular weight heparin following stent implantation in the pig coronary artery.* Basic Res Cardiol, 2000. **95**(3): p. 173-8.

103. Baumbach, A., et al., *Porous balloon delivery of low molecular weight heparin in the dog coronary artery.* Eur Heart J, 1996. **17**(10): p. 1538-45.

104. Hong, M.K., et al., *Feasibility and efficacy of locally delivered enoxaparin via the Channeled Balloon catheter on smooth muscle cell proliferation following balloon injury in rabbits.* Cathet Cardiovasc Diagn, 1997. **41**(3): p. 241-5.

105. Beohar, N., et al., *Antirestenotic effects of a locally delivered caspase inhibitor in a balloon injury model.* Circulation, 2004. **109**(1): p. 108-13.

106. Kibbe, M.R., T.R. Billiar, and E. Tzeng, *Gene therapy for restenosis.* Circ Res, 2000. **86**(8): p. 829-33.

107. Caplice, N. and R. Simari, *Gene Transfer for Coronary Restenosis.* Curr Interv Cardiol Rep, 1999. **1**(2): p. 157-164.

108. Yla-Herttuala, S. and J.F. Martin, *Cardiovascular gene therapy.* Lancet, 2000. **355**(9199): p. 213-22.

109. Kipshidze, N., et al., *Complete vascular healing and sustained suppression of neointimal thickening after local delivery of advanced c-myc antisense at six months follow-up in a rabbit balloon injury model.* Cardiovasc Radiat Med, 2002. **3**(1): p. 26-30.

110. Kipshidze, N., et al., *Local delivery of c-myc neutrally charged antisense oligonucleotides with transport catheter inhibits myointimal hyperplasia and positively affects vascular remodeling in the rabbit balloon injury model.* Catheter Cardiovasc Interv, 2001. **54**(2): p. 247-56.

111. Kibbe, M., T. Billiar, and E. Tzeng, *Nitric oxide synthase gene transfer to the vessel wall.* Curr Opin Nephrol Hypertens, 1999. **8**(1): p. 75-81.

112. Kibbe, M., T. Billiar, and E. Tzeng, *Inducible nitric oxide synthase and vascular injury.* Cardiovasc Res, 1999. **43**(3): p. 650-7.

113. Shears, L.L., 2nd, et al., *Efficient inhibition of intimal hyperplasia by adenovirus-mediated inducible nitric oxide synthase gene transfer to rats and pigs in vivo.* J Am Coll Surg, 1998. **187**(3): p. 295-306.

114. Ooboshi, H., et al., *Improvement of relaxation in an atherosclerotic artery by gene transfer of endothelial nitric oxide synthase.* Arterioscler Thromb Vasc Biol, 1998. **18**(11): p. 1752-8.

115. Kibbe, M.R., et al., *Adenovirus-mediated gene transfer of human inducible nitric oxide synthase in porcine vein grafts inhibits intimal hyperplasia.* J Vasc Surg, 2001. **34**(1): p. 156-65.

116. Hiltunen, M.O., et al., *Intravascular adenovirus-mediated VEGF-C gene transfer reduces neointima formation in balloon-denuded rabbit aorta.* Circulation, 2000. **102**(18): p. 2262-8.

117. Rutanen, J., et al., *Gene transfer using the mature form of VEGF-D reduces neointimal thickening through nitric oxide-dependent mechanism.* Gene Ther, 2005. **12**(12): p. 980-7.

118. Laitinen, M., et al., *Catheter-mediated vascular endothelial growth factor gene transfer to human coronary arteries after angioplasty.* Hum Gene Ther, 2000. **11**(2): p. 263-70.

119. Turunen, M.P., et al., *Peptide-retargeted adenovirus encoding a tissue inhibitor of metalloproteinase-1 decreases restenosis after intravascular gene transfer.* Mol Ther, 2002. **6**(3): p. 306-12.

120. O'Brien, T. and R.D. Simari, *Gene therapy for atherosclerotic cardiovascular disease: a time for optimism and caution.* Mayo Clin Proc, 2000. **75**(8): p. 831-4.

121. Bishop, G.G., et al., *Local adenovirus-mediated delivery of hirudin in a rabbit arterial injury model.* J Vasc Res, 1999. **36**(5): p. 343-52; discussion 430-3.

122. Toyoda, K., et al., *Cationic polymer and lipids enhance adenovirus-mediated gene transfer to rabbit carotid artery.* Stroke, 1998. **29**(10): p. 2181-8.

123. Thierry, B., et al., *Nanocoatings onto arteries via layer-by-layer deposition: toward the in vivo repair of damaged blood vessels.* J Am Chem Soc, 2003. **125**(25): p. 7494-5.

124. Moon, M.C., et al., *Perivascular delivery of losartan with surgical fibrin glue prevents neointimal hyperplasia after arterial injury.* J Vasc Surg, 2004. **40**(1): p. 130-7.

125. Geho, D.H., et al., *Fibronectin-based masking molecule blocks platelet adhesion.* Bioconjug Chem, 2003. **14**(4): p. 703-6.

126. Hill-West, J.L., et al., *Inhibition of thrombosis and intimal thickening by in situ photopolymerization of thin hydrogel barriers.* Proc Natl Acad Sci U S A, 1994. **91**(13): p. 5967-71.

127. West, J.L. and J.A. Hubbell, *Separation of the arterial wall from blood contact using hydrogel barriers reduces intimal thickening after balloon injury in the rat: the roles of medial and luminal factors in arterial healing.* Proc Natl Acad Sci U S A, 1996. **93**(23): p. 13188-93.

128. Tulis, D.A., et al., *YC-1-mediated vascular protection through inhibition of smooth muscle cell proliferation and platelet function.* Biochem Biophys Res Commun, 2002. **291**(4): p. 1014-21.

129. Bohl, K.S. and J.L. West, *Nitric oxide-generating polymers reduce platelet adhesion and smooth muscle cell proliferation.* Biomaterials, 2000. **21**(22): p. 2273-8.

130. Parikh, S.A. and E.R. Edelman, *Endothelial cell delivery for cardiovascular therapy.* Adv Drug Deliv Rev, 2000. **42**(1-2): p. 139-61.

131. Dillavou, E., P. Cupp, and P.M. Consigny, *Delivery of endothelial cells to balloon-dilated rabbit arteries with use of a local delivery catheter.* J Vasc Interv Radiol, 2001. **12**(5): p. 601-5.

132. Consigny, P.M., *Placement of endothelial cells on the luminal surface of denuded arteries in vitro and in vivo.* J Vasc Interv Radiol, 1997. **8**(4): p. 595-604.

133. Thompson, M.M., et al., *The effect of transluminal endothelial seeding on myointimal hyperplasia following angioplasty.* Eur J Vasc Surg, 1994. **8**(4): p. 423-34.

134. Thompson, M.M., et al., *Platelet deposition after angioplasty is abolished by restoration of the endothelial cell monolayer.* J Vasc Surg, 1994. **19**(3): p. 478-86.

135. Walluscheck, K.P., G. Steinhoff, and A. Haverich, *Endothelial cell seeding of de-endothelialised human arteries: improvement by adhesion molecule induction and flow-seeding technology.* Eur J Vasc Endovasc Surg, 1996. **12**(1): p. 46-53.

136. Walluscheck, K.P., G. Steinhoff, and A. Haverich, *Endothelial cell seeding of native vascular surfaces.* Eur J Vasc Endovasc Surg, 1996. **11**(3): p. 290-303.

137. Griese, D.P., et al., *Vascular gene delivery of anticoagulants by transplantation of retrovirally-transduced endothelial progenitor cells.* Cardiovasc Res, 2003. **58**(2): p. 469-77.

138. Consigny, P.M., D.A. Silverberg, and N.J. Vitali, *Use of endothelial cells containing superparamagnetic microspheres to improve endothelial cell delivery to arterial surfaces after angioplasty.* J Vasc Interv Radiol, 1999. **10**(2 Pt 1): p. 155-63.

139. Fujiyama, S., et al., *Bone marrow monocyte lineage cells adhere on injured endothelium in a monocyte chemoattractant protein-1-dependent manner and accelerate reendothelialization as endothelial progenitor cells.* Circ Res, 2003. **93**(10): p. 980-9.

140. Gulati, R., et al., *Modulation of the vascular response to injury by autologous blood-derived outgrowth endothelial cells.* Am J Physiol Heart Circ Physiol, 2004. **287**(2): p. H512-7.

141. Gulati, R., et al., *Autologous culture-modified mononuclear cells confer vascular protection after arterial injury.* Circulation, 2003. **108**(12): p. 1520-6.

142. Cho, H.J., et al., *Mobilized endothelial progenitor cells by granulocyte-macrophage colony-stimulating factor accelerate reendothelialization and reduce vascular inflammation after intravascular radiation.* Circulation, 2003. **108**(23): p. 2918-25.

143. Iwakura, A., et al., *Estrogen-mediated, endothelial nitric oxide synthase-dependent mobilization of bone marrow-derived endothelial progenitor cells contributes to reendothelialization after arterial injury.* Circulation, 2003. **108**(25): p. 3115-21.

144. Werner, N., et al., *Intravenous transfusion of endothelial progenitor cells reduces neointima formation after vascular injury.* Circ Res, 2003. **93**(2): p. e17-24.

145. Werner, N., et al., *Bone marrow-derived progenitor cells modulate vascular reendothelialization and neointimal formation: effect of 3-hydroxy-3-methylglutaryl coenzyme a reductase inhibition.* Arterioscler Thromb Vasc Biol, 2002. **22**(10): p. 1567-72.

146. Urbich, C. and S. Dimmeler, *Endothelial Progenitor Cells: Characterization and Role in Vascular Biology.* Circ Res, 2004. **95**(4): p. 343-353.

147. Nathan, A., M. Nugent, and E. Edelman, *Tissue Engineered Perivascular Endothelial Cell Implants Regulate Vascular Injury.* PNAS, 1995. **92**(18): p. 8130-8134.

148. Nugent, H.M. and E.R. Edelman, *Endothelial implants provide long-term control of vascular repair in a porcine model of arterial injury.* J Surg Res, 2001. **99**(2): p. 228-34.

149. Nugent, H.M., et al., *Perivascular endothelial implants inhibit intimal hyperplasia in a model of arteriovenous fistulae: a safety and efficacy study in the pig.* J Vasc Res, 2002. **39**(6): p. 524-33.

150. Nugent, H.M., C. Rogers, and E.R. Edelman, *Endothelial implants inhibit intimal hyperplasia after porcine angioplasty.* Circ Res, 1999. **84**(4): p. 384-91.

151. Roberts, M.J., M.D. Bentley, and J.M. Harris, *Chemistry for peptide and protein PEGylation.* Adv Drug Deliv Rev, 2002. **54**(4): p. 459-76.

152. Lee, J.H., H.B. Lee, and J.D. Andrade, *Blood compatibility of polyethylene oxide surfaces.* Progress in Polymer Science, 1995. **20**(6): p. 1043-1079.

153. Allen, C., et al., *Controlling the physical behavior and biological performance of liposome formulations through use of surface grafted poly(ethylene glycol).* Biosci Rep, 2002. **22**(2): p. 225-50.

154. Du, H., P. Chandaroy, and S.W. Hui, *Grafted poly-(ethylene glycol) on lipid surfaces inhibits protein adsorption and cell adhesion.* Biochim Biophys Acta, 1997. **1326**(2): p. 236-48.

155. Elbert, D.L. and J.A. Hubbell, *Surface Treatments of Polymers for Biocompatibility.* Annual Review of Materials Science, 1996. **26**(1): p. 365-294.

156. Kim, Y.H., et al., *Enhanced blood compatibility of polymers grafted by sulfonated PEO via a negative cilia concept.* Biomaterials, 2003. **24**(13): p. 2213-23.

157. Veronese, F.M. and J.M. Harris, *Introduction and overview of peptide and protein pegylation.* Adv Drug Deliv Rev, 2002. **54**(4): p. 453-6.

158. Caliceti, P. and F.M. Veronese, *Pharmacokinetic and biodistribution properties of poly(ethylene glycol)-protein conjugates.* Adv Drug Deliv Rev, 2003. **55**(10): p. 1261-77.

159. Chapman, A.P., *PEGylated antibodies and antibody fragments for improved therapy: a review.* Adv Drug Deliv Rev, 2002. **54**(4): p. 531-45.

160. Eliason, J.F., *Pegylated cytokines: potential application in immunotherapy of cancer.* BioDrugs, 2001. **15**(11): p. 705-11.

161. Harris, J.M., N.E. Martin, and M. Modi, *Pegylation: a novel process for modifying pharmacokinetics.* Clin Pharmacokinet, 2001. **40**(7): p. 539-51.

162. Deible, C.R., et al., *Molecular barriers to biomaterial thrombosis by modification of surface proteins with polyethylene glycol.* Biomaterials, 1999. **20**(2): p. 101-9.

163. Deible, C.R., *Molecular barriers to thrombosis formed with protein reactive polyethylene glycol*. 1998. p. xvii, 194 leaves.

164. Deible, C.R., et al., *Molecular barriers to biomaterial thrombosis by modification of surface proteins with polyethylene glycol.* Biomaterials, 1998. **19**(20): p. 1885-93.

165. Muller, M., et al., *Surface modification of PLGA microspheres.* J Biomed Mater Res A, 2003. **66**(1): p. 55-61.

166. Mok, H., et al., *Evaluation of polyethylene glycol modification of first-generation and helper-dependent adenoviral vectors to reduce innate immune responses.* Mol Ther, 2005. **11**(1): p. 66-79.

167. Managit, C., et al., *Targeted and sustained drug delivery using PEGylated galactosylated liposomes.* Int J Pharm, 2003. **266**(1-2): p. 77-84.

168. Alberts, B., *Molecular biology of the cell*. 3rd ed. 1994, New York: Garland Pub. xliii, 1294, [67].

169. Chen, A.M. and M.D. Scott, *Current and future applications of immunological attenuation via pegylation of cells and tissue.* BioDrugs, 2001. **15**(12): p. 833-47.

170. Scott, M.D., A.J. Bradley, and K.L. Murad, *Camouflaged blood cells: low-technology bioengineering for transfusion medicine?* Transfus Med Rev, 2000. **14**(1): p. 53-63.

171. Scott, M.D. and K.L. Murad, *Cellular camouflage: fooling the immune system with polymers.* Curr Pharm Des, 1998. **4**(6): p. 423-38.

172. Scott, M.D., et al., *Chemical camouflage of antigenic determinants: stealth erythrocytes.* Proc Natl Acad Sci U S A, 1997. **94**(14): p. 7566-71.

173. Armstrong, J.K., H.J. Meiselman, and T.C. Fisher, *Covalent binding of poly(ethylene glycol) (PEG) to the surface of red blood cells inhibits aggregation and reduces low shear blood viscosity.* Am J Hematol, 1997. **56**(1): p. 26-8.

174. Chung, H.A., et al., *Casual cell surface remodeling using biocompatible lipid-poly(ethylene glycol)(n): development of stealth cells and monitoring of cell membrane behavior in serum-supplemented conditions.* J Biomed Mater Res A, 2004. **70A**(2): p. 179-85.

175. Stuhlmeier, K.M. and Y. Lin, *Camouflaging endothelial cells: does it prolong graft survival?* Biochim Biophys Acta, 1999. **1428**(2-3): p. 177-90.

176. Panza, J.L., et al., *Treatment of rat pancreatic islets with reactive PEG.* Biomaterials, 2000. **21**(11): p. 1155-64.

177. Lee, D.Y., et al., *Optimization of monomethoxy-polyethylene glycol grafting on the pancreatic islet capsules.* J Biomed Mater Res, 2002. **62**(3): p. 372-7.

178. Contreras, J.L., et al., *A novel approach to xenotransplantation combining surface engineering and genetic modification of isolated adult porcine islets.* Surgery, 2004. **136**(3): p. 537-47.

179. Jang, J.Y., et al., *Immune reactions of lymphocytes and macrophages against PEG-grafted pancreatic islets.* Biomaterials, 2004. **25**(17): p. 3663-9.

180. Xie, D., et al., *Cytoprotection of PEG-modified adult porcine pancreatic islets for improved xenotransplantation.* Biomaterials, 2005. **26**(4): p. 403-12.

181. Deible, C.R., et al., *Creating molecular barriers to acute platelet deposition on damaged arteries with reactive polyethylene glycol.* J Biomed Mater Res, 1998. **41**(2): p. 251-6.

182. Burchenal, J.E., et al., *Polyethylene glycol diisocyanate decreases platelet deposition after balloon injury of rabbit femoral arteries.* J Thromb Thrombolysis, 2002. **13**(1): p. 27-33.

183. Savage, M.D., et al., *Avidin-Biotin Chemistry: A Handbook*. 2nd ed. 1994, Rockford: Pierce Chemical Company. xxvii, 467.

184. Campbell, N.A., *Biology*. 2nd ed. 1990, Redwood City, Calif.: Benjamin/Cummings Pub. Co. 1 v. (various pagings).

185. Richards, F.M., *Avidin-biotin technology. Reflections.* Methods Enzymol, 1990. **184**: p. 3-5.

186. Vermette, P., et al., *Immobilization and surface characterization of NeutrAvidin biotin-binding protein on different hydrogel interlayers.* J Colloid Interface Sci, 2003. **259**(1): p. 13-26.

187. Wilchek, M. and E.A. Bayer, *Introduction to avidin-biotin technology.* Methods Enzymol, 1990. **184**: p. 5-13.

188. Ng, P.P., et al., *An anti-transferrin receptor-avidin fusion protein exhibits both strong proapoptotic activity and the ability to deliver various molecules into cancer cells.* Proc Natl Acad Sci U S A, 2002. **99**(16): p. 10706-11.

189. Yu, A., et al., *Specific cell targeting for delivery of toxins into small-cell lung cancer using a streptavidin fusion protein complex.* DNA Cell Biol, 2000. **19**(7): p. 383-8.

190. Sawai, K., et al., *A novel method of cell-specific mRNA transfection.* Mol Genet Metab, 1998. **64**(1): p. 44-51.

191. Ohno, K., B. Levin, and D. Meruelo, *Cell-specific, multidrug delivery system using streptavidin-protein A fusion protein.* Biochem Mol Med, 1996. **58**(2): p. 227-33.

192. Casalini, P., et al., *Tumor pretargeting: role of avidin/streptavidin on monoclonal antibody internalization.* J Nucl Med, 1997. **38**(9): p. 1378-81.

193. Wilbur, D.S., et al., *Development of new biotin/streptavidin reagents for pretargeting.* Biomol Eng, 1999. **16**(1-4): p. 113-8.

194. Wilbur, D.S., et al., *Biotin reagents for antibody pretargeting. 3. Synthesis, radioiodination, and evaluation of biotinylated starburst dendrimers.* Bioconjug Chem, 1998. **9**(6): p. 813-25.

195. Wilbur, D.S., et al., *Streptavidin in antibody pretargeting. 2. Evaluation Of methods for decreasing localization of streptavidin to kidney while retaining its tumor binding capacity.* Bioconjug Chem, 1998. **9**(3): p. 322-30.

196. Wilbur, D.S., et al., *Streptavidin in antibody pretargeting. Comparison of a recombinant streptavidin with two streptavidin mutant proteins and two commercially available streptavidin proteins.* Bioconjug Chem, 1998. **9**(1): p. 100-7.

197. Goldenberg, D.M., et al., *Radioimmunotherapy: is avidin-biotin pretargeting the preferred choice among pretargeting methods?* Eur J Nucl Med Mol Imaging, 2003. **30**(5): p. 777-80.

198. Karacay, H., et al., *Development of a streptavidin-anti-carcinoembryonic antigen antibody, radiolabeled biotin pretargeting method for radioimmunotherapy of colorectal cancer. Reagent development.* Bioconjug Chem, 1997. **8**(4): p. 585-94.

199. Hoya, K., et al., *A novel intravascular drug delivery method using endothelial biotinylation and avidin-biotin binding.* Drug Deliv, 2001. **8**(4): p. 215-22.

200. Huhtinen, P., et al., *Immunoassay of total prostate-specific antigen using europium(III) nanoparticle labels and streptavidin-biotin technology.* J Immunol Methods, 2004. **294**(1-2): p. 111-22.

201. Veronese, F.M., *Peptide and protein PEGylation: a review of problems and solutions.* Biomaterials, 2001. **22**(5): p. 405-17.

202. Harris, J.M., *Poly(ethylene glycol) chemistry : biotechnical and biomedical applications*. Topics in applied chemistry. 1992, New York: Plenum Press. xxi, 385.

203. Martin, B.M., *Tissue culture techniques : an introduction*. 1994, Boston: Birkhèauser. x, 247.

204. Gaigalas, A.K., et al., *Quantitating Fluorescence Intensity From Fluorophore: Assignment of MESF Values.* J Res Natl Inst Stand Technol, 2005. **110**(2): p. 101-114.

205. Schwartz, A., et al., *Standardizing flow cytometry: construction of a standardized fluorescence calibration plot using matching spectral calibrators.* Cytometry, 1996. **26**(1): p. 22-31.

206. Schwartz, A., et al., *Formalization of the MESF unit of fluorescence intensity.* Cytometry B Clin Cytom, 2004. **57**(1): p. 1-6.

207. Schwartz, A., et al., *Standardizing flow cytometry: a classification system of fluorescence standards used for flow cytometry.* Cytometry, 1998. **33**(2): p. 106-14.

208. Schwartz, A., et al., *Quantitating Fluorescence Intensity from Fluorophore: The Definition of MESF Assignment.* J Res Natl Inst Stand Technol, 2002. **107**(1): p. 83-91.

209. Devore, J.L., *Probability and statistics for engineering and the sciences*. 4th ed. 1995, Belmont: Duxbury Press. xviii, 743 p.

210. Hogg, R.V. and J. Ledolter, *Applied statistics for engineers and physical scientists*. Ed. 2. ed. 1992, New York: Macmillan Publishing Company. xxiii, 472 p.

211. Neter, J., et al., *Applied linear statistical models*. 4th ed. 1996, Chicago: Irwin. xv, 720 p.

212. Mosiman, V.L., et al., *Reducing cellular autofluorescence in flow cytometry: an in situ method.* Cytometry, 1997. **30**(3): p. 151-6.

213. Lee, J.H., J. Kopecek, and J.D. Andrade, *Protein-resistant surfaces prepared by PEO-containing block copolymer surfactants.* J Biomed Mater Res, 1989. **23**(3): p. 351-68.

214. Efremova, N.V., S.R. Sheth, and D.E. Leckband, *Protein-Induced Changes in Poly(ethylene glycol) Brushes: Molecular Weight and Temperature Dependence.* Langmuir, 2001. **17**(24): p. 7628-7636.

215. Herold, D.A., K. Keil, and D.E. Bruns, *Oxidation of polyethylene glycols by alcohol dehydrogenase.* Biochem Pharmacol, 1989. **38**(1): p. 73-6.

216. Weller, G.E.R. and University of Pittsburgh. School of Engineering, *Development and Characterizationof Ultrasound Contrast Microbubblestargeted to Dysfunctional Endothelium*. 2003, University of Pittsburgh: Pittsburgh, PA.

217. Weller, G.E., et al., *Modulating targeted adhesion of an ultrasound contrast agent to dysfunctional endothelium.* Ann Biomed Eng, 2002. **30**(8): p. 1012-9.

218. Weller, G.E., et al., *Ultrasound imaging of acute cardiac transplant rejection with microbubbles targeted to intercellular adhesion molecule-1.* Circulation, 2003. **108**(2): p. 218-24.

219. Villanueva, F.S., et al., *Albumin microbubble adherence to human coronary endothelium: implications for assessment of endothelial function using myocardial contrast echocardiography.* J Am Coll Cardiol, 1997. **30**(3): p. 689-93.

220. Villanueva, F.S., et al., *Microbubbles targeted to intercellular adhesion molecule-1 bind to activated coronary artery endothelial cells.* Circulation, 1998. **98**(1): p. 1-5.

221. Wootton, D.M. and D.N. Ku, *Fluid mechanics of vascular systems, diseases, and thrombosis.* Annu Rev Biomed Eng, 1999. **1**: p. 299-329.

222. Dickerson, J.B., et al., *Limited adhesion of biodegradable microspheres to E- and P-selectin under flow.* Biotechnol Bioeng, 2001. **73**(6): p. 500-9.

223. Blackwell, J.E., et al., *Ligand coated nanosphere adhesion to E- and P-selectin under static and flow conditions.* Ann Biomed Eng, 2001. **29**(6): p. 523-33.

224. Badimon, L., et al., *Characterization of a tubular flow chamber for studying platelet interaction with biologic and prosthetic materials: deposition of indium 111-labeled platelets on collagen, subendothelium, and expanded polytetrafluoroethylene.* J Lab Clin Med, 1987. **110**(6): p. 706-18.

225. Griese, D.P., et al., *Isolation and transplantation of autologous circulating endothelial cells into denuded vessels and prosthetic grafts: implications for cell-based vascular therapy.* Circulation, 2003. **108**(21): p. 2710-5.

226. Zou, J., et al., *Effect of resveratrol on intimal hyperplasia after endothelial denudation in an experimental rabbit model.* Life Sci, 2000. **68**(2): p. 153-63.

227. Doornekamp, F.N., et al., *Fogarty and percutaneous transluminal coronary angioplasty balloon injury induce comparable damage to the arterial wall but lead to different healing responses.* J Vasc Surg, 1996. **24**(5): p. 843-50.

228. Barone, G.W., et al., *Morphological and functional techniques for assessing endothelial integrity: the use of Evans blue dye, silver stains, and endothelial derived relaxing factor.* J Card Surg, 1989. **4**(2): p. 140-8.

229. Shintani, S., et al., *Augmentation of postnatal neovascularization with autologous bone marrow transplantation.* Circulation, 2001. **103**(6): p. 897-903.

230. Du, X., et al., *In vivo US monitoring of catheter-based vascular delivery of gene microspheres in pigs: feasibility.* Radiology, 2003. **228**(2): p. 555-9.

231. Yang, X., *Imaging of vascular gene therapy.* Radiology, 2003. **228**(1): p. 36-49.

232. Vermette, P. and L. Meagher, *Interactions of phospholipid- and poly(ethylene glycol)-modified surfaces with biological systems: relation to physico-chemical properties and mechanisms.* Colloids and Surfaces B: Biointerfaces, 2003. **28**(2-3): p. 153-198.

233. Halperin, A., *Polymer Brushes that Resist Adsorption of Model Proteins: Design Parameters.* Langmuir, 1999. **15**(7): p. 2525-2533.

234. Hansen, P.L., et al., *Osmotic properties of poly(ethylene glycols): quantitative features of brush and bulk scaling laws.* Biophys J, 2003. **84**(1): p. 350-5.

235. Heuberger, M., T. Drobek, and N.D. Spencer, *Interaction forces and morphology of a protein-resistant poly(ethylene glycol) layer.* Biophys J, 2005. **88**(1): p. 495-504.

236. Taylor, J.R., *An introduction to error analysis : the study of uncertainties in physical measurements*. 1982, Mill Valley, Calif.: University Science Books. x, 270.

237. Bird, R.B., W.E. Stewart, and E.N. Lightfoot, *Transport phenomena*. 2nd ed. 2002, New York: J. Wiley. xii, 895.

238. Welty, J.R., C.E. Wicks, and R.E. Wilson, *Fundamentals of momentum, heat, and mass transfer*. 3rd ed. 1984, New York: Wiley. xxii, 803.

239. White, F.M., *Fluid mechanics*. 4th ed. McGraw-Hill series in mechanical engineering. 1999, Boston, Mass.: WCB/McGraw-Hill. xiv, 826.

240. Korenaga, R., et al., *Negative transcriptional regulation of the VCAM-1 gene by fluid shear stress in murine endothelial cells.* Am J Physiol, 1997. **273**(5 Pt 1): p. C1506-15.

241. Gosgnach, W., et al., *Shear stress induces iNOS expression in cultured smooth muscle cells: role of oxidative stress.* Am J Physiol Cell Physiol, 2000. **279**(6): p. C1880-8.